




2017

Genome Editing Approach To Uncover Microtubule-Actin Crosslinking Factor (macf1) Essential Domains In Establishing Oocyte Polarity And Nuclear Positioning

Matias Escobar

University of Pennsylvania, matiesco28@gmail.com

Follow this and additional works at: <https://repository.upenn.edu/edissertations>

 Part of the [Cell Biology Commons](#), [Developmental Biology Commons](#), and the [Genetics Commons](#)

Recommended Citation

Escobar, Matias, "Genome Editing Approach To Uncover Microtubule-Actin Crosslinking Factor (macf1) Essential Domains In Establishing Oocyte Polarity And Nuclear Positioning" (2017). *Publicly Accessible Penn Dissertations*. 2271.
<https://repository.upenn.edu/edissertations/2271>

This paper is posted at ScholarlyCommons. <https://repository.upenn.edu/edissertations/2271>
For more information, please contact repository@pobox.upenn.edu.

Genome Editing Approach To Uncover Microtubule-Actin Crosslinking Factor (macf1) Essential Domains In Establishing Oocyte Polarity And Nuclear Positioning

Abstract

The totipotent egg of most vertebrates is polarized in a so called animal-vegetal (AV) axis that is crucial for early embryonic development. AV polarity is established during early oogenesis through the formation and disassembly of the Balbiani Body (Bb) at the vegetal pole. The Bb is a non-membrane bound large mRNP granule, conserved from insects to humans and composed of mitochondria, RNAs and proteins. The Bb components, which include germ cell determinants, anchor to the vegetal cortex upon Bb dissociation in late stage I oocytes. Importantly, Bb dissociation at the oocyte cortex defines the future vegetal pole of the egg. Our lab discovered in zebrafish the only genes known to function in AV polarity formation in vertebrates: bucky ball and macf1. On one hand, Bucky ball is required for Bb formation, and is thought to act by the formation of amyloid-like fibers that capture Bb components. On the other hand, Macf1 is crucial for Bb dissociation. Macf1 is a conserved and giant multi-domain cytoskeletal linker protein that can interact with microtubules (MTs), actin filaments (AF) and intermediate filaments (IF). Macf1 is the only factor known to regulate Bb dissociation, however the Macf1 and cytoskeleton-dependent mechanism by which Macf1 regulates Bb mRNP granule dissociation and, thus, defines AV polarity in the egg is unknown. Here, we unravel Macf1 function via interrogating, for the first time, individual macf1-encoded domains from its endogenous locus to determine their requirement in Bb dissociation and ultimately in egg polarity establishment. Our results show that the Macf1 actin binding domain is essential for Bb dissociation, whereas the Macf1 plakin repeat domain, which interacts with IF, is dispensable for Macf1 function in this context. The method presented here is applicable to other cytolinkers involved in human diseases.

Degree Type

Dissertation

Degree Name

Doctor of Philosophy (PhD)

Graduate Group

Biology

First Advisor

Mary C. Mullins

Keywords

Balbani Body, Cell Polarity, Crispr/Cas9, Macf1, Oogenesis, RNA localization

Subject Categories

Cell Biology | Developmental Biology | Genetics

GENOME EDITING APPROACH TO UNCOVER MICROTUBULE-ACTIN
CROSSLINKING FACTOR (MACF1) ESSENTIAL DOMAINS IN ESTABLISHING
OOCYTE POLARITY AND NUCLEAR POSITIONING

Matias Escobar-Aguirre

A DISSERTATION

in

Biology

Presented to the Faculties of the University of Pennsylvania

in

Partial Fulfillment of the Requirements for the

Degree of Doctor of Philosophy

2017

Supervisor of Dissertation

Mary Mullins, Ph.D., Professor of Cell and Developmental Biology

Graduate Group Chairperson

Michael Lampson, Ph.D., Professor of Biology

Dissertation Committee

Tatyana Svitkina, Ph.D., Professor of Biology

Erfei Bi, Ph.D., Professor of Cell and Developmental Biology

Stephen DiNardo, Ph.D., Professor of Cell and Developmental Biology

Wei Guo, Ph.D., Professor of Biology

GENOME EDITING APPROACH TO UNCOVER MICROTUBULE-ACTIN
CROSSLINKING FACTOR (MACF1) ESSENTIAL DOMAINS IN ESTABLISHING
OOCYTE POLARITY AND NUCLEAR POSITIONING

COPYRIGHT

2017

Matias Escobar-Aguirre

This work is licensed under the

Creative Commons Attribution-

NonCommercial-ShareAlike 3.0

License

To view a copy of this license, visit

<https://creativecommons.org/licenses/by-nc-sa/3.0/us/>

ACKNOWLEDGMENTS

I would first like to thank my thesis advisor, Mary Mullins. She is a great scientist that shared with me her knowledge and experience. I am very thankful for all her constructive criticism along the way that helped to move this project forward. Mary would usually say “Don’t jump to conclusions too fast”, and I think over the years I have come to fully appreciate that phrase. To do good science, there is no easy process. To understand something, you have to work hard, think and design experiments that address your question from all possible angles, but more importantly, even after you think you have tried everything and are convinced about your results, we need to be aware of our own biases and keep our eyes open for alternative explanations. Mary taught me to feel responsible about our science, and helped me to see it as part of a bigger scientific effort. As I move forward in my scientific career, I feel privileged to have had Mary as my advisor and she has definitely influenced me.

I am very thankful to my thesis committee: Tanya Svitkina, Erfei Bi, Steve Dinardo and Wei Guo. The input they provided was fundamental to move my project forward. All along they were very supportive and helped me to clarify my ideas. Also, I was very grateful to them for understanding my particular situation in relation to my Chilean doctoral fellowship.

The Mullins lab is a great work environment. Since I joined back in 2011 the lab has transition from a mainly post-doc to a PhD student lab. I had the opportunity to learn from former postdocs: Megumi Hashiguchi, Lee Kapp, Elliott Abrams and James Dutko.

It was a great experience to interact with them professionally, intellectually and personally. My big thanks to James Dutko, a great teacher in the lab that is always down for a beer after work. Thanks to a friend and former collaborator in the lab, Hong Zhang. Big thanks to Amy Kugath for keeping the lab up and running, for being a very good friend and caring person. Thank you Ricardo Fuentes, my friend and colleague that was always supportive and willing to help me whenever I needed it. I want to thank the current lab members: Joe, Francesca, Ben, Allison, Hannah, Robyn and Dondra for making the lab a friendly and intellectually stimulating environment. Thanks to Dennis Huang for helping me with genotyping and image analysis of my project. I am grateful also to the fish facility staff; Mona, Bill, Nadine, Erin and Dave for taking care of my fish.

Many thanks to friends outside the Mullins Lab, Juliane Bremer for her critical analysis of every experiment or idea, and for making me company those long hours in the lab after midnight. I want to thank Kristin Lorent for supporting me at every step with good advice and chocolate. Thanks Paula Stein for teaching me to microinject zebrafish oocytes, and for watching and playing soccer with me. I would also like to thank the Granato and Pack labs for their help with reagents and feedback about my project. Michael Granato for supporting the zebrafish community which benefits to all students in the department. Thanks to Mike Pack for his advice on my future career decisions.

I would like to thank other labs outside Penn that shared important reagents for my project: Elaine Fuchs lab for the Macf1 antibody, the Heisenberg lab, Masahiko Hibi and Sampath labs for sharing various zebrafish transgenic lines.

Many thanks to biology PhD students: Ammar, Amita, Swathi, Yang, Jia, Ale, Lukaz, Vince and Leo. We went through a lot together and it was important to keep it fun. I am very grateful to Colleen in the Biology department for caring about the Biology PhD students.

I would like to thank Clara Franzini-Armstrong, Cesar Cardenas and Marioly Muller for giving me the opportunity to come to Penn and supporting me when I decided to do my PhD in the United States.

Thanks to my non-science friends from the Chilean community in Philly, my soccer team WPMC for those great seasons we have played together and to my great friend Dio.

I am very thankful to the Chilean government for providing me with a fellowship to pursue my PhD at Penn. Despite the fact that governmental fellowships have acquired a bad reputation in Chile over the years, I reclaim the importance of such initiatives to promote science development in Chile.

Lastly, I would like to thank my inner circle; to Giselle for being patient and supportive, and my family that although have felt a bit unconnected of my PhD experience, they always made me feel this was a worthwhile experience.

ABSTRACT

GENOME EDITING APPROACH TO UNCOVER MICROTUBULE-ACTIN CROSSLINKING FACTOR (MACF1) ESSENTIAL DOMAINS IN ESTABLISHING OOCYTE POLARITY AND NUCLEAR POSITIONING

Matias Escobar -Aguirre

Mary Mullins

The totipotent egg of most vertebrates is polarized in a so called animal-vegetal (AV) axis that is crucial for early embryonic development. AV polarity is established during early oogenesis through the formation and disassembly of the Balbiani Body (Bb) at the vegetal pole. The Bb is a non-membrane bound large mRNP granule, conserved from insects to humans and composed of mitochondria, RNAs and proteins. The Bb components, which include germ cell determinants, anchor to the vegetal cortex upon Bb dissociation in late stage I oocytes. Importantly, Bb dissociation at the oocyte cortex defines the future vegetal pole of the egg. Our lab discovered in zebrafish the only genes known to function in AV polarity formation in vertebrates: *bucky ball* and *macf1*. On one hand, Bucky ball is required for Bb formation, and is thought to act by the formation of amyloid-like fibers that capture Bb components. On the other hand, Macf1 is crucial for Bb dissociation. Macf1 is a conserved and giant multi-domain cytoskeletal linker protein that can interact with microtubules (MTs), actin filaments (AF) and intermediate filaments (IF). Macf1 is the only factor known to regulate Bb dissociation, however the Macf1 and

cytoskeleton-dependent mechanism by which Macf1 regulates Bb mRNP granule dissociation and, thus, defines AV polarity in the egg is unknown. Here, we unravel Macf1 function via interrogating, for the first time, individual *macf1*-encoded domains from its endogenous locus to determine their requirement in Bb dissociation and ultimately in egg polarity establishment. Our results show that the Macf1 actin binding domain is essential for Bb dissociation, whereas the Macf1 plakin repeat domain, which interacts with IF, is dispensable for Macf1 function in this context. The method presented here is applicable to other cytolinkers involved in human diseases.

TABLE OF CONTENTS

ACKNOWLEDGMENTS.....	III
ABSTRACT	VI
TABLE OF CONTENTS.....	VIII
LIST OF TABLES	XI
LIST OF FIGURES	XII
CHAPTER 1 : GENERAL INTRODUCTION	1
Oocyte polarity regulates the localization of germ cell determinants.....	3
Determinants of the embryonic body axes originate in the polarized oocyte.....	5
Oocyte development and the formation of the Bb.	8
The Bb after 170 years	10
Bb function in RNA localization of germ cell and dorsal determinants.....	10
The Animal pole localization of RNAs	13
Bb assembly and disassembly regulate AV polarity establishment	14

Buckyball	15
Macf1: A cytolinker regulates Bb dissociation	19
CHAPTER 2 :	27
*Microtubule-Actin Crosslinking Factor 1 (Macf1) domain function in Balbiani body dissociation and nuclear positioning	27
Summary	28
Introduction.....	29
Material and Methods.....	33
Ethics Statement	33
Fish lines	33
Fluorescence immunolabeling and RNA in situ hybridization.....	34
Antibodies.....	34
In situ hybridization.....	35
Confocal microscopy and image processing.....	35
Image quantification	35
Live imaging of whole ovaries and isolated oocytes.....	36
Nocodazole, Latrunculin A and cold treatment.....	37
macf1a cDNA sequencing	38
CRISPR/Cas9 Genome editing	39
Results.....	42
Macf1a is essential in Buc relocalization from Bb to oocyte cortex	43

Macf1a functions independently in Bb disassembly and nucleus positioning	45
Actin required for Bb cortical attachment and nucleus positioning, whereas MTs dispensable	47
Genome editing approach to interrogate Macf1a functional domains	49
Macf1a-ABD is essential for Bb disassembly and nucleus positioning	52
Discussion	54
Macf1a may function as a non-canonical linker.....	54
Macf1a in Bb disassembly, IDPs, and P granules.....	54
Drosophila Macf1 ortholog Shot and MTs	57
Macf1a in nuclear positioning	58
 CHAPTER 3 : FUTURE DIRECTIONS.....	 78
 Is Macf1 and actin interaction directly or indirectly mediating Bb disassembly? ...	 80
 Is the rod domain (spectrin repeats) required in establishing oocyte polarity?	 81
 BIBLIOGRAPHY.....	 84

LIST OF TABLES

Table 2.1. Generation of <i>macf1a</i> deletion mutants	75
Table 2.2: Egg phenotype of <i>macf1a</i> mutant females	76
Table 2.3. List of <i>macf1a</i> cDNA primers.....	77

LIST OF FIGURES

Figure 1.1: Function of localized maternal products.....	24
Figure 1.2: RNA localization and AV axis establishment during oogenesis.	25
Figure 2.1: Macf1a is essential in relocalizing Buc from the Bb to the oocyte cortex.....	61
Figure 2.2: Epistasis of <i>buckyball</i> and <i>macf1a</i> in nuclear positioning.	62
Figure 2.3: Localization of Macf1a in stage I oocytes.	63
Figure 2.4: Latrunculin A treatment in stage I oocytes	64
Figure 2.5: Effect of disrupting actin and MTs on the Bb and nuclear positioning.	65
Figure 2.6: Distribution of cytokeratin in stage I oocytes.	67
Figure 2.7: Pipeline for the generation of <i>macf1a</i> ^{ΔABD(CH1)} , <i>macf1a</i> ^{ΔABD(CH1-ch2)} and <i>macf1a</i> ^{ΔPRD/-} mutants.	68
Figure 2.8: CRISPR/Cas9 deletions of Macf1a ABD and PRD.	69
Figure 2.9: Molecular characterization of <i>macf1a</i> domain deletion mutants.	71
Figure 2.10: Phenotypic characterization of <i>macf1a</i> ^{ΔABD(CH1)} , <i>macf1a</i> ^{ΔABD(CH1-CH2)} and <i>macf1a</i> ^{ΔPRD} mutants.	73
Figure 2.11: AV polarity establishment in <i>macf1a</i> mutants.	73
Figure 2.12: Model of Macf1a function in Bb dissociation at the cortex.	74

Chapter 1 : General Introduction

Portions of this chapter were published in "***Localization in Oogenesis of Maternal Regulators of Embryonic Development***", book: Vertebrate Development:

Maternal to Zygotic Control. Escobar-Aguirre M, Elkouby YM, Mullins MC. Adv Exp Med Biol. 2017;953:173-207.

Cell polarity is a universal strategy for organizing the intracellular space to mediate cell function. Cell polarity in development often relies on mechanisms of RNA localization to specific subcellular domains to define the identity of future developing tissues. The totipotent egg of most animals illustrates in a grand way the importance of cell polarity and RNA localization in regulating multiple crucial developmental events. The polarization of the egg arises during its development in oogenesis. RNAs localize asymmetrically in the early oocyte defining its animal-vegetal (AV) axis, which upon further elaboration in mid- and late-oogenesis stages produces a mature egg with specific localized factors along its AV axis that will define the future anterior-posterior (AP) and dorsal-ventral (DV) axes of the embryo. Furthermore, AV polarity confines germ cell determinants to the vegetal pole, from where they redistribute to the cleavage furrows of the 2- and 4-cell stage embryo, ultimately specifying the primordial germ cells (PGCs). The sperm entry region during fertilization is also defined by the AV axis. In frogs and fish sperm enters through the animal pole, similar to the mouse where it enters predominantly in the animal half. Thus, AV polarity establishment and RNA localization are involved in all the major events of early embryonic development (Figure 1.1).

Studies in *Xenopus* have identified many animally and vegetally localized factors that distribute either to the germ cells, the germ layers, or specify the axes in the early embryo (Bubunenko et al., 2002; Claussen and Pieler, 2004; Claussen et al., 2011; Cuykendall and Houston, 2010; Houston et al., 1998; Kaneshiro et al., 2007; Ku and Melton, 1993; Kwon et al., 2002; Rebagliati et al., 1985; Weeks and Melton, 1987).

Genetic screens in the zebrafish or knockdown approaches in *Xenopus* have revealed the function for some of these factors and discovered new ones. In the zebrafish, *bucky ball* (*buc*) and *macf1* genes were identified in a maternal-effect mutant screen in zebrafish and provide the only known genetic entry points for studying the early events of AV polarity establishment during oogenesis (Bontems et al., 2009; Dosch et al., 2004; Gupta et al., 2010; Marlow and Mullins, 2008; Wagner et al., 2004). Vegetally-localized RNAs acting in DV axis formation include *wnt8* in zebrafish (Erter et al., 2001; Lekven et al., 2001; Varga et al., 2007), and *wnt11* in *Xenopus* (Cha et al., 2008; Cha et al., 2009; Ku and Melton, 1993; Tao et al., 2005), while vegetally-localized VegT in *Xenopus* functions in germ layer formation (Clements et al., 1999; Xanthos et al., 2001). Genetic screens in zebrafish also identified *glutamate receptor interacting protein 2* (*grip2a* or *hecate*) (Ge et al., 2014) and *syntabulin* (*tokkaebi*) (Nojima et al., 2010) as key vegetally-localized regulators of DV axis formation in the egg.

Oocyte polarity regulates the localization of germ cell determinants

Animals have developed two primary strategies to specify the germ line. In mammals, the germ cell lineage is induced in the epiblast by the action of BMP4 produced in the extraembryonic ectoderm (Lawson et al., 1999). In other vertebrates, and in most insects, germ cells are specified by the inheritance of the germ plasm (GP), a cytoplasmic aggregate containing RNA and proteins sufficient to determine the primordial germ cell (PGC) fate (Kobayashi et al., 1994)(reviewed (Extavour and Akam, 2003). In zebrafish and *Xenopus*, GP accumulates at the 2- and 4-cell stages at the ends of the cleavage furrows (Figure 1.1C)(Hashimoto et al., 2004; Kloc et al., 2001;

Yoon et al., 1997). Removal of GP diminishes or ablates PGC formation in fish and frogs (Ikenishi et al., 1974; Smith, 1966; Whittington and Dixon, 1975; Yoon et al., 1997; Zust and Dixon, 1975). Conversely, GP transplantation induces PGC formation (Kobayashi et al., 1994), thus providing compelling evidence for GP function in germ cell specification.

In *Xenopus* the GP becomes localized during oogenesis to the oocyte vegetal cortex, where it remains localized in the egg (Figure 1.1A) (Heasman et al., 1984) (Houston and King, 2000; Kloc et al., 2002). In the *Xenopus* embryo the vegetal cells that inherit the GP then adopt the PGC fate (Houston, 2013; Whittington and Dixon, 1975). In zebrafish it is more complex: some GP components localize to the oocyte and egg vegetal pole (e.g. *dazl* RNA) (Kosaka et al., 2007), whereas *vasa* RNA, for instance, is initially vegetally-localized in the oocyte, then becomes radially localized to the oocyte cortex, where it remains in the egg (Kosaka et al., 2007). After egg activation in zebrafish, the GP components from distinct locations accumulate at the cleavage furrows of the 2- and 4-cell stage embryo (Braat et al., 1999; Knaut et al., 2000; Riemer et al., 2015; Yoon et al., 1997). The difference between frog and fish is likely due to the distinct architectures of these embryos. In zebrafish the yolk lies at the vegetal pole of the egg separate from the blastomeres that form in the animal half, whereas in frog the yolk and cytoplasm are not segregated from each other and blastomeres will comprise the entire AV extent of the egg. So in the zebrafish the GP must re-aggregate at the cleavage furrows at the yolk-cytoplasm interface at an animal-vegetal mid-region, whereas in the frog the vegetal-most blastomeres inherit directly the vegetal-oocyte localized GP to become the PGCs.

In both frogs and fish, the germ plasm components are first localized in stage I oocytes to a structure called the Balbiani body (Bb) (Figure 1.1 A,B) (Chang et al., 2004; Heasman et al., 1984; Kloc and Etkin, 1995; Kloc et al., 1998; Kloc et al., 1996; Kosaka et al., 2007; Schnapp et al., 1997; Wilk et al., 2005). Here I will generally use the zebrafish oocyte staging convention (Selman et al., 1993), which is slightly different to that in *Xenopus*. The Bb, also called the Mitochondrial Cloud in *Xenopus*, is a highly conserved structure present from insects to humans where specific RNAs, proteins and organelles, like mitochondria become localized (reviewed (Kloc et al., 2004). These RNAs and proteins, including GP components, passage via the Bb to the oocyte vegetal cortex (Figure 1.1 .1B) (Kloc and Etkin, 1995; Melton, 1987; Wilk et al., 2005; Yisraeli et al., 1989, 1990; Zhou and King, 1996b). Later in this chapter, I will discuss in detail what is known about the Bb function in the oocyte.

Determinants of the embryonic body axes originate in the polarized oocyte

During gastrulation the main body axes are patterned in vertebrate embryos giving rise to a body plan displaying a dorsal-ventral (DV) and anterior-posterior (AP) axes. The factors that guide this remarkable morphogenetic processes can be found polarized in the developing oocyte prior to the emergence of a competent zygote. Maternal factors that localizes to the vegetal pole in the oocyte, later act in the establishment of the DV axis of the embryo (Figure 1.1B) (De Robertis and Kuroda, 2004; Langdon and Mullins, 2011). In both *Xenopus* and zebrafish, the dorsal determinants are localized in the oocyte and end up on the dorsal side of the embryo during gastrulation. These dorsal determinants are Wnt ligands that in *Xenopus*

corresponds to a combination of Wnt11 and Wnt5a, whereas in zebrafish the ligand is Wnt8(Cha et al., 2008; Cha et al., 2009; Tao et al., 2005) (Lu et al., 2011).. The activation of the Wnt pathway by these ligands induces β -catenin nuclear localization on the future dorsal side of the embryo that in combination with other morphogen signaling, like Nodal and FGF, activates the developmental program for the embryo dorsal identity (De Robertis and Kuroda, 2004; Langdon and Mullins, 2011).

Despite using different Wnt ligands, dorsal determinant activity is regulated by similar principles in *Xenopus* and zebrafish. The *wnt* ligand mRNAs are initially localized to the vegetal pole of the egg and zygote (Figure 1.1 B) (Ku and Melton, 1993; Lu et al., 2011; Nojima et al., 2010; Nojima et al., 2004). Upon fertilization in *Xenopus* and egg activation in zebrafish, microtubules reorganize to pave the way for these mRNAs to translocate asymmetrically in an animal direction, resulting in their new localization specifically on the future dorsal side of the embryo (Heasman, 2006; Ku and Melton, 1993; Lu et al., 2011; Tao et al., 2005). Prior to this dorsal transport, these mRNAs are translationally silent. While *wnt8* translation regulation has yet to be elucidated in zebrafish, *wnt11* mRNA in *Xenopus* was shown to load onto polysomes only after detaching from the microtubules at its dorsal destination during cleavage stages (Schroeder et al., 1999). A similar mechanism is expected for zebrafish Wnt8. The coordinated localization and translation regulation of these mRNAs ensures their dorsally-localized activity, and results in a dorsal to ventral Wnt gradient (Figure 1.1B).

Two factors identified in maternal-effect screens in zebrafish, *syntabulin* (*tokkaebi*) and *grip2a* (*hecate*), are localized to the vegetal pole of the egg and play key roles in dorsal determinant translocation following egg activation (Ge et al., 2014; Nojima et al., 2010). Consistent with this role, females mutants for these genes produce ventralized embryos. Syntabulin is a microtubule-motor linker protein that can bind the Kinesin I motor heavy chain, Kif5b (Nojima et al., 2010). Syntabulin protein localizes to the vegetal pole of the egg and translocates asymmetrically in a microtubule-dependent manner, consistent with it playing a role in translocating dorsal determinants on the microtubule array. The *grip2a* mRNA also localizes to the vegetal pole and itself is translocated asymmetrically like the *wnt* transcripts following egg activation (Figure 1.1B) (Ge et al., 2014). In eggs of *grip2a* mutant females, the vegetal pole microtubule network is compromised and the asymmetric translocation of *wnt8* and *grip2a* itself fails (Ge et al., 2014). The vegetal localization of *grip2a* and *syntabulin* are conserved in *Xenopus*, as well as the function of Syntabulin (Colozza and De Robertis, 2014; Nojima et al., 2010). Although, *grip2a* is later localized to PGCs in *Xenopus* (Ge et al., 2014; Kaneshiro et al., 2007; Kirilenko et al., 2008; Tarbashevich et al., 2007).

The *wnt8*, *wnt11*, *syntabulin*, and *grip2a* mRNAs are all localized to the vegetal pole of the egg (Ge et al., 2014; Kirilenko et al., 2008; Ku and Melton, 1993; Lu et al., 2011). Moreover, with the exception of *wnt11* (Ku and Melton, 1993), their localization to the vegetal pole occurs early in oogenesis and is executed by the Balbiani body (Bb) (Kirilenko et al., 2008; Lu et al., 2011; Tarbashevich et al., 2007). These mRNAs localize

to the Bb and the future vegetal pole of the early oocyte, where they remain anchored throughout oogenesis and in the egg. Thus, the AV axis of the oocyte is key to forming the dorsal organizer and subsequently establishing the basic vertebrate embryonic body plan (Figure 1.1).

Oocyte development and the formation of the Bb.

Germline stem cells give rise to oogonial cells which are the oocyte precursors. The process of oocyte specification involves the successive mitotic divisions with incomplete cytokinesis that causes oogonial cells to remain interconnected to their sister cells through cytoplasmic bridges. Thus, oogonia form a cyst in which the oocyte develops during early oogenesis and that is believed to allow for the exchange of factors that ensure synchronous progression. The cyst will eventually breakdown and oocytes become surrounded by somatic follicle cells that proliferate, as the oocyte develops and grows, forming a multilayer in late stage oocytes. After the final mitotic division, oogonia enters meiosis I characterized by a long prophase I where it undergoes genetic recombination and cell growth. Later in oogenesis, the first meiotic division is completed during oocyte maturation, whereas the second meiotic division will only take place after fertilization.

Until recently, the first indication of polarity in the oocyte was the detection of the Balbiani body (Bb) at a mid-diplotene stage of prophase I or earlier asymmetric Bucky ball protein in zebrafish that was more dispersed (Heim et al., 2014; Riemer et al., 2015). It has now been shown in zebrafish that the first stages of Bb formation and oocyte polarization occur much earlier, at the onset of meiosis (Elkouby et al., 2016). In the pre-

meiotic oogonial stages Bb precursor components, such as Bucky ball, GasZ and mitochondria, are distributed symmetrically in the perinuclear cytoplasm (Figure 1.2A). These Bb components initiate their specific and asymmetric localization at the early meiotic zygotene stage where a polarized nuclear configuration known as the chromosomal bouquet is established. Here, the telomeres of the chromosomes move and rotate tethered to the nuclear envelope and become clustered to one pole. The movement is mediated by microtubules along with the centrosome and ultimately facilitates chromosomal pairing and meiotic recombination. (Ding et al., 2007; Link et al., 2014; Sato et al., 2009; Scherthan, 2001; Shibuya et al., 2014a; Shibuya et al., 2014b).

Remarkably, Bb precursors initially localize to the cytoplasmic region that apposes the bouquet telomere cluster and contains the centrosome (Elkouby et al., 2016). Disruption of microtubules causes a loss of telomere clustering of the bouquet with a parallel loss of mitochondrial enrichment to form the Bb precursor aggregate, indicating that the pre-aggregation of mitochondria and the establishment of the bouquet configuration are coordinated (Elkouby et al., 2016). Subsequent to the bouquet stage, the Bb precursor components aggregates within a nuclear cleft that gradually rounds up concomitantly with the pre- Bb aggregates appearing more condensed and spherical, displaying the typical mature Bb of mid-diplotene stages . Altogether, centrosome and telomere cluster association at zygotene stages marks the site for Bb formation and, perhaps, also plays a role in predicting the site for Bb disassembly at late stage I that ultimately defines the oocyte vegetal pole (Elkouby et al., 2016).

The Bb after 170 years

The Bb is a universally conserved structure first described in oocytes from insects around 170 years ago (Cox and Spradling, 2003; Jaglarz et al., 2003; WH, 1845), present in arthropods (Jedrzejowska and Kubrakiewicz, 2007), zebrafish (Marlow and Mullins, 2008), frogs (Dumont, 1978), birds (Carlson et al., 1996; Rodler and Sinowatz, 2013; Ukeshima and Fujimoto, 1991), rodents (Pepling et al., 2007; Weakley, 1967), primates (Barton and Hertig, 1972), to humans (Albamonte et al., 2013; Hertig, 1968). Across all these species, the Bb appears as an aggregate of mitochondria and electron-dense material adjacent to the nucleus. Though the Bb is present in mammalian early oocytes, it is not known if it functions in early oocyte polarity or whether plays a role later, perhaps related to events like the asymmetric formation of the antral cavity.

Bb function in RNA localization of germ cell and dorsal determinants.

Throughout oogenesis, dorsal determinants and germ plasm components distribute within distinct compartments often reflecting the oocyte AV polarity. Early studies in *Xenopus* identified several vegetally-localized RNAs and determined their localization dynamics during oogenesis (Cuykendall and Houston, 2010; Houston et al., 1998). Among them, *Xcat/nanos* (Forristall et al., 1995; Mosquera et al., 1993) and *Vg1/gdf1* (Yisraeli and Melton, 1988) became models for unraveling RNA localization mechanisms. *nanos* RNA localizes to the Bb in stage I oocytes, then translocates via the Bb to the vegetal cortex, where it becomes docked during Bb disassembly at the end of stage I (stage II in frog) of oogenesis. On the other hand, *Vg1* localization to the vegetal

pole begins during stage III and culminates anchoring to the vegetal cortex by stage VI in frog (Mowry and Cote, 1999). The localization patterns of *nanos* and *Vg1* led to defining two pathways of RNA localization, an early pathway for RNAs that are transported via the Bb (also called the METRO pathway) (Kloc and Etkin, 1995; Wilk et al., 2005) and a later pathway for RNAs, like *Vg1*, that localizes at the vegetal cortex after the Bb has disassembled (Mowry and Cote, 1999). These two pathways are further distinct mechanistically in that the early pathway is believed not to require the cytoskeleton, whereas the late pathway requires microtubules for successful localization of RNAs to the vegetal pole.

The delivery of the early pathway mRNAs to a restricted region of the oocyte cortex specifies this region as the vegetal pole, and the process is executed by the Balbiani body. In frogs and zebrafish, transcripts that are localized via the Bb will constitute the germ plasm during early development, such as *dazl*, *vasa*, and *nanos* (Kosaka et al., 2007; Mosquera et al., 1993; Zhou and King, 1996a); others mRNAs encode dorsal determinants and its localizing machinery (like *wnt8*, *grip2a*, and *syntabulin*) (Colozza and De Robertis, 2014; Ge et al., 2014; Kirilenko et al., 2008; Lu et al., 2011; Nojima et al., 2010; Tarbashevich et al., 2007). In addition, the Bb contains mRNA binding proteins (like Rbpm2 (Hermes) (Kosaka et al., 2007; Song et al., 2007)) and RNP scaffold proteins (like GasZ (Marlow and Mullins, 2008; Yan et al., 2004; Yano et al., 2004)).

In the late pathway, RNAs like *Vg1* in frog (Cote et al., 1999), and *bruno-like* and *mago nashi* in zebrafish (Kosaka et al., 2007), localize to the vegetal pole in stage III of

oogenesis, at this stage the Bb has disassembled and its components were loaded to the vegetal cortex earlier. The late vegetal mRNA localization pathway during stages III-V in *Xenopus* depends on microtubules (MTs) that radiate from a dense perinuclear array to the cortex in continuous filaments, and by stage VI oocytes display a perinuclear cap enriched in tubulin at the vegetal side of the nucleus (Gard, 1991). The molecular mechanisms that drive RNA localization are better understood for the late pathway, in particular for the *Xenopus Vg1* RNA (Figure 1.2C). Interestingly, in zebrafish *Vg1 (gdf3)* RNA localizes to the animal pole, instead of the vegetal pole of stage III oocytes. Studies in frog oocytes show that a 340-nt localizing element (LE) in the 3' UTR of *Vg1* contains repetitive sequence motifs necessary for the vegetal localization of injected *Vg1* RNA. These motifs are the sequences UUUCU (VM1) and UUCAC (E2) that are necessary also for localization of RNAs through the early pathway. The clustering of E2 and/or VM1 motifs might be important for LE recognition (Betley et al., 2002; Choo et al., 2005; King et al., 2005).

The current understanding of the RNA localization process in *Xenopus* oocytes suggests that early and late pathways may not represent two independent events, but rather a continuum mechanism of RNA localization though with differences in the role of MTs, which seem required only in the late pathway (chapter 2) (Chang et al., 2004) (Zhou and King, 1996b). Interestingly, when RNAs that localize through the early pathway are injected into stage III oocytes in *Xenopus*, they can still localize to the vegetal cortex (Choo et al., 2005; Claussen et al., 2004). Moreover, the late pathway *Vg1-LE* when injected into stage I oocytes, can localize to the Bb (Choo et al., 2005).

Importantly, these RNAs require the same motifs in their 3'UTRs for early and late pathway localization, suggesting that the RNA-protein machinery functioning in the late pathway may be similar to that used in the early pathway (Choo et al., 2005; Claussen et al., 2004).

The Animal pole localization of RNAs

At the animal pole, the egg is fertilized in frogs and fish and the blastodisc forms in zebrafish. Like at the vegetal pole, RNAs localize to the animal pole during oogenesis, though they localize after the Bb disassembles, suggesting that vegetal pole identity is acquired first. In zebrafish, RNAs like *cyclin B1* (*cycB*) and *pou5f3* (previously called *pou2*) localize to the animal pole in stage II and early stage III, respectively, remaining there in a cortical and tight distribution throughout oocyte maturation (Figure 1.2C) (Howley and Ho, 2000). Interestingly, *Vg1* RNA in zebrafish localizes to the animal pole right below the micropyle (Marlow and Mullins, 2008), unlike in frogs where *Vg1* localizes to the vegetal pole (Mowry and Melton, 1992). As stated earlier, the lack of vegetal pole identity in zebrafish *buc* mutants causes the formation of multiple micropyles and a radial animal identity with no recognizable blastodisc in the egg (Dosch et al., 2004) (Marlow and Mullins, 2008). Similarly, *pou5f3* and *cycB* RNAs show a radial localization in *buc* mutant stage III oocytes, indicating that *Buc* defines the egg AV axis by also restricting the localization of animal RNAs in the oocyte.

In stage IV, zebrafish oocytes undergo maturation. Through this process, oocytes progress from prophase of meiosis I (MI) to metaphase of meiosis II (MII), extruding the first polar body at the animal pole. Several changes occur during this process, including

GV migration to the animal pole and translation of RNAs promoting meiotic progression (Figure 1.2C). Before the oocyte matures, animally-localized RNAs like *cycB*, are translationally repressed. CycB protein is required during oocyte maturation, along with Cdc2 kinase, as part of the Maturation-Promoting Factor (MPF) that drives meiotic progression (Kondo et al., 1997; Masui, 1972; Nagahama and Yamashita, 2008). Thus, *cycB* mRNA localization to the animal pole is important for CycB localized translation and activity, which allows, in conjunction with other factors, oocyte meiotic progression and competence.

Bb assembly and disassembly regulate AV polarity establishment

Two maternal-effect mutants identified in zebrafish, *bucky ball* (*buc*) and *macf1* (*microtubule crosslinking factor 1*), have provided the only known genes required for AV polarity establishment in vertebrates (Figure 1.2B) (Bontems et al., 2009) (Marlow and Mullins, 2008) (Gupta et al., 2010). In contrast to a normal egg with cytoplasm in a distinct blastodisc at the animal pole and yolk at the vegetal pole, *buc* and *macf1* mutant eggs show radially distributed cytoplasm around a centrally-localized yolk. Moreover, the primary defect in *buc* and *macf1* mutants is evident much earlier, specifically during the early Bb localization pathway in stage I oocytes (discussed further in next section). *buc* mutant oocytes fail to form the Bb and RNAs that are normally vegetally localized are instead unlocalized and remain dispersed in the cytoplasm. In contrast, in *macf1* mutants the Bb forms and RNAs localize to it, however, they fail to anchor to the prospective vegetal cortex and instead they remain in an apparent persisting Bb (Gupta

et al., 2010). Thus, Buc and Macf1 provide a molecular link to the early processes by regulating Bb assembly and disassembly.

Buckyball

The *buc* transcript and protein localize to the Bb in zebrafish and, after Bb disassembly, to the oocyte vegetal cortex (Figure 1.2A,B) (Heim et al., 2014; Riemer et al., 2015). Furthermore, Buc protein localizes to the germ plasm in the early embryo (Figure 1.1C) (Riemer et al., 2015), where it can increase PGC number in overexpression experiments (Bontems et al., 2009). So far, two Buc-interacting proteins have been reported: Rbpms2 (Hermes) (Heim et al., 2014) and Kinesin-1 (Campbell et al., 2015; Forbes et al., 2015). Rbpms2 is postulated to function with Buc in Bb formation, whereas Kinesin-1 plays distinct role in germ cell formation. Hence, Buc function connects the early stages of AV polarity and RNA localization with early developmental events of germ line specification.

Studies of the *buc* gene structure show the importance of the introns and 3' UTR to its function in AV polarity establishment. Several transgenes were generated containing either all or none of the *buc* gene introns (*gbuc* or *intronless-buc*, respectively), with a full-length or truncated 3' UTR (Heim et al., 2014). Analysis of eggs from *buc* mutant females carrying a single copy of a transgene showed that the egg AV polarity defect is rescued in a higher ratio using *gbuc* containing the full-length 3'UTR than the truncated version. These results suggest that the *buc*-3'UTR plays a regulatory role, possibly in its localization or translation, however, it is not essential, since some embryos were rescued to wild type. In *buc* mutants, the *buc-intronless* transgenes either

with the full-length or truncated 3'UTR could not rescue egg or oocyte polarity. In fact, these *buc-intronless* transgenes induced a partially penetrant dominant-negative (DN) effect, producing oocytes or eggs with no AV polarity. This DN effect is observed in a *buc* heterozygous or wild type background, with either *buc-intronless* carrying the full-length or truncated 3'UTR.

In another transgene construct where *buc-intronless* carries the original *buc*^{p106} mutation (*bucp106-intronless*) (Bontems et al., 2009; Marlow and Mullins, 2008), it fails to rescue *buc* mutants (Heim et al., 2014), as expected. However, unexpectedly this transgene, when homozygous, induces a DN effect in females. Furthermore, a *buc-intronless* transgene in a wild-type background can cause oocyte polarity defects and formation of what appears to be supernumerary Bbs (Heim et al., 2014). The protein and RNA constituents of these Bbs has not yet been determined but they look like typical Bbs by histological analysis. Additional studies will be needed to determine the nature of these ectopic Bbs: for example, if they arise due to incomplete coalescence of Bb precursors, to formation of new Bbs at distinct time points, or to fragmentation of a Bb. It will also be interesting to determine if these supernumerary Bbs disassemble at the cortex as in wild-type oocytes or if some or all do not, or do so abnormally leading to the AV egg defects observed in these mutants. If these supernumerary Bbs can disassemble and dock their contents to the cortex, one would expect it to lead to an expansion of vegetal pole identity, possibly at the expense of animal identity, the opposite phenotype to a *buc* loss-of-function mutant oocyte.

It is tempting to speculate that Buc may function and be regulated by mechanisms similar to those for the GP and oocyte posterior pole regulator Oskar (Osk) in *Drosophila*. In flies, *osk* mutant females produce embryos that lack PGCs and fail to form abdominal segments (Ephrussi et al., 1991). Like many other localized mRNAs, *osk* RNA relies on 3'UTR motifs for its proper localization, as well as a unique stem-loop sequence within the coding region, and splicing of the first intron. The first intron splicing assembles the exon junction complex (EJC) next to the stem-loop, which together are required for *osk* mRNA transport and posterior pole localization (Ghosh et al., 2012). The *buc-intronless* transgenes suggest the importance of the introns in *buc* regulation or function. However, additional studies will be required to determine the nature of the intron requirement, whether it be for *buc* RNA localization via EJC assembly as with *osk*, or instead due to transcriptional regulatory elements localized within an intron, or to facilitate mRNA transport out of the nucleus, or another mechanism.

Osk and Buc may have some homologous functions in GP assembly. In *Drosophila* at the oocyte posterior pole, *osk* RNA is translated, where accumulation of Osk protein enhances the recruitment of GP components that specify the germ line (Ephrussi and Lehmann, 1992; Glotzer et al., 1997; Jenny et al., 2006; Markussen et al., 1995; Staudt et al., 2005). Heim et al 2014, proposed a similar mechanism in zebrafish for Buc, whereby asymmetric/localized translation of *buc* leads to the recruitment of Bb-localized RNAs, including *buc* RNA, which further produces Bb-localized Buc protein in a positive feedback mechanism of Bb component entrapment and hence Bb formation. One major difference between Osk and Buc is that Osk can bind GP RNA components

directly, whereas Buc appears unable to do so and may rely on other interacting proteins to assemble RNA into the GP, like Rbpms2. Alternatively or in addition, a critical step in oocyte polarity may be Buc protein aggregation. In early stage I oocytes Buc protein is asymmetrically localized but not yet in a single aggregate (Elkouby et al., 2016; Heim et al., 2014), suggesting that a factor may mediate Buc aggregation or that Buc must accumulate to a particular level before it aggregates into a single bolus as the Bb.

The Bb is a large RNP granule that resembles other similar structures; like P-granules in *C. elegans*, polar granules in *Drosophila*, germ granules in germ cells and stress granules. RNP granules are non-membrane bound compartments that isolate its components from the cytoplasm. The Bb tightly aggregates RNAs- like germ cell determinants, proteins and mitochondria in the oocyte. How does Buc regulate Bb assembly? It's becoming more apparent that intrinsically disordered proteins (IDP), that lack a defined tertiary structure, bear properties that serve the assembly of the RNP granules. The MEG family of proteins, for instance, are IDPs that regulate the assembly of P-granules in *C. elegans* (Wang et al., 2014). Similarly, Buc and the frog homolog Xvelo, are both IDPs that regulate the assembly of the Bb RNP granule. Xvelo is highly concentrated in the Bb and assembles an amyloid like matrix in which Bb components are contained. Moreover, Xvelo contains a prion-like domain (PLD) within the N-terminal disordered region that is required for Xvelo localization to the Bb and assembly (Boke et al., 2016). The signals that drive the early Bb assembly by regulating Buc/Xvelo remain to be determined, however, like in P-granules assembly, where dephosphorylation of

MEG-1 and MEG-3 is the key event (Wang et al., 2014), it is possible that in zebrafish changes in the phosphorylation state of Buc/Xvelo regulates Bb formation.

Macf1: A cytolinker regulates Bb dissociation

Macf1 is the only factor known to regulate Bb disassembly. Macf1 is a conserved, giant cytolinker that can interact with all cytoskeleton components and functionally integrate them. In the absence of Macf1, the Bb fails to disassemble and, as a consequence, AV polarity is not established. In addition, the nucleus displays an acentric position in *macf1a* mutants. Thus, Macf1 functions in Bb RNP granule disassembly ensuring the establishment of AV polarity in the egg. Macf1 conserved function suggests a major role for the cytoskeleton in this process.

Macf1 is modular; it is expressed as multiple isoforms with distinct arrays of domains. For instance, Macf1 binds actin through its amino-terminal actin binding domain (ABD) that is composed of two calponin-homology (CH) domains; CH1 and CH2. Certain Macf1 isoforms contain only the CH2 domain and consequently bind actin with lower affinity (Bernier et al., 1996). Another mammalian isoform, Macf1b, is the only isoform that contains a Plakin repeat domain (PRD) for interaction with intermediate filaments (IF) (Lin et al., 2005). On the other hand, most *macf1* isoforms contain a Microtubule binding domain (MTBD) that associates with and stabilizes MTs (Karakesisoglou et al., 2000; Kodama et al., 2003; Subramanian et al., 2003). Macf1 domains operate as independent functional units to provide a range of actions in cytoskeleton integration. In addition to the cytoskeleton binding domains, Macf1 contains several spectrin repeats (SRs) that form linear rods ultrastructurally, giving length and

some flexibility to spectraplakins(Grum et al., 1999), and separating their functional domains, Macf1 also contains a Plakin domain that mediates interaction with desmosomes (Styers et al., 2006) (Smith and Fuchs, 1998) and a EF-hands (Ca²⁺ binding motif) that facilitates MT binding (Bottenberg et al., 2009).

In general, loss of Macf1 in different cell types, including zebrafish oocytes (Gupta et al., 2010), causes disorganized MTs (Karakesisoglou et al., 2000; Lee et al., 2000). In mice, Macf1 is essential for early development and mutant embryos die at gastrulation stage (Chen et al., 2006). In mammalian cells, Macf1 acts as a plus (+) tip MT-binding protein and mediates MT and actin integration at the cell cortex (Kodama et al., 2003; Wu et al., 2008). Keratinocytes require Macf1 for cell migration, where Macf1 integrates MTs and actin cables to maintain focal adhesions (Wu et al., 2008). In invertebrates, the *macf1* homologs *shot* (fly) and *VAB-10* (worm) have diverse functions in axon targeting, nuclear migration, epidermal attachment, and germ cell maintenance (Bosher et al., 2003; Bottenberg et al., 2009; Kim et al., 2011; Lee et al., 2000; Lee and Kolodziej, 2002a, b; Roper and Brown, 2004; Sanchez-Soriano et al., 2009; Subramanian et al., 2003). While the loss of *macf1* affects a variety of tissues and processes in different species, all share failures in cytoskeletal integration that disrupt cellular function.

In the *Drosophila* ovary, Shot, the Macf1 homolog in flies, is required for the organization of the fusome and for oocyte progression. The fusome is a membranous structure that extends between the cytoplasmic bridges of the 16 cells of the oogonial cyst and which functions in oocyte specification (Roper and Brown, 2004). Shot localizes

to the fusome, and functions to recruit MT for the transport of factors, including centrosomes, towards the oocyte. Shot in *Drosophila* probably acts much earlier during oogenesis than Macf1 in zebrafish, since the *macf1* mutant phenotype is visible only around mid-stage I of oogenesis, long after the oogonial cyst stage (Gupta et al., 2010).

In vertebrate oocyte development, microtubules (MT), actin, and intermediate-filament (IF) cytoskeletal components are all detected in different regions of the oocyte. Cytokeratins-a type of intermediate filament, for instance, is first detected in the Bb (Gard et al., 1997), and in the cytoplasm as oogenesis progresses in *Xenopus*. On the other hand, polymerized MT are not detected in the Bb and show intricate cytoplasmic networks in early and late stage *Xenopus* oocytes (Gard, 1991, 1992, 1999; Gard et al., 1995b). Actin distributes cortically and is present also intranuclearly (Gard, 1999; Gupta et al., 2010; Marlow and Mullins, 2008), (Figure 1.2B) (Gupta et al., 2010). Paradoxically, disruption of MT and actin filaments in early stage I oocytes does not affect Bb structure, nor the localization of RNAs to the Bb through the early localization pathway. Nevertheless, Macf1 function suggests that the cytoskeleton is relevant for the early pathway of RNA localization that includes the anchoring of RNAs to the vegetal cortex after Bb disassembly. While phosphorylation of MEG1 and 3 by kinases leads to P-granules disassembly, the signals that trigger Bb disassembly and ultimately define the vegetal pole of the oocyte are still unknown. Thus, elucidating Macf1 function in Bb disassembly will shed light into the unknown processes of cytoskeleton integration that are required for oocyte polarity establishment (Gard et al., 1997).

Macf1 functions in positioning the nucleus of the oocyte in a function that may also involve the cytoskeleton. Nesprins that reside in the outer NE also function in positioning the nucleus in diverse cellular contexts by interacting with the cytoskeleton. Nesprin 1 and 2 can directly interact with the cytoskeleton through their ABD, whereas the Nesprin-3 α isoform lacks the ABD and instead interacts in vitro with the ABD of Plectin and Macf1 (Wilhelmsen et al., 2005) (Postel et al., 2011). Nesprin interacts with the inner nuclear membrane Sun protein, which interacts with the nuclear lamina. Sun-Nesprin establish bridges spanning the nuclear envelope, connecting the nucleoskeleton with the cytoskeleton, referred to as the LINC (Linker of nucleo- and cyto-skeleton) complex (Mellad, Warren et al. 2011, Sosa, Rothballer et al. 2012, Sosa, Kutay et al. 2013)(Crisp et al., 2006; Meinke et al., 2011). The LINC complex is important for nuclear anchorage, nuclear migration, anchoring the MTOC to the nucleus, among other functions (Starr and Fridolfsson, 2010), suggesting that they may act similarly in the oocyte, which is also supported by the Macf1-ABD and Nesprin-3 interaction. Whether Macf1 and the LINC complex acts together in positioning the nucleus remains to be determined.

Spectraplakins are difficult to address functionally, since they are large proteins encoded by long transcripts with a variety of isoforms that challenge traditional cloning and transgenic techniques. Moreover, their function relies on the presence of specific functional domains that are cell type and context dependent. Fortunately, genome-editing approaches offer new possibilities to study them, including in zebrafish, where *macf1* loss of function does not cause embryonic lethality like in mammals (Kodama et

al., 2003). Thus, zebrafish oocytes offer a unique possibility to interrogate the requirement of Macf1 single modules in cell polarity. Such studies will help to understand the relationship between the cytoskeleton, the Bb and the RNA localization machinery that together drive AV polarity establishment during early oogenesis.

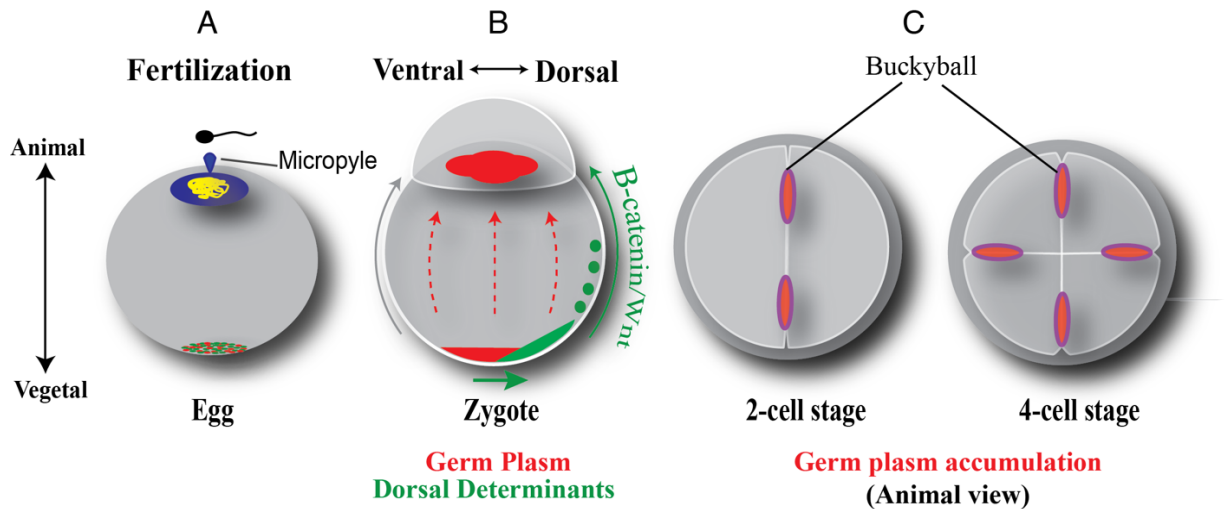


Figure 1.1: Function of localized maternal products.

Establishment of the AV axis in the egg defines the: A) sperm entry region, B) dorsal-ventral (DV) axis, and C) the location of the germ plasm, which specifies the PGCs. A) In frog, fish, and mouse, the oocyte nucleus migrates to the animal pole during oocyte maturation and extrudes the first polar body. Frog and fish eggs are fertilized in the animal half, and in zebrafish the sperm enters through the micropyle that forms at the animal pole. Following fertilization, the second polar body is also extruded at the animal pole. At the egg vegetal pole, the germ plasm (red) and dorsal determinants (green) are localized. B) Upon fertilization, dorsal determinants are transported from the vegetal pole to the future dorsal side of the embryo. Here, activation of the Wnt pathway specifies the dorsal fate. C) The germ plasm, including Bucky ball, accumulates at the cleavage furrows of the 2- and 4-cell stage embryo, illustrated for the zebrafish embryo here.

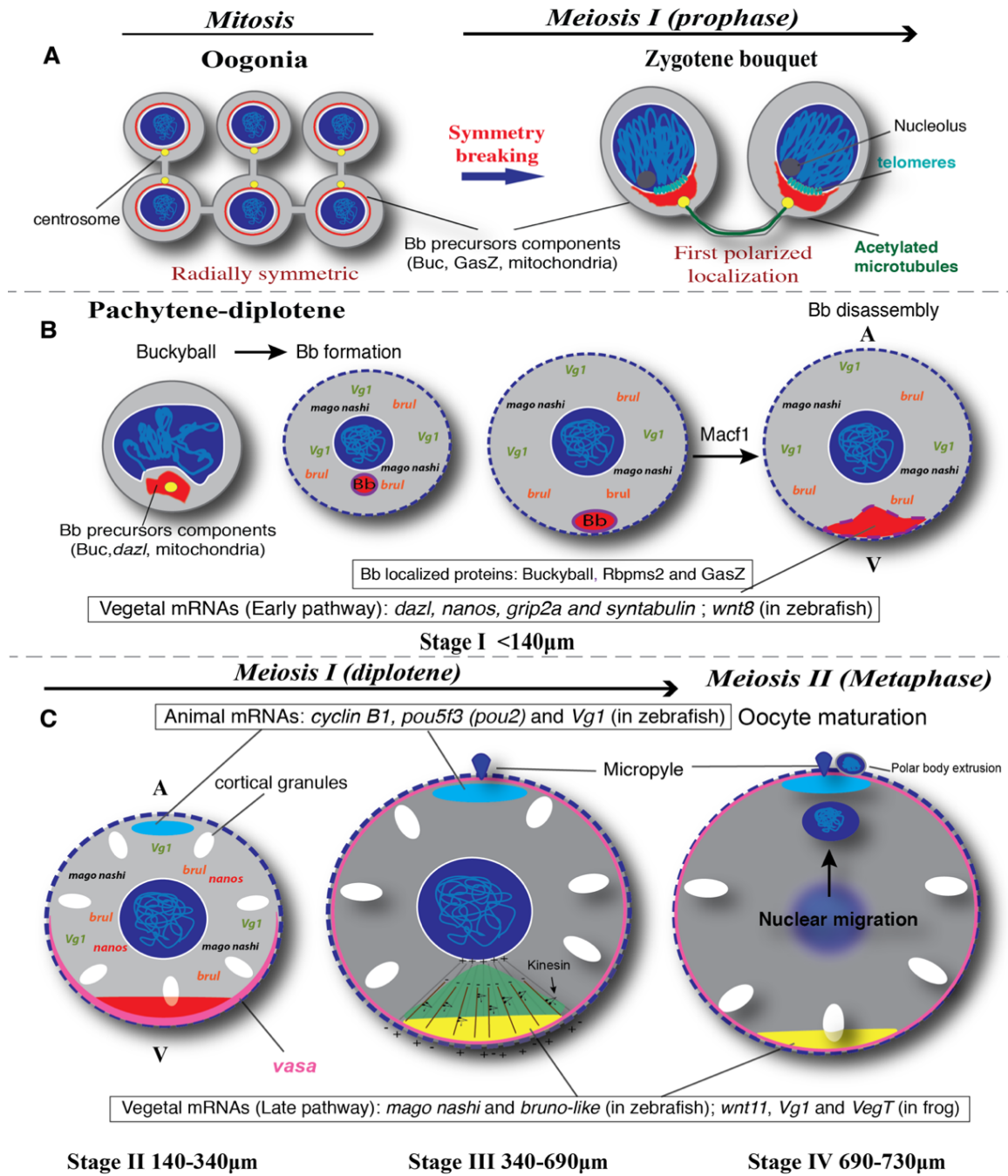


Figure 1.2: RNA localization and AV axis establishment during oogenesis.

A) In pre-meiotic oogonia, Bb precursors are distributed radially in the cytoplasm, telomeres are scattered intranuclearly, and the centrosome (yellow) is at a perinuclear position, possibly positioned facing the cytoplasmic bridge of the last mitotic division. When meiosis initiates, specifically during zygotene stages, Bb precursors (red) localize around the centrosome and adjacent to the telomere cluster (cyan) of the zygotene bouquet configuration. Thus, the nuclear axis of the bouquet configuration predicts the AV axis of the oocyte. At this stage, acetylated tubulin cables (dark green) form and may connect sister oocyte pairs through the cytoplasmic bridges of the last mitotic oogonial division (a pair is shown). B) At the subsequent pachytene stage, a nuclear cleft forms at the centrosome position where Bb precursors aggregate. The nuclear cleft remains throughout pachytene and early diplotene. In mid-diplotene, the nuclear envelope rounds out and the mature spherical Bb forms marking the position of the prospective vegetal pole of the oocyte. The formation of the Bb and its disassembly requires Bucky ball and Macf1 function, respectively. Hence, Bucky ball and Macf1 regulate RNA localization to the vegetal pole through the early pathway and are also required for AV polarity establishment. C) At stage II, Bb RNAs are localized to the vegetal pole (red). Distinct RNAs localize to the animal pole (light blue) and cortical granules (white ovoid) are formed. vasa RNA is broadly localized at the vegetal pole (pink) and expands radially cortically at subsequent stages. At stage III, previously unlocalized RNAs (yellow) are transported to the vegetal pole on microtubules tracks (brown) by the action of molecular motors (late pathway). Thus, at this stage early and late localized RNAs reside at the vegetal cortex (orange). During this stage, additional mRNAs (e.g. Vg1 in zebrafish) are localized animally (light blue) and the micropyle becomes evident at the animal pole. In stage IV, the oocyte matures, the nucleus migrates to the animal pole and the nuclear envelope disassembles in frogs, fish, and the mouse. At this stage, the oocyte transitions from diplotene of meiosis I to metaphase of meiosis II, extruding the first polar body at the animal pole in all 3 species.

Chapter 2 :

***Microtubule-Actin Crosslinking Factor 1 (Macf1) domain function in Balbiani body dissociation and nuclear positioning**

This chapter has been submitted for publication in Plos Genetics as: **Matias Escobar-Aguirre**, Hong Zhang, Allison Jamieson-Lucy and Mary C. Mullins. Microtubule-Actin Crosslinking Factor 1 (Macf1) domain function in Balbiani body dissociation and nuclear positioning

Summary

Animal-vegetal (AV) polarity of most vertebrate eggs is established during early oogenesis through the formation and disassembly of the Balbiani Body (Bb). The Bb is a large mRNP granule, conserved from insects to humans, composed of mitochondria, mRNA, and proteins. The components of the Bb, which have amyloid-like properties, include germ cell and axis determinants of the embryo that anchor to the vegetal cortex upon Bb disassembly. Our lab discovered in zebrafish the only gene known to function in Bb disassembly, *microtubule-actin crosslinking factor 1a* (*macf1a*). Macf1 is a conserved, giant multi-domain cytoskeletal linker protein that can interact with microtubules (MTs), actin filaments (AF), and intermediate filaments (IF). In *macf1a* mutant oocytes the Bb fails to dissociate, the nucleus is acentric, and AV polarity of the oocyte and egg fails to form. The cytoskeleton-dependent mechanism by which Macf1a regulates Bb mRNP granule dissociation was unknown. We found that disruption of AFs phenocopies the *macf1a* mutant phenotype, while MT disruption does not. We determined that cytokeratins (CK), a type of IF, are enriched in the Bb. We found that Macf1a localizes to the Bb and the nucleus, indicating a direct function in their regulation. We thus tested if Macf1a functions via its actin binding domain (ABD) and plectin repeat domain (PRD) to integrate cortical actin and Bb CK, respectively, to mediate Bb dissociation at the oocyte cortex. We developed a CRISPR/Cas9 approach to delete the exons encoding these domains from the *macf1a* endogenous locus, while maintaining the open reading frame. Our analysis shows that Macf1a functions via its

ABD to mediate Bb mRNP granule dissociation and nuclear positioning, while the PRD is dispensable. We propose that Macf1a does not function via its canonical mechanism of linking two cytoskeletal systems together in dissociating the Bb. Instead our results suggest that Macf1a functions by linking one cytoskeletal system, cortical actin, to another structure, the Bb, where Macf1a is localized. Through this novel linking process, it dissociates the Bb at the oocyte cortex, thus specifying the AV axis of the oocyte and future egg. To our knowledge, this is also the first study to use genome editing to unravel the module-dependent function of a cytoskeletal linker.

Introduction

Cellular polarity is the organization of intracellular space into cytoplasmic domains, and mediates cellular function across diverse cell types. For instance, oocytes are polarized in many species with the formation of the Balbiani Body (Bb) adjacent to the nucleus. The Bb is a large RNP granule conserved from insects to mammals that tightly aggregates RNAs, proteins and mitochondria. Like other RNPs, the Bb in vertebrates is a non-membrane bound compartment that isolates its content from the cytoplasm. In the early stage I oocyte, the Bb forms through the assembly of Bucky ball amyloid-like fibers that capture Bb components and give rise to a large Bb RNP granule (Boke et al., 2016; Bontems et al., 2009; Marlow and Mullins, 2008). Later, by the end of stage I, the Bb dissociates at the oocyte cortex and its components become docked at the now defined oocyte vegetal pole, thus, establishing the animal-vegetal (AV) axis of the oocyte and future egg, which in turn defines the anterior-posterior axis of the embryo (Escobar-Aguirre et al., 2016). Hence, elucidating the mechanism of Bb disassembly is

relevant to understanding two conserved and linked processes; the establishment of cell polarity and the disassembly of an amyloid-like structure such as the large Bb RNP granule.

The two proteins known to be necessary for Bb function in zebrafish, Bucky ball (Buc) and Microtubule-actin crosslinking factor 1a (Macf1a), were discovered via a zebrafish maternal-effect mutant screen in our lab. In eggs from *buc* or *macf1a* mutant females, the cytoplasm fails to segregate to form the blastodisc at the animal pole, and instead is radially distributed around the yolk (Dosch et al., 2004). Lacking AV polarity, development aborts shortly thereafter (Dosch et al., 2004). During early stage I of oogenesis, Bucky ball is required for Bb formation, and the *Xenopus* Buc ortholog, Xvelo, is the most abundant protein in the frog Bb (Boke et al., 2016). *buc* mutant oocytes lack a Bb and RNAs normally carried within the Bb are dispersed throughout the cytoplasm and never localize to the vegetal pole (Bontems et al., 2009; Heim et al., 2014; Marlow and Mullins, 2008). Xvelo self-aggregates *in vitro* and *in vivo* forming a matrix of amyloid-like fibers that is thought to entrap mitochondria to create the Bb. These amyloid-like aggregates are very stable and difficult to disrupt (Boke et al., 2016). However, the Bb naturally disassembles by the end of stage I of oogenesis. Macf1 is the only known functional player in this process. In *macf1a* mutant oocytes the Bb forms and accumulates RNA normally, however, the Bb becomes enlarged and never disassembles (Gupta et al., 2010). *macf1a* mutant oocytes also display an acentric nucleus phenotype. It is unknown if this phenotype is functionally linked to AV polarity and Bb disassembly. Understanding the role of Macf1 in Bb dissociation could provide

insight into the dissociation of similar amyloid-like aggregations in pathological conditions.

Macf1 is a conserved, giant cytolinker that can interact with all cytoskeleton components: microtubules (MTs), actin filaments (AF) and intermediate filaments (IF). Macf1 is modular in that distinct domains can interact with each of these cytoskeleton components, and it is expressed as multiple isoforms with diverse arrays of domains (Karakesisoglou et al., 2000; Kodama et al., 2003; Lin et al., 2005). Macf1 functions in a variety of tissues and processes in different species, all integrating the cytoskeleton in cellular functions. In mice, Macf1 is essential for early development and mutant embryos die during gastrulation (Chen et al., 2006). In mammalian cells, Macf1 acts as a plus (+) tip MT-binding protein and mediates MT and actin integration at the cell cortex (Kodama et al., 2003; Wu et al., 2008). Keratinocytes require Macf1 for cell migration, where Macf1 integrates MTs and actin cables to maintain focal adhesions (Wu et al., 2008). In invertebrates, the *macf1* homologs, *shot* (fly) and *VAB-10* (worm), have diverse functions in axon targeting, nuclear migration, epidermal attachment, and germ cell maintenance (Bosher et al., 2003; Bottenberg et al., 2009; Kim et al., 2011; Lee et al., 2000; Lee and Kolodziej, 2002a, b; Roper and Brown, 2004; Sanchez-Soriano et al., 2009; Subramanian et al., 2003).

How Macf1 interacts with the cytoskeleton to disassemble the Bb and establish oocyte polarity remains undetermined (Chang et al., 2004; Gard et al., 1997; Messitt et al., 2008). Technical constraints have restricted the study of *macf1*, since it is a large gene spanning ~300 kb of the zebrafish genome, with the longest predicted ORF of ~25

kb (NCBI: XP_001920094.1). Using transgenes for such large transcripts is difficult and subject to variable expression due to heterogeneous insertion sites. Thus, to unambiguously determine how Macf1 acts in AV polarity establishment, we targeted the *macf1* endogenous gene to address Macf1 domain function in its normal physiological context.

Here we investigated the localization and function of Macf1 and the cytoskeleton in regulating the Bb and oocyte nucleus positioning. We found that Macf1 and cytokeratins (a type of IF) localize to the Bb, and that Macf1 associates with actin at the cortex upon Bb disassembly. Disruption of cortical actin in late stage I oocytes causes detachment of Bb components from the cortex, partially phenocopying the *macf1* mutant. In contrast, disruption of MTs does not affect the Bb or nuclear positioning. Based on these results, we tested the hypothesis that Macf1 functions via its ABD and/or PRD (IF binding domain) to regulate Bb disassembly at the cortex. To test this, we used CRISPR/Cas9 genome editing technology to delete these domains by targeting the *macf1* endogenous gene. The method harnesses the modular structure of the Macf1 cytoskeleton-binding domains to specifically interrogate single Macf1 domain functions in Bb disassembly and nucleus positioning. Our results reveal that the Macf1 ABD is essential for Bb disassembly and correct nuclear positioning. Surprisingly, we found that the Macf1 PRD domain is dispensable for both of these processes. To our knowledge, this is the first study to use genome editing to precisely target the module-dependent function of a cytoskeletal linker.

Material and Methods

Ethics Statement

All animal studies were approved by the University of Pennsylvania Institutional Animal Care and Use Committee (Protocol number 804214). Animal care and use adhered to the National Institutes of Health Guide for the Care and Use of Laboratory Animals.

Fish lines

Ovaries were collected from 3 to 12 month old adult fish of TU wild type, *macf1a*^{p6cv} (Gupta et al., 2010), *macf1a*^{sa12708} (Sanger Center Mutation Resource), *buc*^{p106} (Bontems et al., 2009; Marlow and Mullins, 2008), *Tg(ef1a:dlk-GFP)* (Tran et al., 2012), *Tg(actb1:lifeact-GFP)* (Behrnt et al., 2012) and *Gt(macf1a-citrine)*^{ct68a} (Trinh le et al., 2011). For genotyping we used the following primers and PCR conditions:

macf1a^{p6cv} For: GCCGACGACCACTTTTAGAG Rev: CCTGTCTGCCATCCTCAAAC.

Denaturing: 94°C, 1:00 min. Annealing: 58°C, 45 sec. Extension: 72°C, 45 sec. X 30 cycles. PCR product wild type: 201bp, *macf1a*^{p6cv}: 170bp. Run in 3% agarose gel.

macf1a^{sa12708} KASPar™ genotyping following protocol of LGC Genomics (Smith and Maughan, 2015).

Gt(macf1a-citrine)^{ct68a} F: ACGTAAACGGCCACAAGTTC Rev:

AAGTCGTGCTGCTTCATGTG. Denaturing: 94°C, 1:00 min. Annealing: 60°C, 45 sec.

Extension: 72°C, 30 sec. X 30 cycles.

Fluorescence immunolabeling and RNA in situ hybridization

Ovaries were dissected from euthanized females and digested with 1.5 mg/ml collagenase I (Sigma-Aldrich) for 15 minutes in L-15 Medium (Sigma-Aldrich). Ovaries were fixed according to the acid fixation method (Fernandez and Fuentes, 2013) and kept overnight in 4% formaldehyde. Following washes in PBS, ovaries were kept in cold methanol at -20°C for at least 6 hours before use. For immunostaining, ovaries were washed and rehydrated in decreasing methanol percentages (75%, 50%, 25%) and washed finally in PBS 3 times (x). Ovaries were incubated in blocking solution containing PBS (0.3% Triton X-100, 1% BSA) for 1.5 to 2h. Primary antibodies were diluted in blocking solution and incubated overnight at 4°C. Ovaries were washed in blocking solution 4x15min and incubated with secondary antibodies in blocking solution for 90 min. Ovaries were washed in PBT (0.1% Triton) 4x15min and lastly incubated in PBT with DAPI (1:1000) and DiOC₆ (1ug/ml) (Calbiochem) for 1-2 h. Then they were washed in PBT 4x10min, transferred into vectashield (Vector labs) and mounted for imaging.

Antibodies

Buc antibody was developed by YenZym (San Francisco, CA, USA). Buc epitope: residues 1-15 MEGINNNSQPMGVGQ were used to generate rabbit polyclonal antibodies as described (Heim et al., 2014). Primary antibodies used were Buc (1:500), Macf1/ACF7 (1:100) (Karakesisoglou et al., 2000), CK type II (1:50) (Progen) and GFP (1:500) (Life Technologies) for staining of *Gt(macf1a-citrine)^{ct68a}* ovaries. Secondary

antibodies used were anti-rabbit IgG, or anti-mouse IgG1, Alexa 488, Alexa 594, Alexa 633 (all 1:1000, Molecular Probes).

In situ hybridization

Whole mount in situ hybridization was performed using the RNA-HCR method (Choi et al., 2010) following the company protocol (Molecular Instruments).

Confocal microscopy and image processing

Images were acquired on a Zeiss LSM 710 confocal microscope using a 40X lens. The acquisition setting was set between samples and experiments to: XYresolution= 512x512 pixels pinhole adjusted to 1.1 μ m of Z thickness, increments between stack images were 1 μ m, laser power and gain were set for each antibody. Acquired images were adjusted only in contrast/brightness. All Figure were made using Adobe Photoshop and Illustrator CC 2014.

Image quantification

Buc Bb/Buc Total ratio

We acquired confocal z-stacks encompassing the entire Buc signal and observed that Buc localized to the Bb showed greater signal intensity than Buc relocalizing to the cortex upon Bb disassembly. Using built-in filters in imageJ software we were able to segment the total Buc signal (Buc in the Bb and relocalized to the cortex) and separately the more intense Buc signal in the Bb only. Buc z-stack images were acquired as explained above and processed by subtracting background and applying a median filter (5 pixel radius). Then, we used imageJ software to create a z-projection of the images.

In these conditions, we applied the threshold check from the BioVoxxel toolbox and chose the Otsu and Intermode algorithms as the most accurate thresholds in segmenting total Buc and Buc in the Bb, respectively. Next, we measured the area segmented by each filter to calculate Buc Bb/Total Buc ratio. The oocyte area was calculated by segmenting the whole oocyte surface using the percentile algorithm in the DAPI channel. DAPI labels the follicle cell nuclei that surround the oocyte, and thus outline the oocyte, which was used to calculate the oocyte diameter. Due to the consistent, quality labeling of Buc, only when necessary were the thresholds adjusted manually.

Cytokeratin puncta measurements

Cytokeratin puncta were quantified using a MATLAB (Version 8.2.0.701 R2013b 64-bit, MathWorks) script. All images were pre-processed to reduce noise and to separate each oocyte into a single image. Cytokeratin positive puncta were identified using a simple threshold. The oocytes were sectioned into three regions (cytoplasm, nucleus, and Balbiani body) according to the intensity of DiOC₆ staining. Additionally, a region of just the perimeter of the cytoplasm was defined as any cytoplasm within one Balbiani-body-diameter of the cytoplasmic membrane. Puncta density was calculated as puncta per area for each region.

Live imaging of whole ovaries and isolated oocytes

Ovaries were dissected from adult fish (3 to 12 months) in L-15 media (60% in Hanks solution with gentamycin (50µg/ml) (Gibco)) supplemented with FBS (10%) and insulin (15µg/ml) at 28°C. In the media, further dissection of the ovary was performed to

isolate small pieces containing mainly stage I oocytes. The ovaries were placed in a glass bottom dish and embedded in low-melt agarose (0.5%) prepared in the media solution. The dish was filled with media solution containing MitoTracker (500 nM, Molecular Probes) for 2-3 hours, then the media was replaced once and ovaries kept in the media throughout the imaging.

Nocodazole, Latrunculin A and cold treatment

Nocodazole (50 μ M) (EMD Milipore) and latrunculin A (Sigma-Aldrich) (20 μ g/ml) were used to destabilize MTs and actin, respectively. When live imaging began, ovaries had been exposed to the drugs in the incubation media for no longer than 15-20 min. The control group was treated with DMSO in the same conditions. We used Mitotracker staining to monitor oocyte health and viability during the treatment.

For analysis of LatA treatment in fixed samples, ovaries from the same fish were divided into Latrunculin A (Sigma-Aldrich) (20 μ g/ml) and DMSO treated groups with two replicates for each condition. We tested incubation times of 6, 12 and 20 hours. After the treatment, ovaries were fixed as above and stained for Buc. We measured the oocyte diameter and analyzed the effect of LatA treatment only in stage I oocytes.

For cold treatment, ovaries were dissected as explained previously; ovaries were kept in culture media, and divided in tubes placed in ice in a cold room (4°C) and incubator at 28°C for 120min, then ovaries were fixed and processed for immunostaining.

macf1a cDNA sequencing

To generate *macf1a* cDNA we used the Superscript First-cDNA synthesis system (Invitrogen). First, using the *macf1a* predicted sequence (~25 kb) (NCBI: XP_001920094.1), primers were designed to amplify a large piece of *macf1a* cDNA (~19 kb) made from ovary RNA. Forward: CCACCGAAAAACAGGAGAACAC; Reverse: GCTCCACTTGAAACCTCTTCGC. Instead a ~6.5 kb product was obtained that was cloned into pCR-XL-TOPO (Invitrogen) (kindly provided by Tripti Gupta). We sequenced the 6.5 kb cDNA and found that it contained three regions from the *macf1a* predicted cDNA sequence: bp 3767- 4482, 12314-15370 and 20453-23180. The 4482-12314 gap corresponds to exon 35-39; exon 35 contains the Macf1a PRD (~7 kb) domain. We amplified from ovary cDNA ~1.5 kb of exon 35 (NCBI:XP_001920094.1) using primers from exon 35 and flanking exon 34. We also amplified and sequenced exon 39, but we did not test exons 36-38. In the ~25 kb predicted transcript (NCBI: XP_001920094.1), 29 spectrin repeats are predicted. We identified 13 spectrin repeats in the 6.5 kb cDNA spanning sequences 12314-15370, and another 13 were identified in cDNA by sequencing the gap in the 6.5 kb cDNA between 15370-20453 bp, corresponding to exons 57-75, for a total of 26 spectrin repeats. To complete the *macf1a* cDNA, we performed 5' RACE, amplifying overlapping fragments upstream of 3955 bp of the 25 kb predicted transcript (NCBI:XP_001920094.1) to assemble a fragment containing the *macf1a* ABD and Plakin domains. Using 3' RACE from the 23,180 bp position, we assembled a fragment containing the MTBD (~3 kb).

CRISPR/Cas9 Genome editing

macf1a deletion mutants were created using CRISPR-Cas9 mediated mutagenesis. The intron targets selected conserved the *macf1a* ORF and contained a PAM sequence for Cas9 targeting. The sgRNAs to target *macf1a* introns were purchased from the University of Utah Mutation Generation and Detection Core, which cloned them into plasmids containing an upstream T7 promoter and flanked by a *Dra*I restriction site. To synthesize sgRNAs, we used the T7 MEGAshortscript kit (Ambion) and a clean-up step with MEGAclear kit (Ambion), following the manufacturer's protocol. For injections, we mixed sgRNAs (Table 1) and Cas9 protein (180-200 pg) (purchased from the University of Utah Mutation Generation and Detection Core for Crispr reagents) and injected 1.2-1.5 nl of the CRISPR mix into one-cell stage zebrafish embryos. At 24 to 48 hpf, a fraction (~25%) of the injected embryos were euthanized and DNA was extracted. We performed HRMA analysis on single embryos using MeltDoctor HRM Master Mix (Applied Biosystems) to determine the mutation rate, and PCR analysis to detect genomic deletions. When a high (~80-100%) mutation rate was obtained, the remaining injected embryos were raised to adulthood and then outcrossed to screen for germline transmission of deletion mutations by PCR analysis.

HRMA primers:

Intron 3. Product: 120bp.

Forward (For) AACCTGTTGGTTCCATTTGAAGTAT

Reverse (Rev) GATTTGCTCAACCCCTTGCTCA

Intron 5. Product: 132bp

For TGCAGCAGACTGGAGATGAA

Rev GGATAGAGAGGAAGCCCGGA

Intron 8. Product: 127bp

For CCAGAGCAGAACAAACCCTA

Rev TGAACAAATCATTGCAGATG

Intron 34. Product: 109bp

For AGTCAGTTCCGGGCAGCATA

Rev ACACACTGATCGAGGTTTCGG

Intron 38. Product: 167bp

For GCATACGTGGACATACGTGA

Rev GTCCAGGTTCTGATTGGCTG

For PCR deletion analysis, we combined three primers to amplify the wild type and mutant alleles. PCR conditions:

Denaturing: 94°C, 1:00 min

Annealing: Primers 1) and 2) 59°C, 45 sec; 3) 58°C, 1 min.

Extension: 72°C, 45 sec

X 30 cycles.

1) Deletion ABD (CH1) primers: wild type: 420bp; deletion: 520bp.

Intron 3 For TTCCACATCTGGGTTTGTGT

Intron 3 Rev TCTCAGGCTGAAACACATCTGA

Intron 5 Rev CTGGATGAGGACAGGAGGGA

2) Deletion ABD (CH1-CH2) primers: wild type: 420 bp; deletion: 505 bp.

Intron 3 For TTCCACATCTGGGTTTGTGT

Intron 3 Rev TCTCAGGCTGAAACACATCTGA

Intron 8 Rev CATAACAGCCTCTTCACCACTGT

3) Deletion PRD primers: wild type: 420 bp; deletion: 505 bp.

Intron 34 For CTAACAGCTGCCGGGAGAAA

Intron 34 Rev ACACACTGATCGAGGTTTCGG

Intron 38 Rev AATAGTGCCTCTGCTCTGGC

sgRNA scaffold sequence:

[GTTTTAGAGCTAGAAATAGCAAGTTAAAATAAGGCTAGTCCGTTATCAACTTGAAAA
AGTGGCACCGAGTCGGTGCT]

Target site sequences:

macf1 Intron 3: [GACATGGACTTCTTAC**ATGG**]

macf1 Intron 5: [GTGTCTACCAGTGAGAG**GCAG**]

macf1 Intron 8 (reverse strand): [TACAGATGGCCACAGG**TAAG**]

macf1 Intron 34 (reverse strand): [GGTGCGATAGGGTGAG**AAGC**]

macf1 Intron 38 (reverse strand): [GGTCGTGGAGAGCTATA**AACA**]

Results

In the zebrafish genome two paralogs of *macf1* are present, *macf1a* and *macf1b*. *macf1a* is expressed during oogenesis and a mutation in *macf1a* causes the AV oocyte and egg polarity phenotype reported previously (Gupta et al., 2010) and is the focus of this study. The largest predicted *macf1a* open reading frame (ORF) in zebrafish is very large: ~25 kb, encoding a protein of ~8,000 amino acids (NCBI: XP_001920094.1). To determine the domain composition of *macf1a* transcripts in oogenesis, we sequenced *macf1a* cDNA from the ovary. We detected all predicted cytoskeleton interaction domains and other conserved domains typical of Macf1 in *macf1a* ovary cDNA, including the N-terminal ABD followed by the Plakin domain, 29 Spectrin repeats, and at the C-terminus, two EF-hands (Ca²⁺ binding motif) and a GAS2 MTBD for MT interaction (Figure 2.1A).

The predicted ORF (NCBI: XP_001920094.1) of gene *macf1a* also contains the PRD domain between the Plakin domain and the Spectrin repeats, similar to the *macf1b* isoform in the mouse (Lin et al., 2005) (Figure 2.1A). Like the mouse *macf1b* isoform, the PRD domain in zebrafish is contained in one large exon (exon 35) of ~7 kb. Since it is challenging to isolate 7 kb cDNA products without amplifying genomic DNA for this large exon, we instead used a primer in flanking exon 34 and an exon 35 primer to amplify part of exon 35 from ovary cDNA. We sequenced ~2 kb from each side of the PRD showing that it is expressed during oogenesis (Figure 2.1A). Importantly, we also sequenced a cDNA that lacks the PRD and 13 Spectrin repeats; in this transcript exon 34 is joined to exon 40, as well as 56 to 76, indicating that alternative splicing generates

a transcript lacking exons 35-39, and 57-75 (Figure 2.1A, transcript variant). This indicates that more than one *macf1a* isoform in the ovary is generated, as also reported in the mouse (Karakesisoglou et al., 2000; Lin et al., 2005). Altogether, we detected all Macf1a functional domains in *macf1a* cDNA, including the PRD, encompassing 94 of the 98 predicted exons (Figure 2.1A) of the longest *macf1a* ORF.

We previously isolated the *macf1a*^{p6cv} allele (Dosch et al., 2004), which is a 31 bp deletion causing a frameshift in the ORF (Gupta et al., 2010). For this allele, the C-terminal half of the protein is predicted to be truncated at amino acid 5315 of the longest predicted zebrafish Macf1a isoform (>8000 amino acids) by a premature stop codon (Figure 2.1A, *p6cv* (stop)) (Dosch et al., 2004; Gupta et al., 2010) (NCBI: XP_001920094.1). We obtained a second *macf1a* mutant allele from the Sanger Zebrafish Mutation Project (<http://www.sanger.ac.uk/science/collaboration/zebrafish-mutation-project>), *macf1a*^{sa12708}, which shows an indistinguishable phenotype to *macf1a*^{p6cv} mutants, including Bb enlargement, failure of Bb disassembly, and acentric positioning of the nucleus (Figure 2.1B). The new allele is a nonsense point mutation affecting codon 553 near the N-terminus of Macf1a (Figure 2.1A, *sa12708* (stop)). These two alleles contain premature stop codons at very different locations in the ORF and yet display the same defects, which provides strong evidence that both are strong loss-of-function or null alleles.

Macf1a is essential in *Buc* relocalization from *Bb* to oocyte cortex

The Bb progresses during stage IB of oogenesis from its initial location adjacent to the nucleus, to the oocyte cortex by late stage IB where it disassembles. To

characterize this process in *macf1a* mutants, we followed protein and RNA markers of the Bb in mutant and wild type (WT) stage IB oocytes ranging from ~50 to 140 μm in diameter (Selman et al., 1993). The Bb markers we selected were Buc, the only protein known to be required for Bb formation in vertebrates, and *dazl*, an mRNA component of the germ plasm (Figure 2.1B-D). To examine *dazl* RNA localization, we used the highly sensitive hybridization chain reaction (HCR) method that allows detection of low RNA concentrations with minimal background (Choi et al., 2010). We observed that Buc is recruited to the Bb in the absence of Macf1a (Figure 2.1D'-D''), similar to *dazl* and other previously examined Bb components (Ge et al., 2014; Gupta et al., 2010) (Figure 2.1B). Unlike in WT, in *macf1a* mutants Buc and *dazl* fail to localize to the vegetal cortex and instead remain in a persistent and enlarged Bb (Figure 2.1B-D).

We used the Buc immunofluorescence localization pattern to quantify the progression of Bb disassembly during stage I of oogenesis in WT and *macf1a* mutant oocytes (Figure 2.1C-D''). In late stage IB WT oocytes, as the Bb disassembles at the cortex (Figure 2.1C'), Buc dissociates from the Bb and localizes to the vegetal cortex (Figure 2.1C''). To quantitatively evaluate Bb disassembly, we identified the Bb by Buc immunostaining, then compared the signal intensity of Buc within the Bb (Figure 2.1E) versus outside the Bb (Figure 2.1E') during disassembly (see methods). We measured the total Buc immunofluorescence area versus Buc localized to the Bb to estimate a Bb disassembly ratio (Bb Buc/Buc total) along with oocyte diameter throughout stage I (Figure 2.1F). In 60 micron (μm) early stage IB oocytes (Figure 2.1C) when the mature, compact Bb has formed (Elkouby et al, 2016), the Buc disassembly ratio is ~1. This ratio

decreases to ~0 towards the end of stage I when the Bb disassembles and Buc is unloaded at the cortex (Figure 2.1F).

Using this method, we found that the Bb disassembles progressively and reached the midway point (0.6 to 0.4 Buc disassembly ratio) in oocytes 115 to 125 μm in diameter (Figure 2.1F). In the largest WT IB oocytes (135 to 160 μm in diameter) the disassembly ratio was 0.15. In contrast, the Bb disassembly ratio in *macf1a*^{p6cv} and *macf1*^{sa12708} mutant oocytes of a similar diameter range did not appreciably decrease below 1 (Figure 2.1F, red squares and green triangles). These results demonstrate that Macf1a is essential to dissociate the Bb RNP granule and relocalize Buc, the essential Bb-forming protein, from the Bb to the cortex to establish AV oocyte polarity. Furthermore, this analysis indicates that the Bb does not dissociate during a short window of time, but rather disassembles over a period of oocyte growth that corresponds to an almost 2-fold increase in volume (from 120 μm to 145 μm diameter).

Macf1a functions independently in Bb disassembly and nucleus positioning

Mutant *macf1a* oocytes display both an asymmetrically positioned nucleus and a Bb dissociation defect. These defects may represent two independent functions of Macf1a, one in Bb disassembly and one in nuclear positioning, or one of the defects may be a secondary effect caused by the other defect. For example, the enlarged, persistent Bb of *macf1a* mutants could displace the nucleus, causing it to become acentric. To determine if the Bb defect causes the nucleus to become asymmetric, we generated double mutants of *macf1a* and the *buc* mutant, which never forms a Bb. We hypothesized that if Macf1a functions independently in Bb disassembly and nuclear

positioning, then a *buc*^{p106re};*macf1a*^{p6cv} double mutant should display an absence of the Bb and a nuclear positioning phenotype. However, if the Bb is absent and the nucleus is no longer acentric in the double mutant, then the nuclear defect can be considered a secondary effect of the Bb defect in *macf1a* mutants. We analyzed *buc*;*macf1a* double mutant oocytes and found that the Bb was absent, while the acentric nuclear phenotype remained (Figure 2.2A-H). These results strongly support Macf1a functioning independently in Bb disassembly and nuclear positioning.

We next tested if Macf1a regulates Bb disassembly and nucleus positioning directly by associating with the Bb and nucleus or if it acts via an indirect mechanism, for example, by localizing to the oocyte cortex and regulating these processes. To investigate this question, we examined the intracellular localization of Macf1a protein in stage I WT oocytes using an antibody against mouse Macf1 (Karakesisoglou et al., 2000) and took advantage of a zebrafish gene trap line, Gt(*macf1a-citrine*)^{ct68a}, inserted in a *macf1a* intron between exon 57 and exon 58 (Figure 2.1A) (Trinh le et al., 2011). Using the Macf1 antibody, we found that Macf1a localizes to the Bb and intranuclearly (Figure 2.3A). Importantly, no immunostaining was observed in the *macf1a*^{sa12708} mutant allele, indicating the specificity of the antibody to Macf1a (Figure 2.3D). In later stage I oocytes, Macf1a localization recapitulated the dynamics of Bb disassembly at the vegetal cortex, progressively dissociating from the Bb and localizing to the oocyte cortex (Figure 2.3A-C). The Citrine insertion into Macf1a also showed similar localization to the Bb and followed its dynamics (Figure 2.3E-G), though seems not to recapitulate the nuclear distribution we observed with Macf1 antibody. It is possible that certain Macf1

isoforms localize to the nucleus and those, among others, splice out the citrine exon. Importantly, these results support a model where Macf1a functions directly in the Bb to regulate its dissociation and anchoring to the oocyte cortex. Macf1a localization to the nucleus suggests a direct role for it in positioning the nucleus.

Actin required for Bb cortical attachment and nuclear positioning, whereas MTs dispensable

Macf1a contains binding domains for several different cytoskeletal elements and acts to integrate cytoskeletal systems in other models, thus we expect that Macf1a interacts with the oocyte cytoskeleton to regulate Bb dissociation and nuclear positioning. To determine which cytoskeletal components interact with Macf1a, we examined the distribution of actin and MTs in stage I oocytes. With this purpose, we performed live imaging experiments using the transgenes Tg(*actb1:lifeact-GFP*) (Behrndt et al., 2012) and Tg(*ef1a:dclk-GFP*) (Tran et al., 2012) to visualize actin and MTs, respectively. Actin appeared as a thick cortical layer and intranuclearly, as shown in live and fixed samples (Figure 2.4A-B; 2.5 A-B) (Gupta et al., 2010). In agreement with previous reports on fixed tissue in *Xenopus* (Gard, 1991), MT networks in live oocytes were present throughout the cytoplasm and were enriched perinuclearly (Figure 2.5 G-L). However, neither actin (Figure 2.5A) nor MTs (Figure 2.5 G-L) appeared enriched in the Bb in stage IB oocytes, though we detected stable MTs (acetylated) (Figure 2.5O) in the Bb (10/25 oocytes), they did not distribute preferentially in the Bb.

We then tested the function of cytoskeletal components in stage I oocytes using pharmacological inhibitors. To test actin function, we disrupted actin filaments with

Latrunculin A (LatA) and evaluated whether this affected the Bb and/or nuclear positioning. We determined that after 6 hours (h) (Figure 2.4C, G) actin filaments were moderately affected, and only after 10-12h of LatA treatment (Figure 2.4A-B, D, I), were actin filaments greatly reduced. We treated ovaries with LatA for 12h and a longer treatment of 20h, then fixed and stained for Buc. After 12h of LatA treatment (Figure 2.4F, J), we observed in a few oocytes an effect in which Buc appears detached from the oocyte cortex (Figure 2.4J) (4/22 oocytes) and some oocytes displayed an acentric nucleus (3/22 oocytes). However, after 20h of LatA treatment these effects are stronger, while in control conditions the Bb remains at the cortex (Figure 2.5C-D), in LatA treated oocytes the Bb appears closer to the nucleus as in a pre-disassembly stage (Figure 2.5E-F). Additionally, the nucleus was acentric in many oocytes (15/40 oocytes) (Figure 2.5F). Thus, disruption of actin partially phenocopies the *macf1a* mutant phenotype, suggesting that Macf1a may interact with cortical actin to mediate Bb disassembly and nuclear positioning.

We addressed MT function in live imaging by treating ovaries with nocodazole for 2 (Figure 2.5 G-H) and 10 h (h) (Figure 2.5 I-L) and by incubating them at 4°C to also depolymerize stable MTs (Figure 2.5 M-T). In both cases, we found that depolymerization of MTs did not affect the Bb or nuclear positioning. This suggests that MTs do not play a role in regulating the Bb structure, nuclear positioning or in cortical attachment like we observed for actin.

Finally, we examined the distribution of IF using a Pan-Cytokeratin (CK) type II antibody. We found that CK was distributed in a punctate pattern in the Bb and cortically

in stage 1B oocytes (Figure 2.6A). We quantified the CK distribution using a custom MATLAB program and found that CK puncta density is significantly enriched in the Bb (3-fold increase) compared to the cytoplasm (Figure 2.6C-D). Interestingly, in *macf1a* mutants CK puncta were still detected in the Bb (Figure 2.6B-C). However, CK and the Bb were not present at the cortex, and instead CK accumulated around the nucleus, similar to the detachment of other components from the cortex in *macf1a* mutants (Figure 2.6B). Thus, Macf1a may function in Bb disassembly via integrating CK in the Bb to actin at the cortex.

Genome editing approach to interrogate Macf1a functional domains

The modular domain structure of Macf1a allows us to interrogate Macf1a by targeting specific cytoskeleton-binding functions. We postulated that Macf1a mediates Bb disassembly by binding cortical actin via its Actin binding domain (ABD) and by binding CK within the Bb via its Plectin repeat domain (PRD), integrating the cortical actin and CK and therefore disassembling the Bb at the oocyte cortex. Results supporting this hypothesis are that CK and Macf1a are both enriched in the Bb and actin depolymerization disrupts Bb cortical anchoring. In addition, because we observed Macf1a localized to the nucleus and disruption of actin causes acentric nuclear positioning, the Macf1a-ABD may be required to position the nucleus in the oocyte. To interrogate Macf1a-ABD and -PRD function in oocyte polarity, we developed a CRISPR/Cas9 approach to make large deletions in the endogenous *macf1a* gene. We designed sgRNAs targeting the introns flanking the ABD and the PRD encoding exons to remove each domain (Figure 2.8, and see methods). Importantly, the deleted exons did

not alter the reading frame of the *macf1a* ORF. Our strategy (Figure 2.7) was to first inject each sgRNA singly with Cas9 protein into 1-cell stage embryos to confirm high frequency cutting. Cutting efficiency was assayed by PCR amplification of genomic DNA spanning the target site, followed by high resolution melt analysis (HRMA) of the PCR product (Dahlem et al., 2012). We increased the amount of sgRNA injected until every embryo showed CRISPR-induced HRMA shifts (Table1). Then we targeted specific *macf1a* domains by simultaneously injecting two sgRNAs with Cas9 into 1-cell embryos. We optimized the sgRNA concentration to obtain high frequencies of deletions without embryo abnormalities. We detected the deletions by PCR analysis of genomic DNA, then sequenced the PCR products to confirm that deletions were consistent with our predictions. We raised F0 injected fish and tested for germline transmission in F1 embryos (Table 1, Figure 2.7).

The Macf1a-ABD is composed of two calponin-homology (CH) domains: CH1 and CH2. Macf1a isoforms can contain either the full ABD with CH1-CH2 or the CH2 domain alone (Bernier et al., 1996), so we designed CRISPR deletions of the CH1 domain and both CH1-CH2. To delete *macf1a*-ABD(CH1) we targeted introns 3 and 5, deleting exons 4 and 5, which spans 70% of the CH1 coding sequence (Figure 2.8B). To delete *macf1a*-ABD (CH1-CH2) we targeted introns 3 and 8, removing exons 4-8, which encompass 85% of the entire *macf1a*-ABD (Figure 2.8B). We succeeded in deleting 10.3 kb and 17.8 kb of genomic DNA to remove the Macf1a-ABD(CH1) and the Macf1a-ABD(CH1-CH2) through germ line transmitted mutations (Figure 2.8 A-C).

The Macf1a-PRD is entirely contained within exon 35 (NCBI: XP_001920094.1). We targeted the immediately preceding intron 34; however, due to the small size of introns 35-37, and to preserve the transcript ORF, we chose intron 38 as the second CRISPR target for deleting the PRD (Figure 2.8C). Importantly, the 174 amino acid region encoded by exons 36-38 that were targeted for deletion does not appear to include key components of Macf1a functional domains (based on a SMART domain prediction). We succeeded in deleting 9.1 kb of genomic DNA to remove the Macf1a-PRD in a germ line transmitted allele (Figure 2.9).

From the *macf1ΔABD* mutant we sequenced ovary cDNA spanning exons 3 to 8 that encode the ABD and confirmed the lack of the intended exons in *macf1ΔABD* (CH1) and *macf1ΔABD* (CH1-CH2) (Figure 2.8A, B, 2.9A). For the PRD, we detected in both WT and *macf1aΔPRD* mutant oocytes a small RT-PCR band (~750 bp) (Figure 2.9C) that sequence analysis showed corresponds to an alternatively spliced transcript that does not include exons 35-39, as discussed above (*macf1a* cDNA results). In addition, we detected a larger band (970bp) only present in the *macf1ΔPRD* mutant that sequence analysis showed is generated by the deletion of exons 35 (PRD) to 38. We amplified ~1.5 kb from the flanking exon 34 into exon 35 in WT (confirmed by sequence analysis), which was absent in *macf1aΔPRD* *-/-* mutants (Figure 2.9C). Together, these results confirmed that we deleted the PRD from the *macf1a* endogenous locus and, generated a transcript lacking the Macf1a-PRD.

In summary, we deleted the exons encoding the Macf1a ABD and PRD from the *macf1a* gene by using CRISPR/Cas9 technology. The transcript produced from the

genome-edited mutants lack these specific domains but preserve the *macf1a* transcript ORF.

Macf1a-ABD is essential for Bb disassembly and nuclear positioning

To determine the role of the Macf1a ABD in Bb progression and nuclear positioning, we analyzed the ovaries of *macf1a* Δ *ABD* deletion mutants. To be able to examine the phenotype in the F1 generation, we crossed *macf1a* deletion mutant heterozygous females to *macf1a*^{sa12708} heterozygous mutant males to obtain 50% transheterozygous (Figure 2.7) ovaries expressing Macf1a mutant protein lacking the CH1 domain (*macf1a* Δ *ABD(CH1)*/*macf1a*^{sa12708}) or the entire ABD (CH1-CH2) (*macf1a* Δ *ABD(CH1-CH2)*/*macf1a*^{sa12708}). We found that in both cases the oocytes display a fully penetrant *macf1a* null mutant phenotype; the nucleus is acentric and the Bb fails to disassemble (Figure 2.10A). In the next generation (F2), the *macf1a* Δ *ABD(CH1-CH2)* homozygous mutant shows a *macf1a* null phenotype in the ovary, whereas in *macf1a* Δ *ABD(CH1)* homozygous the *macf1a* null phenotype is not fully penetrant in the ovary (Figure 2.10A). Importantly, the Macf1a mutant protein (Macf1a Δ *ABD(CH1)*) is localized to the Bb in the mutant as in WT, and it shows similar levels of expression in immunostaining (Figure 2.10B).

Similar to the *macf1a*^{sa12708} mutant phenotype, Buc remains localized in the persisting, enlarged Bb of *macf1a* Δ *ABD(CH1)*/*macf1a*^{sa12708}, *macf1a* Δ *ABD(CH1)*, *macf1a* Δ *ABD(CH1-CH2)*/*macf1a*^{sa12708} and *macf1a* Δ *ABD(CH1-CH2)* oocytes (Figure 2.10A). AV

polarity establishment is also affected in these mutants (2.11) (Table 2). The incomplete penetrance of the mutant phenotype in *macf1a*^{ΔABD(CH1)} ovaries is consistent with that observed in the eggs phenotype, and suggest that in certain conditions Macf1a with only the CH1-ABD is not sufficient for Macf1 function in the oocyte and egg (see discussion)(Figure 2.10C, table2). These findings showing the requirement of Macf1 ABD support a mechanism of Macf1 mediating Bb RNP granule dissociation at the cortex, nuclear positioning, and that is essential for defining the AV axis (Figure 2.12 model).

Unexpectedly, when we analyzed the ovaries of the *macf1a*^{ΔPRD} / *macf1a*^{sa12708} and *macf1a*^{ΔPRD} deletion mutants, which lack the domain that can interact with IF, Bb disassembly was not affected (Figure 2.10A). In *macf1a*^{ΔPRD} mutant oocytes, Buc localizes to the Bb normally and the nucleus is centrally located as in WT. Furthermore, eggs from *macf1a*^{ΔPRD} / *macf1a*^{sa12708} and *macf1a*^{ΔPRD} mutant females (2.11B, table 2) display normal AV polarity and development. These results show that the Macf1a-PRD is not required to localize Macf1a to the Bb or to disassemble the Bb RNP granule. Thus the Macf1a-PRD is dispensable for Macf1a function in AV polarity and nuclear positioning.

Discussion

Macf1a may function as a non-canonical linker

Macf1a is a cytolinker that integrates cytoskeleton components in different cellular contexts (Alves-Silva et al., 2012; Karakesisoglou et al., 2000; Kodama et al., 2003; Sanchez-Soriano et al., 2009; Wu et al., 2008); however, a function for Macf1a in dissociating a large mRNP granule like the Bb is unprecedented, and so it is unclear how it may integrate MTs, actin, or IFs in Bb disassembly. Here, we developed a novel approach to unravel Macf1a domain-dependent function by interrogating, for the first time, the very large endogenous *macf1a* gene through CRISPR-Cas9 mediated exon deletions (Figure 2.8). We found that the Macf1a ABD is essential for Bb disassembly, whereas the IF interacting domain of Macf1a, the PRD, is dispensable. Since we did not detect MT enrichment in the Bb, nor a defect when MTs were depolymerized (Figure 2.5I-V), it is possible that Macf1a does not function as a cytoskeletal linker in this context. Rather it may link Bb components to the oocyte cortex through its ability to bind cortical actin and localize to the Bb (Figure 2.12). Thus, it may function to link two structures together, but not through its canonical cytoskeletal specific cross-linking function.

Macf1a in Bb disassembly, IDPs, and P granules

C. elegans P-granules have become an excellent model for studying the assembly/disassembly dynamics of RNP granules. P granules form via the assembly of MEG proteins, which are intrinsically disordered proteins (IDPs) acting like a scaffold for P granule condensation (Wang et al., 2014). MEG is the target of kinases and

phosphatases that regulate the disassembly and assembly of P granules, respectively, and are crucial in establishing the anterior-posterior axis of the embryo (Brangwynne et al., 2009; Wang et al., 2014). Similarly, Buc and its ortholog in *Xenopus* Xvelo are IDPs functioning in Bb RNP granule formation. The N-terminal region of Xvelo contains a prion-like domain required for Xvelo assembly in an amyloid-like matrix that can enclose Bb components (Boke et al., 2016). In zebrafish oocytes, Bb cortical disassembly defines the future oocyte and egg vegetal pole, and Macf1a is the only known factor to function in this process. Our data show that Buc remains localized in a persistent Bb in *macf1a* mutants, suggesting that Macf1a either directly triggers Bb disassembly at the cortex or is required to mediate Bb component interaction with cortical factors that trigger Bb disassembly.

Our results show that deletion of the Macf1a (CH1) domain in an otherwise intact Macf1a protein that localizes to the Bb causes a failure in Bb RNP granule dissociation. These defects are indistinguishable from those of the two *macf1a* nonsense alleles A *macf1a* mutant lacking the CH1 binding domain, leaving intact the CH2 domain in *macf1a*^{ΔABD(CH1)}/*macf1a*^{sa12708} transheterozygotes also exhibits a fully penetrant mutant phenotype, however, the phenotype shows incomplete penetrance in *macf1a*^{ΔABD(CH1)} homozygous mutants. This suggests that *macf1a*^{ΔABD(CH1)} is an hypomorphic allele; unable to restore function over the null allele (transheterozygous) but partially restoring function in a homozygous condition. Interestingly, Macf1 and other Spectraplakins generate isoforms lacking the ABD (CH1) that bind actin with less affinity

(Karakesisoglou et al., 2000; Leung et al., 1999). This suggests that in the oocyte, the Macf1a CH1 ABD is frequently not sufficient for linking the Bb to cortical actin.

These results indicate that the Macf1a-ABD interacts with cortical actin to anchor the Bb to the oocyte cortex where it undergoes dissociation. Consistently, actin disruption phenocopied some aspects of the *macf1a* mutant phenotype, causing the detachment of the Bb from the cortex. It is possible that Macf1a interaction with actin is sufficient to trigger Bb disassembly, or that other factors are required in addition to Macf1a. P granules, for instance, disassemble upon phosphorylation of structural components (Wang et al., 2014), thus, Buc may be phosphorylated at the cortex in a Macf1a-ABD dependent manner.

Our analysis shows that the Bb does not disassemble all at once, but instead dissociates progressively during a period of about two-fold growth in oocyte volume. During this period the Bb becomes progressively smaller, although remains largely spherical, with Macf1a, Buc and other Bb components relocating as puncta to the oocyte cortex. We hypothesize that the Bb dissociates progressively with peripheral regions dissociating prior to more internal regions. During this process, it remains unclear whether Bb components fully dissolve at the cortex upon disassembly and then reassemble in aggregates that are docked cortically in a two- step process, or if the Bb fragments into smaller granules, with each granule anchored in a single step to the oocyte cortex. Either way, the Macf1a-ABD is a key activity in the process, which could be accompanied with modifications to Buc and/or other Bb components that act in Bb dissociation at the cortex.

Drosophila Macf1 ortholog Shot and MTs

Shot, the *Macf1* ortholog in *Drosophila*, also plays a key role in establishing oocyte polarity. Shot is required for anchoring MTs to the anterior and lateral oocyte cortex by interacting with the MT minus-end binding protein Patronin, which together with Shot functions as a noncentrosomal MT organizing center (Nashchekin et al., 2016). The Shot-ABD is required for its localization to cortical actin and to bring Patronin to the oocyte cortex. The MT network organized by Shot/Patronin is key to setting up anterior-posterior polarity of the *Drosophila* oocyte. Both *Macf1a* and Shot function through their ABDs and localize with actin at the oocyte cortex, however, the mechanisms by which they act are likely distinct. In *Drosophila*, the assembly of MTs is downstream of Shot polarized cortical localization, which is regulated by Par-1, whereas *Macf1a* localizes at the oocyte cortex after Bb disassembly. Nevertheless, a role for *Macf1a* more broadly in linking MTs to the cortex is consistent with an absence of MTs at the cortex in zebrafish *macf1a* mutant oocytes (Gupta et al., 2010), where it could act with Patronin to organize the MT network at a stage when the centrosome is absent (Elkouby et al., 2016).

Our live imaging data suggest that disruption of MTs does not affect the Bb. In keratinocytes and fibroblasts *Macf1a* localizes to MTs, and can function as a plus tip binding protein, stabilizing them (Karakesisoglou et al., 2000; Kodama et al., 2003). However, MTs are not enriched in the Bb and disruption of the MT network with nocodazole and cold treatment does not affect Bb morphology, RNA localization or cortical attachment (Figure 2.5I-V) (Chang et al., 2004; Gard, 1991; Gard et al., 1995a;

Gard et al., 1997; Kloc and Etkin, 1995). Thus, we do not consider a role for MTs or the Macf1a-MTBD currently in Bb disassembly. Nevertheless, since Macf1a stabilizes MTs and connects them to cortical actin in other cell types (Karakesisoglou et al., 2000; Kodama et al., 2003; Wu et al., 2008), we cannot rule out a contribution of MTs, until the conditions for culturing zebrafish oocytes allow in vivo visualization of Bb disassembly dynamics and the role of MTs in the process can be addressed. Future studies interrogating the Macf1a-MTBD will also clarify its contribution in oogenesis.

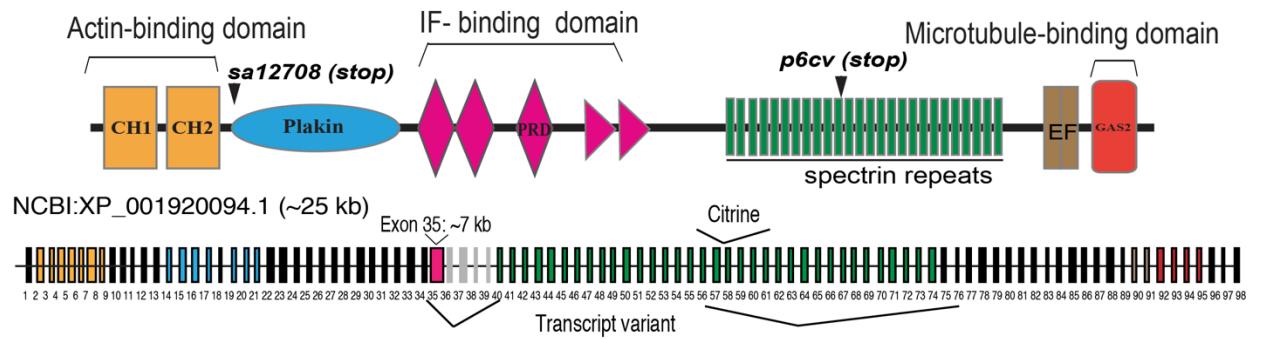
Macf1a in nuclear positioning

We found here that Macf1a localizes perinuclearly in the oocyte, suggesting that Macf1a plays a direct role in positioning the nucleus centrally in the oocyte. Further evidence from the *macf1a;buc* double mutant that lacks a Bb but displays an acentric nucleus, shows that the *macf1a* mutant nuclear localization defect is not caused by the Bb defect (Figure 2.2). Macf1a may interact with proteins residing in the nuclear envelope (NE) to connect the nucleus to the cytoskeleton. Although Nesprins residing in the outer NE interact with MTs to regulate nuclear positioning (Brosig et al., 2010; Crisp et al., 2006; Laporte et al., 2003; Link et al., 2014; Lombardi and Lammerding, 2011; Meinke et al., 2011; Sosa et al., 2012), our data indicate that disruption of MTs does not affect nuclear positioning. Rather, we found that actin disruption often leads to acentric nuclear positioning (Figure 2.5H), albeit we did not detect actin filaments around the nucleus and instead as an intranuclear mesh. Considering that the Macf1a ABD is required for nuclear positioning, it is possible that the Macf1a ABD interacts with cytoplasmic or perinuclear actin filaments that are undetectable in our conditions or,

alternatively, that the Macf1a ABD interacts with a yet unknown partner in positioning the nucleus. Future studies will be required to deduce the mechanism.

In summary, we developed a genome editing approach using CRISPR-Cas9 to interrogate the cytolinker function of Macf1a. With this approach, we identified the Macf1a ABD as essential for Bb RNP granule disassembly and, thus, for establishing AV polarity of the oocyte and egg. The Macf1a ABD is also required for centric nucleus positioning in the oocyte. Moreover, we determined that the Macf1a PRD is dispensable for Macf1a function in oogenesis indicating that Macf1a does not interact with CKs to regulate Bb dissociation or nucleus localization. This is the first study to address Macf1a functional domains by targeting its endogenous locus. Although the use of CRISPR technology is widespread nowadays, applications like the one presented here take a step further in developing more powerful and elegant genome editing approaches than solely generating null alleles, to reveal a deeper understanding of basic cellular mechanisms. We expect that applying similar strategies will be valuable to understand the function of other modular proteins like Macf1, including the related genes *dystonin* (Guo et al., 1995), *dystrophin* (Koenig et al., 1987) and *plectin* (Bouameur et al., 2014), which like *macf1* (Jorgensen et al., 2014) can lead to complex human diseases

A *macf1* cDNA sequenced:



B

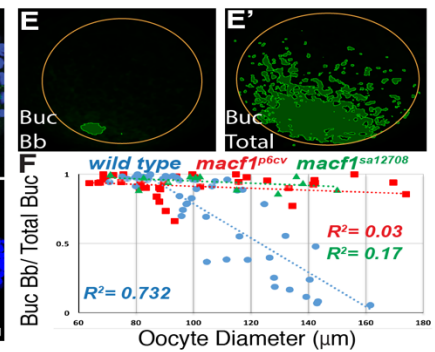
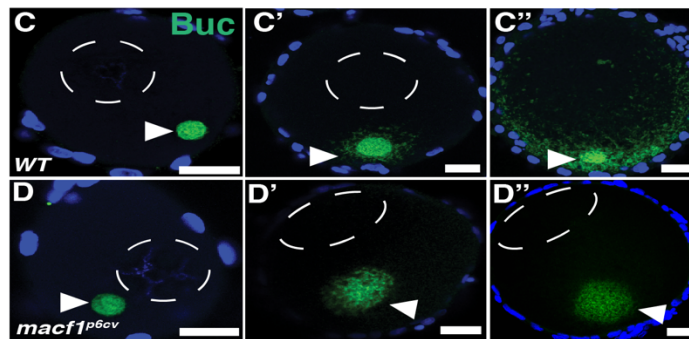
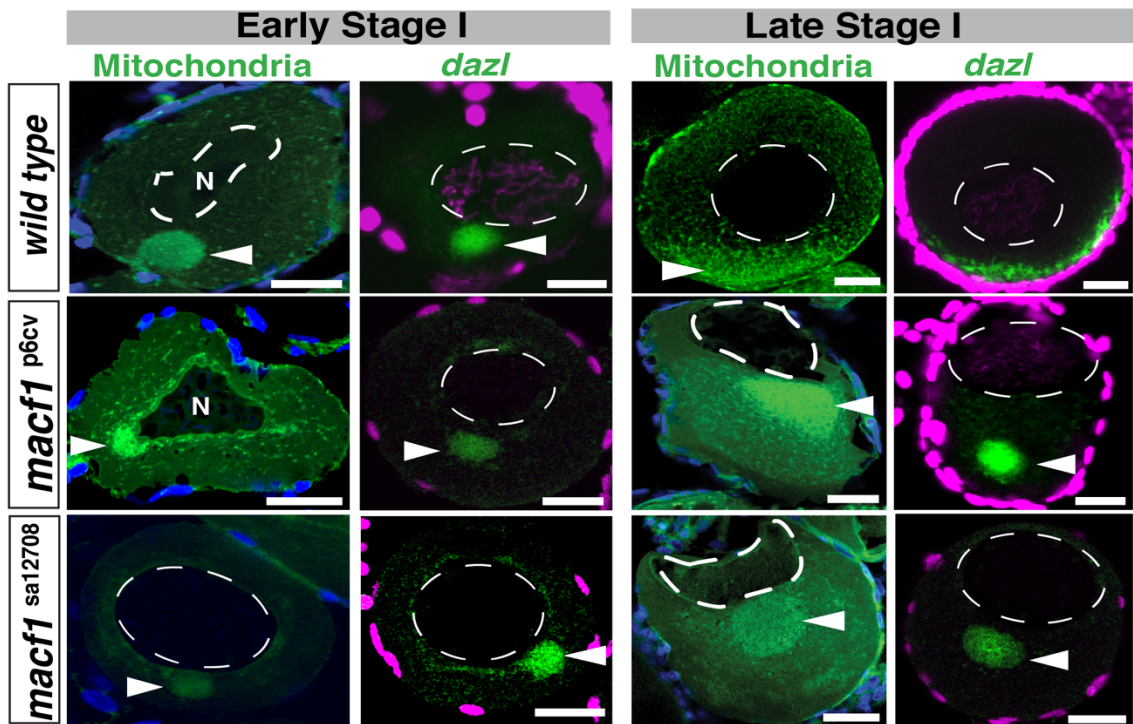


Figure 2.1: Macf1a is essential in relocalizing Buc from the Bb to the oocyte cortex.

macf1a ovary cDNA from zebrafish was sequenced to determine the Macf1a domains that are expressed. CH= calponin-homology domain (yellow); PRD= Plectin repeat domain (pink); EF= Ca²⁺ binding domain (brown); Gas2: MT binding domain (red); IF= Intermediate filament. The exons are numbered and color-coded according to the domains. The premature stop codon locations in mutant alleles, *macf1a*^{sa12708} and *macf1a*^{p6cv}, are shown. B) DiOC6 staining (mitochondria, green) and *dazl* in situ (green) in early and late stage I oocytes, labeling in WT the Bb prior to disassembly (early stage I) and the disassembled Bb at the cortex (late stage I). *macf1a*^{p6cv} and *macf1a*^{sa12708} mutant oocytes display a normal Bb in early stage I, but in late stage I the Bb enlarges and never disassembles. In addition, *macf1a* mutants show an acentric nuclear position compared to WT. DiOC6: N > 5 ovaries, >30 WT, *macf1a*^{p6cv}, and *macf1a*^{sa12708} oocytes. *dazl* in situ: N= 5 ovaries, >30 WT, 25 *macf1a*^{p6cv} and 35 *macf1a*^{sa12708} oocytes. C-D) Buc staining (green) to visualize Bb disassembly in stage I oocytes in WT and *macf1a* mutants (C-D, images correspond to different oocytes). E) Quantification method for Bb disassembly during stage I. The two images (E-E') correspond to a Z-stack from C'' where green represents the areas of Buc Bb and Buc total of oocytes that were segmented according to Buc signal intensity (see methods). The yellow circle marks the oocyte perimeter, which was used to estimate the oocyte diameter. F) Bb disassembly versus oocyte size (60 μm early stage I to 160 μm late stage I) in WT (blue), *macf1a*^{p6cv} and *macf1a*^{sa12708} mutants (green). Buc Bb: Total Buc (a quantitative measure of Bb disassembly) decreases as oocyte diameter (μm) increases in WT (R² = 0.732), but not in *macf1a*^{p6cv} (R² = 0.03) and *macf1a*^{sa12708} (R² = 0.17). N > 3 ovaries, WT and mutant oocytes. DAPI staining labels DNA (blue or magenta) and marks follicle cells. Images are single optical sections, except for E-E'. Arrowheads indicate Bb and N the nucleus. Scale bar: 20 μm. All images are representative from at least 3 experiments.

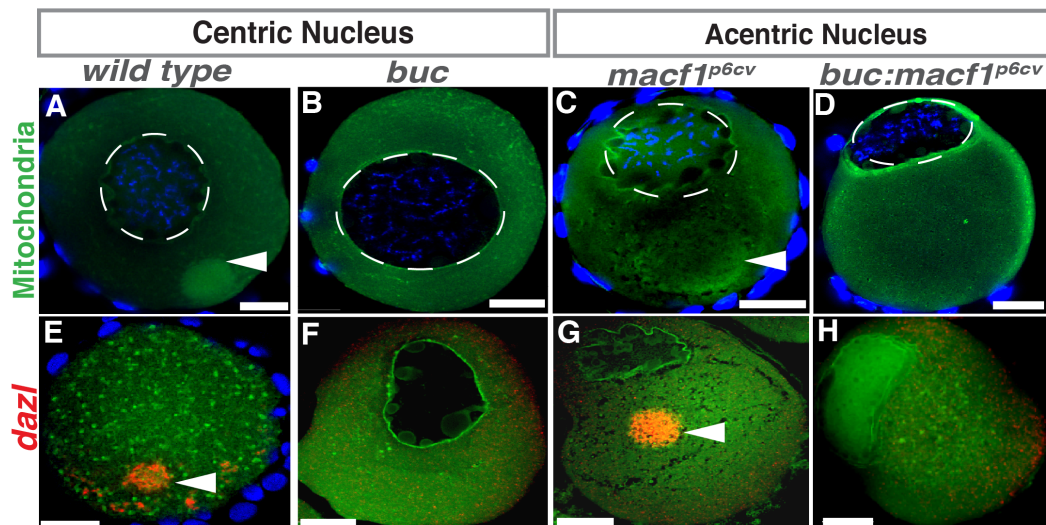


Figure 2.2: Epistasis of *buckyball* and *macf1a* in nuclear positioning.

A-D) DiOC6 staining (mitochondria, green) and *dazl* in situ (E-H, red) in stage I oocytes label the Bb. (A, E) WT with centered nucleus and Bb present. (B, F) *buc* mutant with centered nucleus, absent Bb, and unlocalized *dazl*. (C, G) *macf1a* mutant with acentric nucleus and Bb enlarged. (D, H) *macf1a^{p6cv}; buc* double mutant with acentric nucleus, absent Bb, and unlocalized *dazl*. DAPI (blue) stains DNA (A-D). *DiOC₆*: N > 3 ovaries; >30 WT, >30 *macf1a^{p6cv}*, 15 *buc^{p106}*, 24 *macf1a^{p6cv}; buc^{p106}* oocytes. *dazl* in situ N = 3 ovaries; 10 *buc^{p106}*, 7 *macf1a^{p6cv}*, 14 *macf1a^{p6cv}; buc^{p106}* oocytes. Representative images from 2 experiments. Dotted white lines outline the nucleus. Images are a sum of 3 single optical confocal sections. Arrowheads indicate the Bb. Scale bar: 20 μm (C-D).

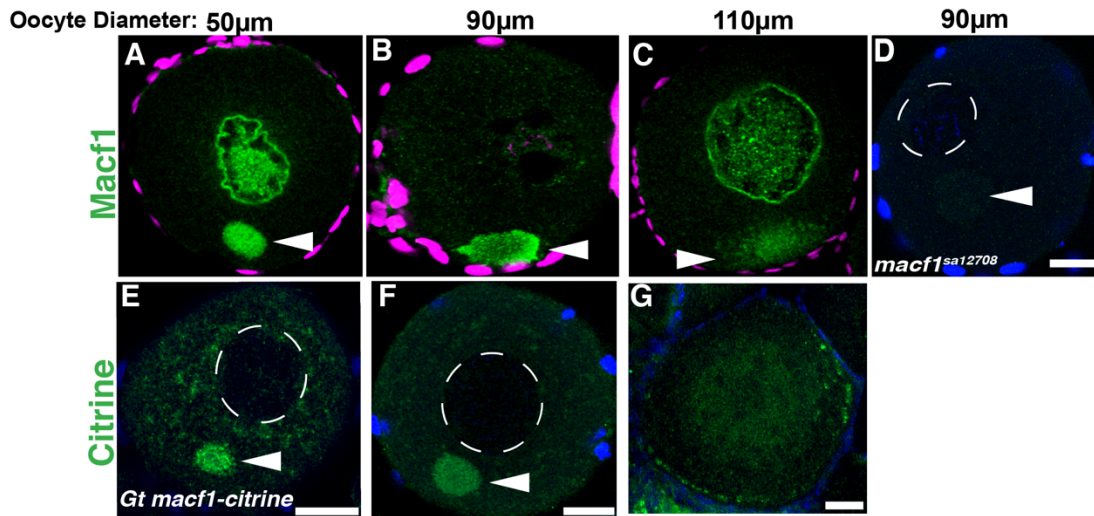


Figure 2.3: Localization of Macf1a in stage I oocytes.

A-C) Macf1a immunostaining (green) in stage I oocytes shows localization perinuclearly and within the Bb (50µm), and later at the cortex during Bb disassembly (B, C). D) In a *macf1a*^{sa12708} mutant oocyte Macf1a staining was negative. E-G) GFP staining in *Gt(macf1a-citrine)*^{ct68a} line also shows Macf1a-citrine localization to the Bb and at the cortex during disassembly. DAPI (blue/magenta) stains DNA. A-D) N> 5 ovaries, 53 WT and 18 *macf1a*^{sa12708} oocytes. E-G) 3 ovaries, 44 oocytes of *Gt(macf1a-citrine)*^{ct68a/+}. Representative images from 3 experiments. Dotted white lines outline the nucleus. Images are a sum of 3 single optical confocal sections. Arrowheads indicate the Bb. Scale bars: 20µm.

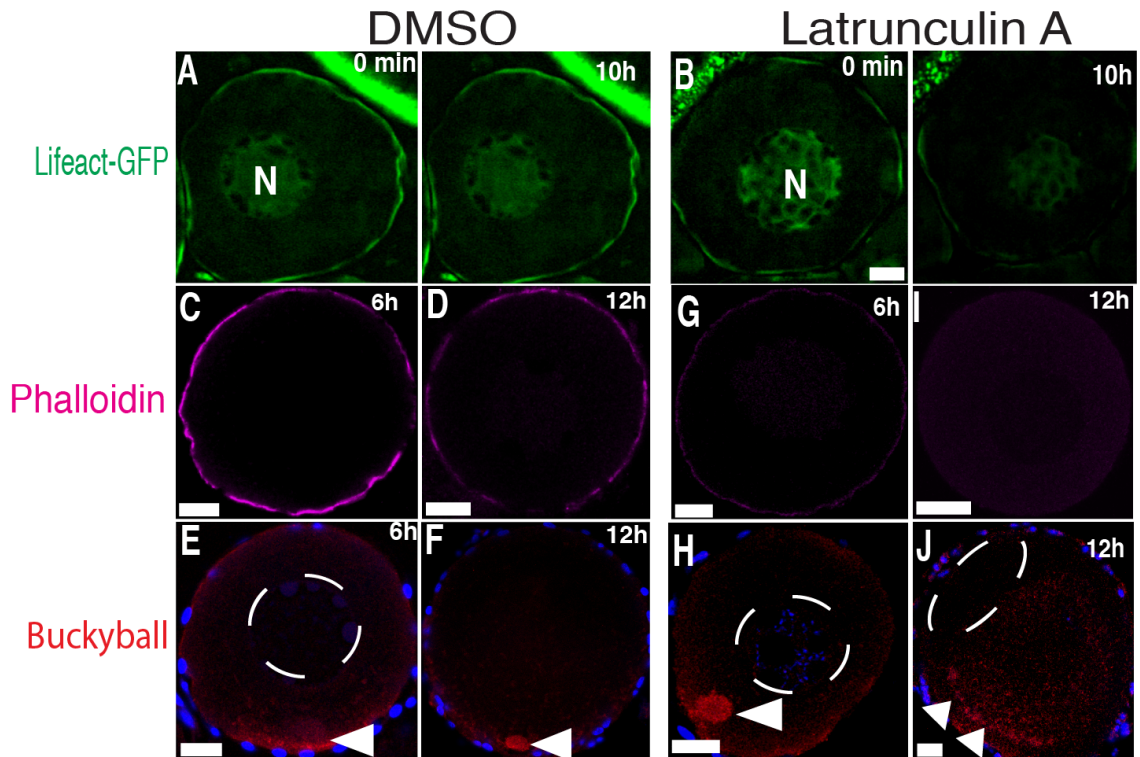


Figure 2.4: Latrunculin A treatment in stage I oocytes

A-B). Stills from live imaging of *Tg(actb1:lifeact-GFP)* oocytes showing actin filaments (green) before and after treatment with DMSO(A) or LatA (B). N= 3 ovaries; 11 DMSO and 23 LatA oocytes. After 10 h of treatment with LatA, Lifeact-GFP fluorescence decreases (B). C-F) Ovaries treated with DMSO or LatA (G-J), then fixed and stained for Buc (red) (E,F, H, and J) and phalloidin (magenta) (C, D, G and I). Arrowheads point to Buc in Bb and cortex. 6h, 18 DMSO and 22 LatA treated oocytes were analyzed finding no effect in Bb or nucleus. After 12h, 19 DMSO and 22 LatA treated oocytes were analyzed, with 4/22 showing Buc cortical detachment and 3/22 acentric nucleus. N > 5 ovaries. Scale bar: 20 μ m.

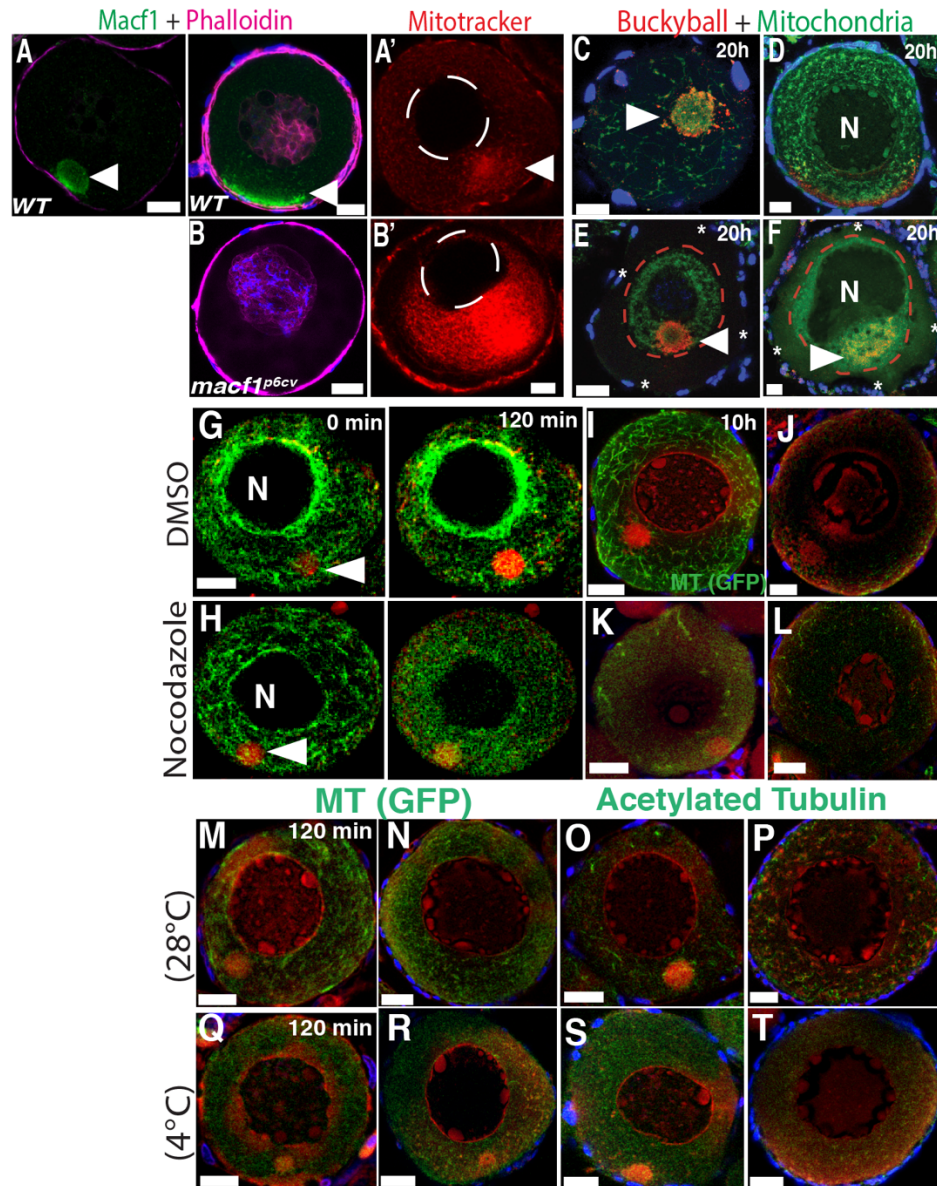


Figure 2.5: Effect of disrupting actin and MTs on the Bb and nuclear positioning.

A) Macf1 (green) and phalloidin staining in WT (A) and phalloidin in *macf1a*^{p6cv} mutant (B) oocytes labeling cortical and intranuclear actin. A) Macf1a is at the cortex upon Bb disassembly in WT and actin is absent from the Bb. N= 3 ovaries, 5 WT and 10 *macf1a*^{p6cv} mutant oocytes. A',

B') WT (A') and *macf1a*^{66cv} mutant (B') live stage I oocytes stained with MitoTracker to visualize the cortical detachment of mitochondria in *macf1a* mutant. N= 3 ovaries, 22 WT and 7 *macf1a*^{66cv} oocytes. C-F) Ovaries treated with DMSO (C-D) or LatA (E-F) for 20 h, then fixed and stained for mitochondria (DiOC6, green) and Buc (red). Asterisks and red dotted line mark the cortical detachment of mitochondria and Buc in LatA treated oocytes (E,-F). The number of oocytes imaged that showed the mitochondrial cortical detachment in DMSO and LatA treated was 3/25 and 25/40, respectively. F) The oocytes that displayed an acentric nucleus after LatA treatment was 15 of 40 oocytes. N > 5 ovaries. G-H) Stills from live imaging of Tg(*ef1a:dclk-GFP*) to visualize MTs (green) and Mitotracker (mitochondria, red) to visualize the Bb. Time series of live stage I oocytes treated with DMSO (G, control) or nocodazole (H) . N>5 ovaries, 75 DMSO and 73 nocodazole treated oocytes. I-L) Ovaries from Tg (EMTB-3GFP) treated with DMSO (I, J) and nocodazole (K, L) for 10h, and stained for MTs (GFP) and mitochondria (DiOC₆). M-T) Cold treatment (4°C) for 120min to depolymerize stable MTs. Incubation at 28°C (M-P) or 4°C (Q-T) of Tg(*ef1a:dclk-GFP*) (M, N; Q, R) and wild type ovaries stained for acetylated tubulin (O, P; S, T) to visualize MTs. N>5 ovaries, 53 (28°C) and 50 (4°C) oocytes. Arrowheads indicate the Bb. Scale bar: 20µm.

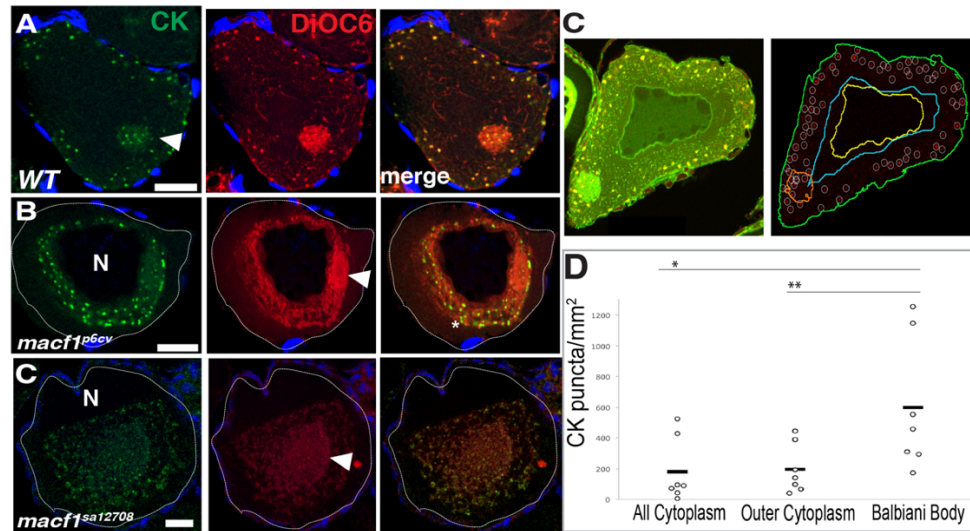


Figure 2.6: Distribution of cytokeatin in stage I oocytes.

A-B) Cytokeatin (CK, green) immunostaining and DiOC6 labeling (Bb, red) in ovary tissue sections. A) In WT, CK puncta are distributed within the Bb (arrowhead) and cortically, whereas in a *macf1^{ap6cv}* and *macf1^{sa12708}* mutant oocyte (B-C) CKs are devoid from the cortex (white outline) and are around the nucleus. C-D) Quantification of CK enrichment in the Bb. C) DiOC6 staining pattern was used to segment the oocyte into regions of interest (ROI). Outlines show identified plasma membrane (green), nucleus (yellow) and Bb (orange). All cytoplasm defined by the area between yellow and green lines, and outer cytoplasm is between cyan and green lines. White circles around identified CK puncta. CK puncta density was measured in each region of interest (ROI). D) Graph of CK enrichment (CK puncta/mm²) in All cytoplasm, outer cytoplasm, and Bb. Points represent single oocytes. Black bar shows the mean. p-values, *, ** <0.01. DAPI (blue) stains the follicle cell nuclei (A-B). Images are single optical sections. Scale bar: 20µm. N > 5 ovaries, > 30 WT and > 20 *macf1^{ap6cv}* oocytes. N= 2 ovaries and 10 oocytes *macf1^{sa12708}* 7 oocytes were used for quantification. Images are representative of 3 experiments.

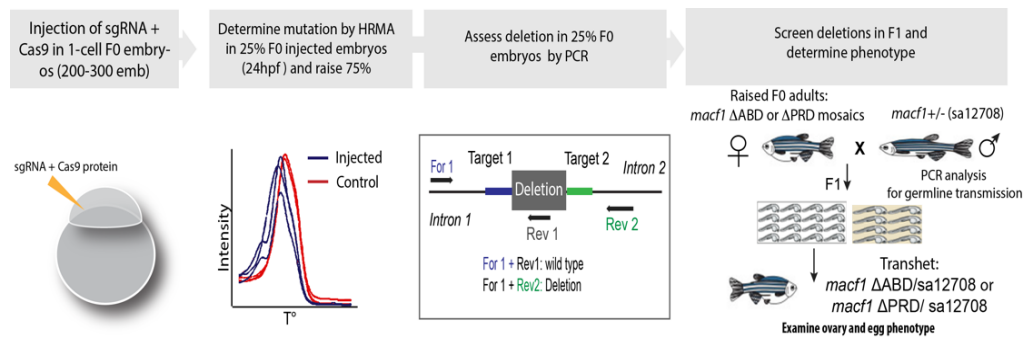


Figure 2.7: Pipeline for the generation of *macf1a*^{ΔABD(CH1)}, *macf1a*^{ΔABD(CH1-c)} and *macf1a*^{ΔPRD/-} mutants.

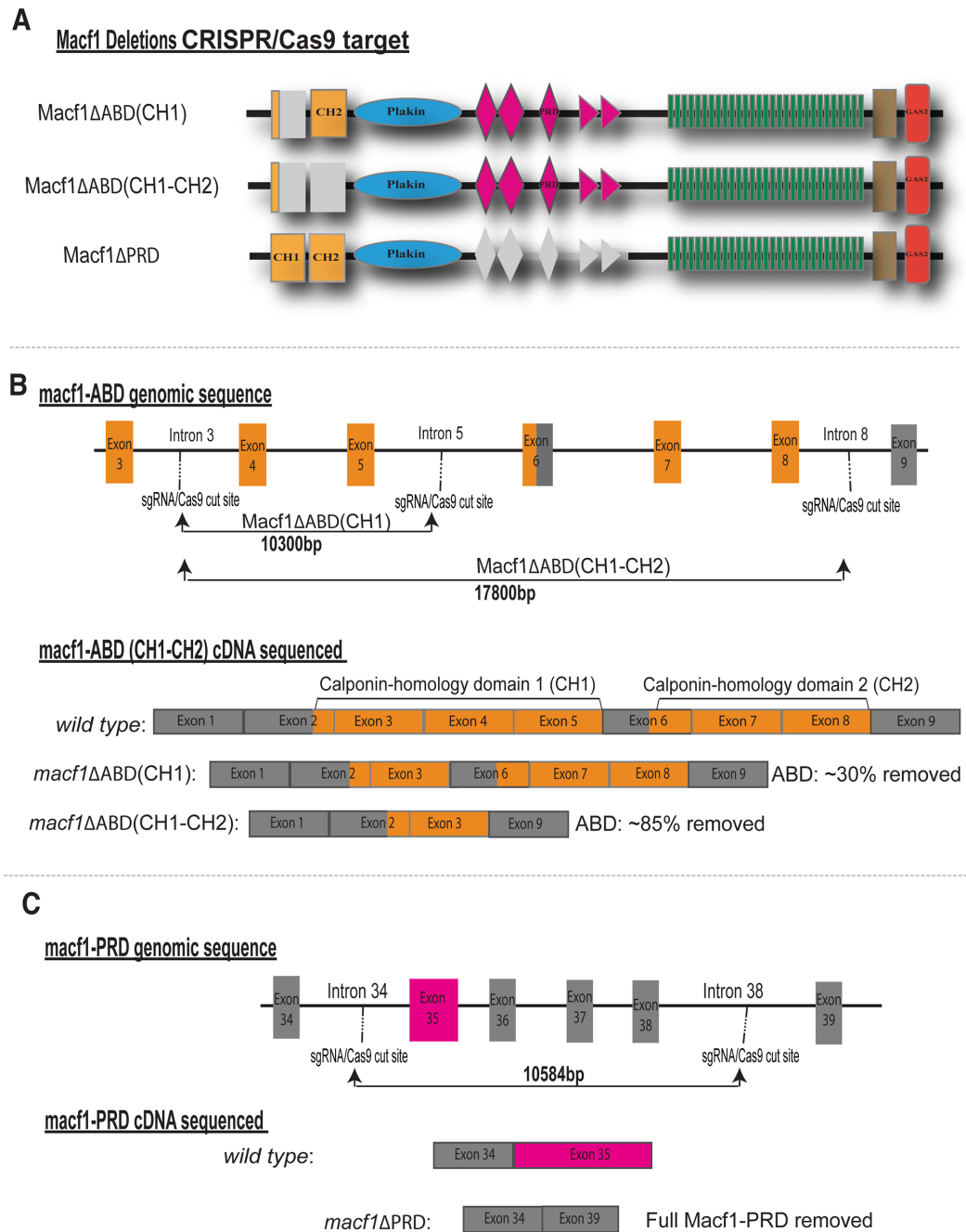


Figure 2.8: CRISPR/Cas9 deletions of Macf1a ABD and PRD.

A) Illustrates the Macf1a protein generated by the genomic deletions and the nomenclature to refer to each deletion mutant. Exons encoding the ABD are

highlighted in yellow and the PRD in pink, whereas the absent domains are in gray. B-C) Schematizes the CRISPR/Cas9 approach to delete the ABD and PRD, showing the targeted introns, the size of the genomic deletion, and the deleted exons from the coding sequence (cDNA). B) Sequencing of cDNA confirmed deletion of intended exons coding for 70% of the CH1 ABD and 85% of the full CH1-CH2 ABD. C) Illustrates the deletion of exon 35, coding for the PRD, and exons 36-38.

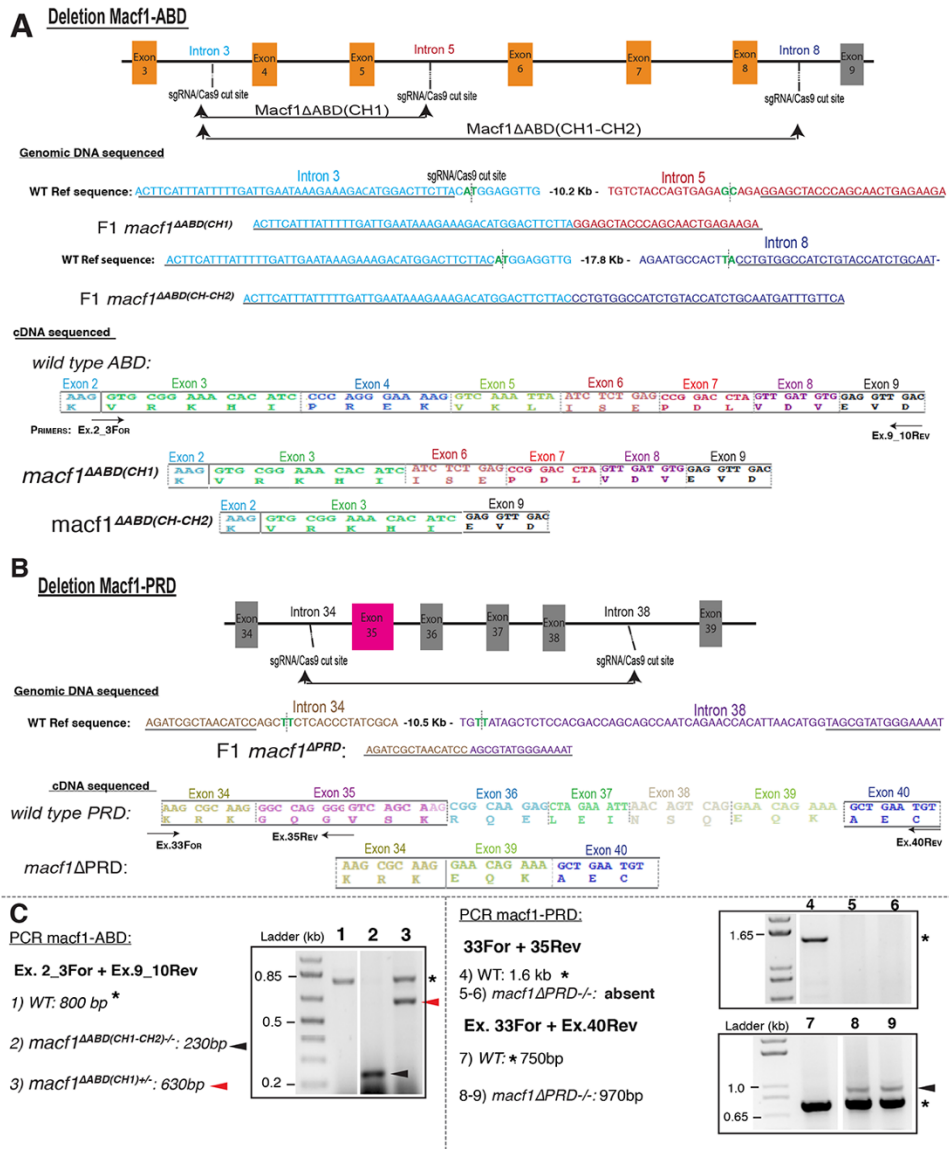


Figure 2.9: Molecular characterization of *macf1a* domain deletion mutants.

A) Detection of *macf1a*-ABD (CH1) and (CH1-CH2) deletions in the *macf1a* gene and cDNA. Scheme indicates intron targets for deleting *macf1a* ABD (CH1) and (CH1-CH2). Partial genomic sequence of introns 3 and 5 in WT and the genomic size between the selected CRISPR target sites is indicated. In green the predicted Cas9 cut site and the underlying gray line marks the joined sites of introns after Cas9 cutting and repair. Below is the cDNA sequence for *macf1a*^{ΔABD(CH1)} and *macf1a*^{ΔABD(CH1-CH2)}. The exon composition (only the first few amino acids are shown) in WT compared to mutants confirms the intended exon deletions in *macf1a*^{ΔABD(CH1)} and *macf1a*^{ΔABD(CH1-CH2)}. The primer locations for amplifying *macf1a* cDNA are indicated. B) Detection of *macf1a*-PRD domain deletion in the *macf1a* gene and cDNA. Scheme indicates intron targets for deleting the *macf1a*-PRD. Partial genomic sequence of introns 34 and 38 in WT indicating the genomic size between the selected CRISPR target sites, in green the predicted Cas9 cut site, and the underlying gray line marks the joined sites of introns 34 and 38 after Cas9 cutting and repair. Below is the deleted genomic DNA and cDNA sequence for *macf1a*^{ΔPRD}. The primer locations for amplifying *macf1a* cDNA are indicated. The exons 36-39 in lighter tone have not been sequenced. C) PCR products from ovary cDNA amplifying *macf1a* ABD and PRD. Primer combinations and expected PCR product sizes are shown along with the bands detected in WT and mutants (lanes 1-3, ABD; 4-9, PRD). Arrowheads (black and red) indicate the mutant bands at the expected size and asterisks indicate the WT bands.

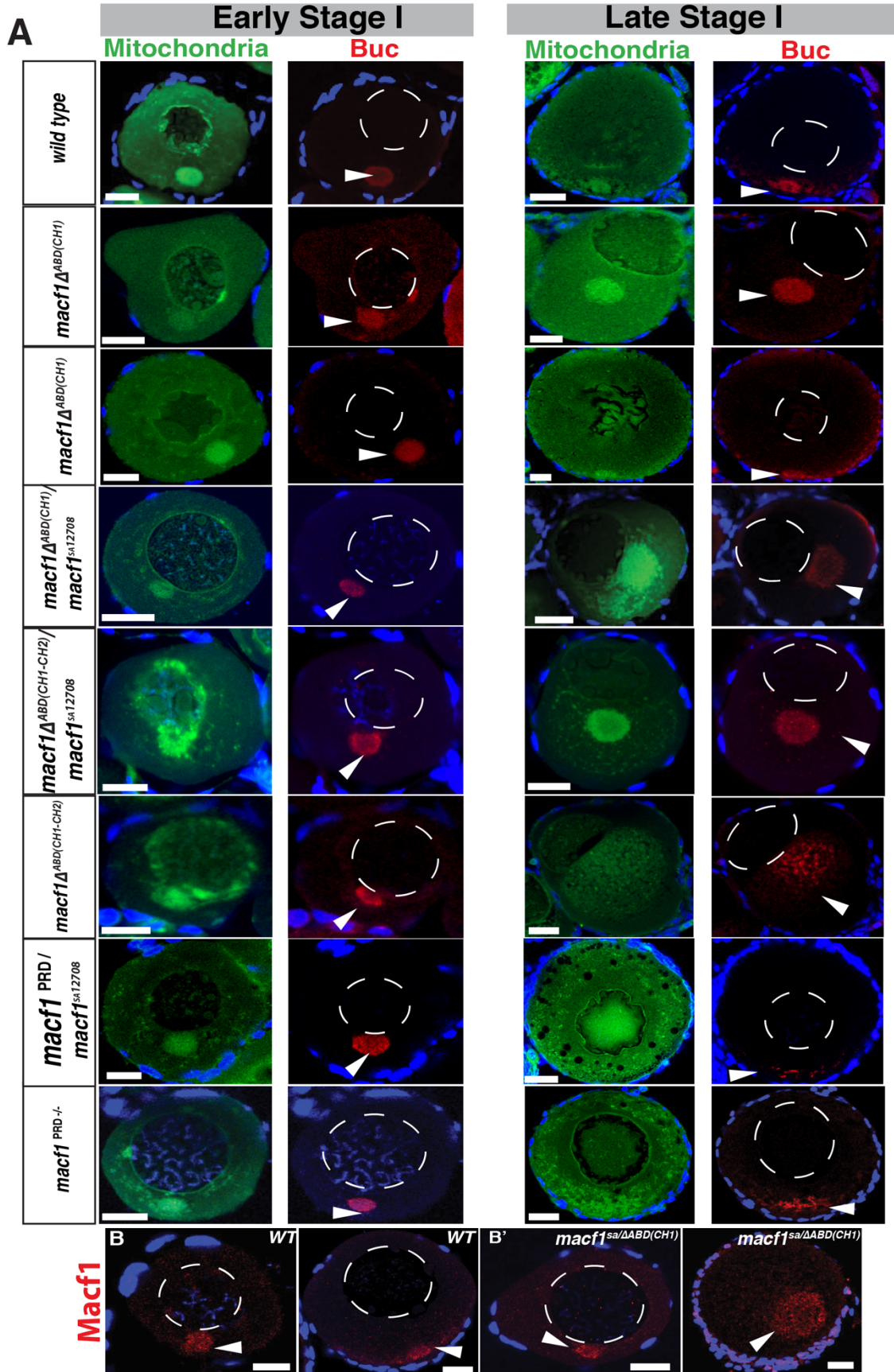


Figure 2.10: Phenotypic characterization of $macf1a^{\Delta ABD(CH1)}$, $macf1a^{\Delta ABD(CH1-CH2)}$ and $macf1a^{\Delta PRD}$ mutants.

A) DiOC₆ (mitochondria, green) and Buc (red) staining in early and late stage I oocytes. $macf1a^{\Delta ABD(CH1)}$ ovaries display wild type and $macf1a$ null phenotype due to incomplete penetrance. In $macf1a$ null phenotype the Bb is normal in early stage I, but in late stage I oocytes the Bb enlarges and never disassembles at the cortex. In addition, mutants show an acentric nucleus in late stage I oocytes, like null mutants. $macf1a^{\Delta ABD(CH1)}/macf1a^{sa12708}$, $macf1a^{\Delta ABD(CH1-CH2)}/macf1a^{sa12708}$ and $macf1a^{\Delta ABD(CH1-CH2)}/macf1a^{sa12708}$ ovaries display $macf1a$ null phenotype, whereas $macf1a^{\Delta PRD}/macf1a^{sa12708}$ and $macf1a^{\Delta PRD}$ homozygous mutant oocytes show no phenotype; the Bb disassembles normally at the cortex and the nucleus is centrally positioned. DiOC₆ and Buc; N> 3 ovaries, > 31 $macf1a^{\Delta ABD(CH1)}$ >25 $macf1a^{\Delta ABD(CH1)}/macf1a^{sa12708}$, 11 $macf1a^{\Delta ABD(CH1-CH2)}/macf1a^{sa12708}$, 22 $macf1a^{\Delta ABD(CH1-CH2)}$, 15 $macf1a^{\Delta PRD}/macf1a^{sa12708}$ and 24 $macf1a^{\Delta PRD/-}$ oocytes. B-B') Macf1a immunostaining (red) in wild type and $macf1a^{\Delta ABD(CH1)}/macf1a^{sa12708}$ (N> 3 ovaries, 20 oocytes).

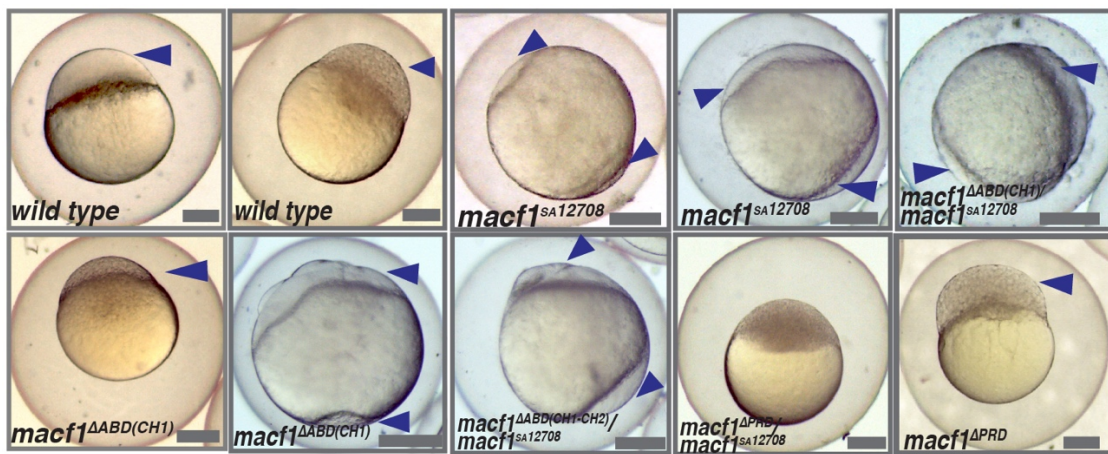


Figure 2.11: AV polarity establishment in $macf1a$ mutants.

AV polarity in wild type, and lack of polarity in *macf1a*^{sa12708}, *macf1a*Δ^{ABD(CH1)}/*macf1a*^{sa12708} and *macf1a*Δ^{ABD(CH1-CH2)}/*macf1a*^{sa12708} mutant eggs, where the cytoplasm (arrowheads) surrounds the yolk instead of forming the blastodisc. In *macf1a*Δ^{ABD(CH1)} mutants the egg phenotype shows incomplete penetrance. Late blastula embryos from *macf1a*Δ^{PRD}/*macf1a*^{sa12708} and *macf1a*Δ^{PRD} mutant females displays normal AV polarity and development. DAPI (blue) stains the DNA. Dotted white lines outline the nucleus. Images are single optical sections. Arrowheads in (A-B, for Buc, Macf1a) indicate the Bb. Scale bar: (A-B) 20μm and (C) 100 μm.. Scale bar: 100μm.

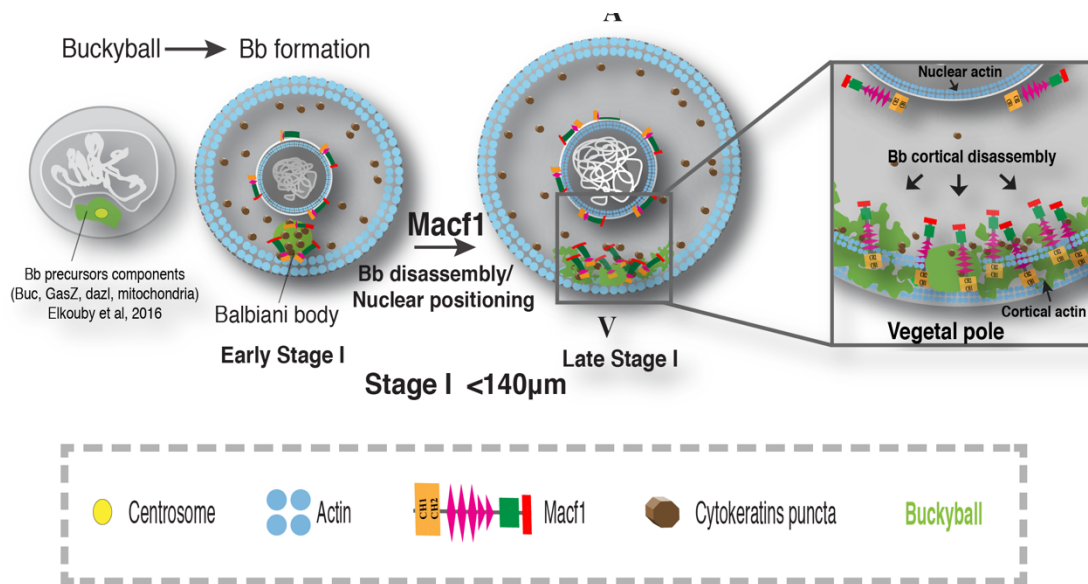


Figure 2.12: Model of Macf1a function in Bb dissociation at the cortex.

In early stage I oocytes, Bb precursors first aggregate in a nuclear cleft around the centrosome. As stage I progresses the centrosome is lost and the Bb rounds up into a mature Bb (Elkouby et al 2016). From this position next to the nucleus the Bb will later reach the oocyte cortex. The mature Bb contains Buc and Macf1a that regulate Bb

formation and disassembly, respectively. We postulate that Macf1a in the Bb does not function as a cytolinker linking two cytoskeletal systems together. Instead, Macf1a links the Bb to the oocyte cortex via its localization to the Bb and by interaction with cortical actin via the Macf1a ABD. The Bb dissociates progressively during a period of about two-fold growth in oocyte volume. During this period the Bb becomes progressively smaller, although remains largely spherical, with Macf1a, Buc and other Bb components relocating as puncta to the oocyte cortex. We hypothesize that Macf1a acts directly in this relocalization process, which may occur via dissolution and reaggregation or via the Bb fragmenting and relocalizing to the oocyte cortex in a Macf1a-dependent manner. In either case, the Bb would dissociate progressively over time with peripheral regions dissociating prior to more internal ones. Once the Bb dissociates at the cortex, the oocyte vegetal pole is defined.

Table 2.1. Generation of macf1a deletion mutants

Targeted macf1 introns and domains in the region	¹ Indel efficiency	Deletion size	² Positive F0 / Total tested	³ Positive F1 / Total tested	Positive adult F1/ Total tested
I3+I5: Calponin-homology 1 (Actin-binding)	I3: 96% I5: 87.5%	10.3 Kb	1/9	3/24	3/30
I3+I8: Calponin-homology 1&2 (Actin-binding)	I3: 96% I8: 83%	17.8 Kb	1/28	1/4	3/20
I34+I38: PRD (IF-binding)	I34: 82.5% I38:90%	9.1 Kb	1/15	6/18	4/24

¹The percentage corresponds to F0 embryos that showed indels from the total of embryos injected (Fig. S1).

² Ratio represents the number of F0 adult females that showed germline transmission in the F1 for the indicated deletions.

³ The number of F1 embryos carrying the deletion from the F1 progeny screened.

Table 2.2: Egg phenotype of *macf1a* mutant females

Genotype	WT AV polarity (N° eggs)	No AV polarity (N° eggs)	Total N° females
<i>wild type</i>	46	0	2
<i>macf1</i> ^{SA12708}	0	81	2
<i>macf1</i> ^{ΔABD(CH1)} / <i>macf1</i> ^{SA12708}	4 (2.8)	142 (97.2)	4
<i>macf1</i> ^{ΔABD(CH1)}	319 (70)	137 (30)	9
<i>macf1</i> ^{ΔABD(CH1-CH2)} / <i>macf1</i> ^{SA12708}	5 (3.0)	160 (97.5)	4
<i>macf1</i> ^{ΔPRD} / <i>macf1</i> ^{SA12708}	116	0	2
<i>macf1</i> ^{ΔPRD}	200 (5)	0	5

* In parenthesis is the percentage from total number of eggs.

Table 2.3. List of *macf1a* cDNA primers

NCBI: XP_001920094.1. (start position)	Sequence	NCBI: XP_001920094.1. (start position)	Sequence
691	GCTGAAGATGTTGATGTGCCG	11565	GCGAACCTCAATGTGTCTCACC
1455	CAGGAAGGGTCATTTCTCTACGG	11565	GGTGAGACACATTGAGGTTCCG
1886	GCAAACCTGCTGGAACATTCGTC	11565	GCGAACCTCAATGTGTCTCACC
2633	TGCCATCTGTGTGTTCCACCG	12181	GCATCATTGAGACCAACGGC
2645	TTAGGGGAGGAACGGTAAAC	14194	AGTGTGGATGACTACAGGCAGACC
3050	AGAGCATCAAGTCTCACCTGGAGG	14488	TTAGTTGGGCTCTTGGCAGG
3388	TTCTGACCTGACTTTCTGCCGC	14488	TTAGTTGGGCTCTTGGCAGG
3767	CCACCGAAAAACAGGAGAACAC	16214	GGATTGCCGAATGTGAGGTAAG
3788	TGTCAGTTGTTCCGGGCTGTG	16592	CGTCCAGGCTTTTGTGTCTAC
3878	AACTGGATGAGTGCCAGACC	16801	CAGTGTCTCATCATTGGAGTCC
4103	GTGATGCGCTACGAAGACTGG	16931	GCCTGTGAAGCCAAGAGTCAG
4231	GATGTGCGACAAGTGATGGCTC	17546	TTGGTATCAGTTCCTCTGTGTCC
4550	CACAGCATGGCCTCATAGAC	18513	CAATCAATGGCTGGATAGAGTGG
4613	GTCAGGCTGGAAAAGACCAC	19014	GAGAGACGCACTGAAGGTGAAGC
5234	CTGTTCAAGCTTGGCCTGATG	19167	CTGGTAATCAGAGTCTCAGTTTCG
5282	CCCTGTTGTAGCTGTCGTG	19590	AACGATGGCAGGAGTTGTCC
5691	ATCTGTCAGTTCCTCGTACCCCC	20481	TCACACTCACGCCACACTGGATA
5842	CGCTTAGTCTGCTAAAACCAG	21053	CCAAAATGGAAGACAGAAGGGG
5894	CTGGTATGGCAAGTTTTTTGAGC	21089	AAACCTGTCCAGTGAACGG
5904	GTTCAACTGGTATGGCAAGG	21588	GGTTTATGACACCACAGTGCCTTC
6586	TCTGGTCCTTCAAAGATGC	21746	AAACTGACCAGAGAACAGGAGGG
7764	GGGGGAACTACCAGCGATAAG	22269	ACACAGCGAGAATGGCTTCG
7764	GGGGGAACTACCAGCGATAAG	22271	AAGCCATTCTCGCTGTGTGC
8357	CCTGTAAGGCTCTGTCAATGCTC	22704	TGGTAATCCTCGCTCACTCAG
8357	CCTGTAAGGCTCTGTCAATGCTC	22861	GACTTCTGTGGTTTCATCCAACG
10679	CTATGCGTCACTCAGCCAATAATG	23158	GCTCCACTTGAACCTCTTCGC
		24880	GGTGCTCCGTCACGAAAGAAC

Chapter 3 : Future Directions

A few years ago, Buckyball and Macf1 emerged as novel factors regulating the establishment of oocyte cell polarity, via the assembly and disassembly of the Bb mRNP granule, respectively. More recently, Buc was shown to contain a prion-like domain that induces the formation of amyloid like fibers in the process of Bb assembly (Boke et al., 2016). These findings situated the Bb as an emerging model to study physiological association and dissociation of amyloid-like aggregates.

Currently, Macf1a is the only known factor required for Bb mRNP granule dissociation (Gupta et al., 2010) and we determined that Macf1-ABD is essential for Bb dissociation at the oocyte cortex. In macf1 mutants, the Bb persists in the cytoplasm and never disassembles, thus, suggesting that Bb anchoring to the cortex is key in the dissociation process. For the future, it is important to address how Bb dissociation is triggered, whether the Macf1-ABD and actin directly mediates Bb dissociation, or additional factors are required in the oocyte cortex or cytoplasm.

From all Macf1 functional domains, we determined that in establishing oocyte polarity the Macf1-ABD is essential, while the Macf1- PRD is dispensable, and the MTBD may not be required since MT disruption does not affect the Bb. However, it is unknown if the Macf1 long rod domain, composed of 29 SRs, is essential for Macf1 function. Moreover, is unclear the requirement of the rod domain in other cell types is unclear (Applewhite et al., 2010; Karakesisoglou et al., 2000; Kodama et al., 2003; Lee and Kolodziej, 2002b). Thus, addressing the requirement of the Macf1a rod domain in Bb dissociation will contribute to fill a gap in the knowledge of the requirement for Macf1 SRs.

Is Macf1 and actin interaction directly or indirectly mediating Bb disassembly?

A remaining question is whether the Macf1a-ABD and actin cortical association is sufficient to drive Bb dissociation or, instead, if other factors are required to act downstream of Macf1a. One hypothesis is that the Macf1a-ABD and actin are only required to anchor the Bb, with an additional or no role in Bb dissociation, whereas a cortical or cytoplasmic factor acts on the Bb to initiate its full dissociation. Such factor(s) could be present in the oocyte cytoplasm or cortex and act from mid-stage I onwards since at that point the Bb is dissociating. Alternatively, no other factors are required and Macf1a in the Bb through its association with cortical actin is sufficient to drive Bb dissociation.

Although the current methods in zebrafish (chapter 2) and *Xenopus* (Chang et al., 2004) are unable to recapitulate the dynamics of Bb dissociation in vivo, recent advances from our lab and others (Boke et al., 2016) have shown that the Bb can be isolated from stage I oocytes to study it in vitro. Moreover, the cytoplasm and cortices can also be extracted from *Xenopus* oocytes and eggs (Field et al., 2014; Sive et al., 2007). Hence, a new approach that combines isolated Bbs and cellular fractions from oocytes, may be able to recreate Bb dissociation in vitro without the constraints of Bb progression in vivo.

The incubation of isolated Bbs with actin filaments should reveal whether it is sufficient to drive Bb dissociation, or only to attach the Bb. The effect of incubating Bbs with cytoplasmic and cortical fractions will address if additional factors are required to trigger Bb dissociation. Based on our findings (chapter 2) showing that *macf1a* mutants

(*macf1a*^{sa12708}, *macf1a*^{p6cv} and *macf1a*^{ΔABD}) fail to disassemble the Bb and persist in the cytoplasm, it seems unlikely that a cytoplasmic factor triggers Bb dissociation. Rather, Bbs are expected to associate with oocyte cortices in an actin and Macf1 dependent manner and induce Bb dissociation.

The effect of the different extracts on isolated Bbs from wild type and *macf1a*^{ΔABD} mutants can be evaluated by live imaging using tagged Buckyball (Riemer et al., 2015), or in fixed and stained samples with Buc antibody (chapter2). The parameters to evaluate are: Bb dissociation rate (method in chapter 3) at different time points, and the colocalization with actin filaments. Results from these experiments in isolated Bbs will address whether Macf1-ABD and actin interaction is mediating or driving Bb dissociation.

Is the rod domain (spectrin repeats) required in establishing oocyte polarity?

Macf1 belongs to the Spectrin family of proteins, characterized by containing a spectrin repeats (SRs) module (chapter 1) forming a linear rod that is believed to provide length, flexibility and space between functional domains (Grum et al., 1999). Dystrophin is also a member of this family and its critical for muscle function, connecting via the N-terminal ABD the cytoskeleton to the plasma membrane through the C-terminal β-Dystroglycan, with the N-term and C-term separated by 24SRs (Ervasti, 2007). Similarly, Macf1 contains 29 SRs (chapter 2) spacing the N-terminal ABD and C-terminal MTBD. Macf1a and Dystrophin have analogous structures and functions, linking large cytoplasmic structures; the Bb and contractile apparatus to the cell cortex, respectively. Thus, despite acting in different cell types, SRs function may be similar in both.

Dystrophin loss of function leads to Duchene muscular Dystrophy (DMD) in humans, characterized by severe and progressive muscle degeneration. Though most mutations causing DMD are null, in some cases, mutations produce in frame deletions that generate smaller Dystrophin versions and associate with milder forms of the disease (Kerr et al., 2001) known as Becker Muscular Dystrophy (BMD). A particular case of BMD contains an in-frame mutation in *dystrophin* that deletes ~30 exons in the rod domain, generating a Dystrophin lacking ~70% of the rod domain that is unable to completely restore protein function (Palmucci et al., 1994). Though the exact mechanism is unknown, it suggests that SRs number and length may be critical for Dystrophin function.

It remains unclear the contribution of the rod domain to Macf1 function, since variable results are obtained in different biological contexts (see chapter 1). Based on our data (chapter 2), showing that Macf1a-ABD is required for Bb dissociation, it is tempting to speculate that a long rod domain may facilitate the linking of the Bb to the cortex. Future experiments should address the Macf1a-rod domain requirement by deleting SRs from the *macf1a* endogenous locus and examining the resulting oocyte phenotype.

We expect that deleting most or all SRs will cause Bb and nuclear positioning defects, although they may not be fully penetrant defects. If only Bb or nuclear positioning are affected, it would suggest that Macf1a may have different SRs requirement for these two processes. We expect that deleting only a few (~30-40%) Macf1 SRs will function normally since it will still contain most of the spectrin rod domain.

However, if we observed otherwise, and the mutant displays a Bb or nucleus defect, then it would suggest that the length of the rod domain is critical for Macf1a function in oocyte polarity.

BIBLIOGRAPHY

Albamonte, M.I., Albamonte, M.S., Stella, I., Zuccardi, L., and Vitullo, A.D. (2013). The infant and pubertal human ovary: Balbiani's body-associated VASA expression, immunohistochemical detection of apoptosis-related BCL2 and BAX proteins, and DNA fragmentation. *Hum Reprod* 28, 698-706.

Alves-Silva, J., Sanchez-Soriano, N., Beaven, R., Klein, M., Parkin, J., Millard, T.H., Bellen, H.J., Venken, K.J., Ballestrem, C., Kammerer, R.A., *et al.* (2012). Spectraplakins promote microtubule-mediated axonal growth by functioning as structural microtubule-associated proteins and EB1-dependent +TIPs (tip interacting proteins). *J Neurosci* 32, 9143-9158.

Applewhite, D.A., Grode, K.D., Keller, D., Zadeh, A.D., Slep, K.C., and Rogers, S.L. (2010). The spectraplakin Short stop is an actin-microtubule cross-linker that contributes to organization of the microtubule network. *Mol Biol Cell* 21, 1714-1724.

Barton, B.R., and Hertig, A.T. (1972). Ultrastructure of annulate lamellae in primary oocytes of chimpanzees (*Pan troglodytes*). *Biol Reprod* 6, 98-108.

Behrndt, M., Salbreux, G., Campinho, P., Hauschild, R., Oswald, F., Roensch, J., Grill, S.W., and Heisenberg, C.P. (2012). Forces driving epithelial spreading in zebrafish gastrulation. *Science* 338, 257-260.

Bernier, G., Mathieu, M., De Repentigny, Y., Vidal, S.M., and Kothary, R. (1996). Cloning and characterization of mouse ACF7, a novel member of the dystonin subfamily of actin binding proteins. *Genomics* 38, 19-29.

Betley, J.N., Frith, M.C., Graber, J.H., Choo, S., and Deshler, J.O. (2002). A ubiquitous and conserved signal for RNA localization in chordates. *Curr Biol* 12, 1756-1761.

Boke, E., Ruer, M., Wuhr, M., Coughlin, M., Lemaitre, R., Gygi, S.P., Alberti, S., Drechsel, D., Hyman, A.A., and Mitchison, T.J. (2016). Amyloid-like Self-Assembly of a Cellular Compartment. *Cell* *166*, 637-650.

Bontems, F., Stein, A., Marlow, F., Lyautey, J., Gupta, T., Mullins, M.C., and Dosch, R. (2009). Bucky ball organizes germ plasm assembly in zebrafish. *Curr Biol* *19*, 414-422.

Bosher, J.M., Hahn, B.S., Legouis, R., Sookhareea, S., Weimer, R.M., Gansmuller, A., Chisholm, A.D., Rose, A.M., Bessereau, J.L., and Labouesse, M. (2003). The *Caenorhabditis elegans* vab-10 spectraplakin isoforms protect the epidermis against internal and external forces. *J Cell Biol* *161*, 757-768.

Bottenberg, W., Sanchez-Soriano, N., Alves-Silva, J., Hahn, I., Mende, M., and Prokop, A. (2009). Context-specific requirements of functional domains of the Spectraplakin Short stop in vivo. *Mech Dev* *126*, 489-502.

Bouameur, J.E., Favre, B., and Borradori, L. (2014). Plakins, a versatile family of cytolinkers: roles in skin integrity and in human diseases. *J Invest Dermatol* *134*, 885-894.

Braat, A.K., Zandbergen, T., van de Water, S., Goos, H.J., and Zivkovic, D. (1999). Characterization of zebrafish primordial germ cells: morphology and early distribution of vasa RNA. *Dev Dyn* *216*, 153-167.

Brangwynne, C.P., Eckmann, C.R., Courson, D.S., Rybarska, A., Hoege, C., Gharakhani, J., Julicher, F., and Hyman, A.A. (2009). Germline P granules are liquid droplets that localize by controlled dissolution/condensation. *Science* *324*, 1729-1732.

Brosig, M., Ferralli, J., Gelman, L., Chiquet, M., and Chiquet-Ehrismann, R. (2010). Interfering with the connection between the nucleus and the cytoskeleton affects nuclear rotation, mechanotransduction and myogenesis. *Int J Biochem Cell Biol* *42*, 1717-1728.

- Bubunenko, M., Kress, T.L., Vempati, U.D., Mowry, K.L., and King, M.L. (2002). A consensus RNA signal that directs germ layer determinants to the vegetal cortex of *Xenopus* oocytes. *Dev Biol* *248*, 82-92.
- Campbell, P.D., Chao, J.A., Singer, R.H., and Marlow, F.L. (2015). Dynamic visualization of transcription and RNA subcellular localization in zebrafish. *Development* *142*, 1368-1374.
- Carlson, J.L., Bakst, M.R., and Ottinger, M.A. (1996). Developmental stages of primary oocytes in turkeys. *Poult Sci* *75*, 1569-1578.
- Cha, S.W., Tadjuidje, E., Tao, Q., Wylie, C., and Heasman, J. (2008). Wnt5a and Wnt11 interact in a maternal Dkk1-regulated fashion to activate both canonical and non-canonical signaling in *Xenopus* axis formation. *Development* *135*, 3719-3729.
- Cha, S.W., Tadjuidje, E., White, J., Wells, J., Mayhew, C., Wylie, C., and Heasman, J. (2009). Wnt11/5a complex formation caused by tyrosine sulfation increases canonical signaling activity. *Curr Biol* *19*, 1573-1580.
- Chang, P., Torres, J., Lewis, R.A., Mowry, K.L., Houliston, E., and King, M.L. (2004). Localization of RNAs to the mitochondrial cloud in *Xenopus* oocytes through entrapment and association with endoplasmic reticulum. *Mol Biol Cell* *15*, 4669-4681.
- Chen, H.J., Lin, C.M., Lin, C.S., Perez-Olle, R., Leung, C.L., and Liem, R.K. (2006). The role of microtubule actin cross-linking factor 1 (MACF1) in the Wnt signaling pathway. *Genes Dev* *20*, 1933-1945.
- Choi, H.M., Chang, J.Y., Trinh le, A., Padilla, J.E., Fraser, S.E., and Pierce, N.A. (2010). Programmable in situ amplification for multiplexed imaging of mRNA expression. *Nat Biotechnol* *28*, 1208-1212.
- Choo, S., Heinrich, B., Betley, J.N., Chen, Z., and Deshler, J.O. (2005). Evidence for common machinery utilized by the early and late RNA localization pathways in *Xenopus* oocytes. *Dev Biol* *278*, 103-117.

- Claussen, M., Horvay, K., and Pieler, T. (2004). Evidence for overlapping, but not identical, protein machineries operating in vegetal RNA localization along early and late pathways in *Xenopus* oocytes. *Development* *131*, 4263-4273.
- Claussen, M., and Pieler, T. (2004). Xvelo1 uses a novel 75-nucleotide signal sequence that drives vegetal localization along the late pathway in *Xenopus* oocytes. *Dev Biol* *266*, 270-284.
- Claussen, M., Tarbashevich, K., and Pieler, T. (2011). Functional dissection of the RNA signal sequence responsible for vegetal localization of XGrip2.1 mRNA in *Xenopus* oocytes. *Rna Biol* *8*, 873-882.
- Clements, D., Friday, R.V., and Woodland, H.R. (1999). Mode of action of VegT in mesoderm and endoderm formation. *Development* *126*, 4903-4911.
- Colozza, G., and De Robertis, E.M. (2014). Maternal syntabulin is required for dorsal axis formation and is a germ plasm component in *Xenopus*. *Differentiation* *88*, 17-26.
- Cote, C.A., Gautreau, D., Denegre, J.M., Kress, T.L., Terry, N.A., and Mowry, K.L. (1999). A *Xenopus* protein related to hnRNP I has a role in cytoplasmic RNA localization. *Mol Cell* *4*, 431-437.
- Cox, R.T., and Spradling, A.C. (2003). A Balbiani body and the fusome mediate mitochondrial inheritance during *Drosophila* oogenesis. *Development* *130*, 1579-1590.
- Crisp, M., Liu, Q., Roux, K., Rattner, J.B., Shanahan, C., Burke, B., Stahl, P.D., and Hodzic, D. (2006). Coupling of the nucleus and cytoplasm: role of the LINC complex. *J Cell Biol* *172*, 41-53.
- Cuykendall, T.N., and Houston, D.W. (2010). Identification of germ plasm-associated transcripts by microarray analysis of *Xenopus* vegetal cortex RNA. *Dev Dyn* *239*, 1838-1848.
- Dahlem, T.J., Hoshijima, K., Jurynech, M.J., Gunther, D., Starker, C.G., Locke, A.S., Weis, A.M., Voytas, D.F., and Grunwald, D.J. (2012). Simple methods for generating and detecting locus-specific mutations induced with TALENs in the zebrafish genome. *Plos Genet* *8*, e1002861.

- De Robertis, E.M., and Kuroda, H. (2004). Dorsal-ventral patterning and neural induction in *Xenopus* embryos. *Annual review of cell and developmental biology* 20, 285-308.
- Ding, X., Xu, R., Yu, J., Xu, T., Zhuang, Y., and Han, M. (2007). SUN1 is required for telomere attachment to nuclear envelope and gametogenesis in mice. *Dev Cell* 12, 863-872.
- Dosch, R., Wagner, D.S., Mintzer, K.A., Runke, G., Wiemelt, A.P., and Mullins, M.C. (2004). Maternal control of vertebrate development before the midblastula transition: mutants from the zebrafish I. *Dev Cell* 6, 771-780.
- Dumont, J.N. (1978). Oogenesis in *Xenopus laevis* (Daudin). VI. The route of injected tracer transport in the follicle and developing oocyte. *J Exp Zool* 204, 193-217.
- Elkouby, Y.M., Jamieson-Lucy, A., and Mullins, M.C. (2016). Oocyte Polarization Is Coupled to the Chromosomal Bouquet, a Conserved Polarized Nuclear Configuration in Meiosis. *Plos Biol* 14, e1002335.
- Ephrussi, A., Dickinson, L.K., and Lehmann, R. (1991). Oskar organizes the germ plasm and directs localization of the posterior determinant nanos. *Cell* 66, 37-50.
- Ephrussi, A., and Lehmann, R. (1992). Induction of germ cell formation by oskar. *Nature* 358, 387-392.
- Erter, C.E., Wilm, T.P., Basler, N., Wright, C.V., and Solnica-Krezel, L. (2001). Wnt8 is required in lateral mesendodermal precursors for neural posteriorization in vivo. *Development* 128, 3571-3583.
- Ervasti, J.M. (2007). Dystrophin, its interactions with other proteins, and implications for muscular dystrophy. *Biochim Biophys Acta* 1772, 108-117.
- Escobar-Aguirre, M., Elkouby, Y.M., and Mullins, M.C. (2016). Localization in Oogenesis of Maternal Regulators of Embryonic Development

. In *Vertebrate Development: Maternal to Zygotic Control*, F. Pelegri, M. Danilchik, and A. Sutherland, eds. (Gewerbestr. 11, 6330 Cham, Switzerland: Springer International Publishing), pp. 173-208.

Extavour, C.G., and Akam, M. (2003). Mechanisms of germ cell specification across the metazoans: epigenesis and preformation. *Development* *130*, 5869-5884.

Fernandez, J., and Fuentes, R. (2013). Fixation/permeabilization: new alternative procedure for immunofluorescence and mRNA in situ hybridization of vertebrate and invertebrate embryos. *Dev Dyn* *242*, 503-517.

Field, C.M., Nguyen, P.A., Ishihara, K., Groen, A.C., and Mitchison, T.J. (2014). *Xenopus* egg cytoplasm with intact actin. *Methods Enzymol* *540*, 399-415.

Forbes, M.M., Rothhamel, S., Jenny, A., and Marlow, F.L. (2015). Maternal *dazap2* Regulates Germ Granules by Counteracting Dynein in Zebrafish Primordial Germ Cells. *Cell Rep* *12*, 49-57.

Forristall, C., Pondel, M., Chen, L., and King, M.L. (1995). Patterns of localization and cytoskeletal association of two vegetally localized RNAs, *Vg1* and *Xcat-2*. *Development* *121*, 201-208.

Gard, D.L. (1991). Organization, nucleation, and acetylation of microtubules in *Xenopus laevis* oocytes: a study by confocal immunofluorescence microscopy. *Dev Biol* *143*, 346-362.

Gard, D.L. (1992). Microtubule organization during maturation of *Xenopus* oocytes: assembly and rotation of the meiotic spindles. *Dev Biol* *151*, 516-530.

Gard, D.L. (1999). Confocal microscopy and 3-D reconstruction of the cytoskeleton of *Xenopus* oocytes. *Microsc Res Tech* *44*, 388-414.

Gard, D.L., Affleck, D., and Error, B.M. (1995a). Microtubule organization, acetylation, and nucleation in *Xenopus laevis* oocytes: II. A developmental transition in microtubule organization during early diplotene. *Dev Biol* *168*, 189-201.

Gard, D.L., Cha, B.J., and King, E. (1997). The organization and animal-vegetal asymmetry of cytokeratin filaments in stage VI *Xenopus* oocytes is dependent upon F-actin and microtubules. *Dev Biol* *184*, 95-114.

Gard, D.L., Cha, B.J., and Schroeder, M.M. (1995b). Confocal immunofluorescence microscopy of microtubules, microtubule-associated proteins, and microtubule-organizing centers during amphibian oogenesis and early development. *Curr Top Dev Biol* *31*, 383-431.

Ge, X., Grotjahn, D., Welch, E., Lyman-Gingerich, J., Holguin, C., Dimitrova, E., Abrams, E.W., Gupta, T., Marlow, F.L., Yabe, T., *et al.* (2014). Hecate/Grip2a acts to reorganize the cytoskeleton in the symmetry-breaking event of embryonic axis induction. *Plos Genet* *10*, e1004422.

Ghosh, S., Marchand, V., Gaspar, I., and Ephrussi, A. (2012). Control of RNP motility and localization by a splicing-dependent structure in oskar mRNA. *Nat Struct Mol Biol* *19*, 441-449.

Glotzer, J.B., Saffrich, R., Glotzer, M., and Ephrussi, A. (1997). Cytoplasmic flows localize injected oskar RNA in *Drosophila* oocytes. *Curr Biol* *7*, 326-337.

Grum, V.L., Li, D., MacDonald, R.I., and Mondragon, A. (1999). Structures of two repeats of spectrin suggest models of flexibility. *Cell* *98*, 523-535.

Guo, L., Degenstein, L., Dowling, J., Yu, Q.C., Wollmann, R., Perman, B., and Fuchs, E. (1995). Gene targeting of BPAG1: abnormalities in mechanical strength and cell migration in stratified epithelia and neurologic degeneration. *Cell* *81*, 233-243.

Gupta, T., Marlow, F.L., Ferriola, D., Mackiewicz, K., Dapprich, J., Monos, D., and Mullins, M.C. (2010). Microtubule actin crosslinking factor 1 regulates the Balbiani body and animal-vegetal polarity of the zebrafish oocyte. *Plos Genet* *6*, e1001073.

Hashimoto, Y., Maegawa, S., Nagai, T., Yamaha, E., Suzuki, H., Yasuda, K., and Inoue, K. (2004). Localized maternal factors are required for zebrafish germ cell formation. *Dev Biol* *268*, 152-161.

Heasman, J. (2006). Maternal determinants of embryonic cell fate. *Semin Cell Dev Biol* 17, 93-98.

Heasman, J., Quarmby, J., and Wylie, C.C. (1984). The mitochondrial cloud of *Xenopus* oocytes: the source of germinal granule material. *Dev Biol* 105, 458-469.

Heim, A.E., Hartung, O., Rothhamel, S., Ferreira, E., Jenny, A., and Marlow, F.L. (2014). Oocyte polarity requires a Bucky ball-dependent feedback amplification loop. *Development* 141, 842-854.

Hertig, A.T. (1968). The primary human oocyte: some observations on the fine structure of Balbiani's vitelline body and the origin of the annulate lamellae. *Am J Anat* 122, 107-137.

Houston, D.W. (2013). Regulation of cell polarity and RNA localization in vertebrate oocytes. *Int Rev Cell Mol Biol* 306, 127-185.

Houston, D.W., and King, M.L. (2000). A critical role for *Xdazl*, a germ plasm-localized RNA, in the differentiation of primordial germ cells in *Xenopus*. *Development* 127, 447-456.

Houston, D.W., Zhang, J., Maines, J.Z., Wasserman, S.A., and King, M.L. (1998). A *Xenopus* DAZ-like gene encodes an RNA component of germ plasm and is a functional homologue of *Drosophila* *boule*. *Development* 125, 171-180.

Howley, C., and Ho, R.K. (2000). mRNA localization patterns in zebrafish oocytes. *Mech Dev* 92, 305-309.

Ikenishi, K., Kotani, M., and Tanabe, K. (1974). Ultrastructural changes associated with UV irradiation in the "germinal plasm" of *Xenopus laevis*. *Dev Biol* 36, 155-168.

Jaglarz, M.K., Nowak, Z., and Bilinski, S.M. (2003). The Balbiani body and generation of early asymmetry in the oocyte of a tiger beetle. *Differentiation* 71, 142-151.

Jedrzejska, I., and Kubrakiewicz, J. (2007). The Balbiani body in the oocytes of a common cellar spider, *Pholcus phalangoides* (Araneae: Pholcidae). *Arthropod Struct Dev* 36, 317-326.

Jenny, A., Hachet, O., Zavorszky, P., Cyrklaff, A., Weston, M.D., Johnston, D.S., Erdelyi, M., and Ephrussi, A. (2006). A translation-independent role of oskar RNA in early *Drosophila* oogenesis. *Development* *133*, 2827-2833.

Jorgensen, L.H., Mosbech, M.B., Faergeman, N.J., Graakjaer, J., Jacobsen, S.V., and Schroder, H.D. (2014). Duplication in the microtubule-actin cross-linking factor 1 gene causes a novel neuromuscular condition. *Sci Rep* *4*, 5180.

Kaneshiro, K., Miyauchi, M., Tanigawa, Y., Ikenishi, K., and Komiyama, T. (2007). The mRNA coding for *Xenopus* glutamate receptor interacting protein 2 (XGRIP2) is maternally transcribed, transported through the late pathway and localized to the germ plasm. *Biochem Biophys Res Commun* *355*, 902-906.

Karakesisoglou, I., Yang, Y., and Fuchs, E. (2000). An epidermal plakin that integrates actin and microtubule networks at cellular junctions. *J Cell Biol* *149*, 195-208.

Kerr, T.P., Sewry, C.A., Robb, S.A., and Roberts, R.G. (2001). Long mutant dystrophins and variable phenotypes: evasion of nonsense-mediated decay? *Hum Genet* *109*, 402-407.

Kim, H.S., Murakami, R., Quintin, S., Mori, M., Ohkura, K., Tamai, K.K., Labouesse, M., Sakamoto, H., and Nishiwaki, K. (2011). VAB-10 spectraplakin acts in cell and nuclear migration in *Caenorhabditis elegans*. *Development* *138*, 4013-4023.

King, M.L., Messitt, T.J., and Mowry, K.L. (2005). Putting RNAs in the right place at the right time: RNA localization in the frog oocyte. *Biol Cell* *97*, 19-33.

Kirilenko, P., Weierud, F.K., Zorn, A.M., and Woodland, H.R. (2008). The efficiency of *Xenopus* primordial germ cell migration depends on the germline mRNA encoding the PDZ domain protein Grip2. *Differentiation* *76*, 392-403.

Kloc, M., Bilinski, S., Chan, A.P., Allen, L.H., Zearfoss, N.R., and Etkin, L.D. (2001). RNA localization and germ cell determination in *Xenopus*. *Int Rev Cytol* *203*, 63-91.

- Kloc, M., Bilinski, S., and Etkin, L.D. (2004). The Balbiani body and germ cell determinants: 150 years later. *Curr Top Dev Biol* 59, 1-36.
- Kloc, M., and Etkin, L.D. (1995). Two distinct pathways for the localization of RNAs at the vegetal cortex in *Xenopus* oocytes. *Development* 121, 287-297.
- Kloc, M., Larabell, C., Chan, A.P., and Etkin, L.D. (1998). Contribution of METRO pathway localized molecules to the organization of the germ cell lineage. *Mech Dev* 75, 81-93.
- Kloc, M., Larabell, C., and Etkin, L.D. (1996). Elaboration of the messenger transport organizer pathway for localization of RNA to the vegetal cortex of *Xenopus* oocytes. *Dev Biol* 180, 119-130.
- Kloc, M., Zearfoss, N.R., and Etkin, L.D. (2002). Mechanisms of subcellular mRNA localization. *Cell* 108, 533-544.
- Knaut, H., Pelegri, F., Bohmann, K., Schwarz, H., and Nusslein-Volhard, C. (2000). Zebrafish vasa RNA but not its protein is a component of the germ plasm and segregates asymmetrically before germline specification. *J Cell Biol* 149, 875-888.
- Kobayashi, S., Amikura, R., and Okada, M. (1994). Localization of mitochondrial large rRNA in germinal granules and the consequent segregation of germ line. *Int J Dev Biol* 38, 193-199.
- Kodama, A., Karakesisoglou, I., Wong, E., Vaezi, A., and Fuchs, E. (2003). ACF7: an essential integrator of microtubule dynamics. *Cell* 115, 343-354.
- Koenig, M., Hoffman, E.P., Bertelson, C.J., Monaco, A.P., Feener, C., and Kunkel, L.M. (1987). Complete cloning of the Duchenne muscular dystrophy (DMD) cDNA and preliminary genomic organization of the DMD gene in normal and affected individuals. *Cell* 50, 509-517.
- Kondo, T., Yanagawa, T., Yoshida, N., and Yamashita, M. (1997). Introduction of cyclin B induces activation of the maturation-promoting factor and breakdown of germinal vesicle in growing zebrafish oocytes unresponsive to the maturation-inducing hormone. *Dev Biol* 190, 142-152.

Kosaka, K., Kawakami, K., Sakamoto, H., and Inoue, K. (2007). Spatiotemporal localization of germ plasm RNAs during zebrafish oogenesis. *Mech Dev* 124, 279-289.

Ku, M., and Melton, D.A. (1993). Xwnt-11: a maternally expressed *Xenopus* wnt gene. *Development* 119, 1161-1173.

Kwon, S., Abramson, T., Munro, T.P., John, C.M., Kohrmann, M., and Schnapp, B.J. (2002). UUCAC- and vera-dependent localization of VegT RNA in *Xenopus* oocytes. *Curr Biol* 12, 558-564.

Langdon, Y.G., and Mullins, M.C. (2011). Maternal and zygotic control of zebrafish dorsoventral axial patterning. *Annu Rev Genet* 45, 357-377.

Laporte, C., Vetter, G., Loudes, A.M., Robinson, D.G., Hillmer, S., Stussi-Garaud, C., and Ritzenthaler, C. (2003). Involvement of the secretory pathway and the cytoskeleton in intracellular targeting and tubule assembly of Grapevine fanleaf virus movement protein in tobacco BY-2 cells. *Plant Cell* 15, 2058-2075.

Lawson, K.A., Dunn, N.R., Roelen, B.A., Zeinstra, L.M., Davis, A.M., Wright, C.V., Korving, J.P., and Hogan, B.L. (1999). Bmp4 is required for the generation of primordial germ cells in the mouse embryo. *Genes Dev* 13, 424-436.

Lee, S., Harris, K.L., Whittington, P.M., and Kolodziej, P.A. (2000). short stop is allelic to kakapo, and encodes rod-like cytoskeletal-associated proteins required for axon extension. *J Neurosci* 20, 1096-1108.

Lee, S., and Kolodziej, P.A. (2002a). The plakin Short Stop and the RhoA GTPase are required for E-cadherin-dependent apical surface remodeling during tracheal tube fusion. *Development* 129, 1509-1520.

Lee, S., and Kolodziej, P.A. (2002b). Short Stop provides an essential link between F-actin and microtubules during axon extension. *Development* 129, 1195-1204.

Lekven, A.C., Thorpe, C.J., Waxman, J.S., and Moon, R.T. (2001). Zebrafish *wnt8* encodes two *wnt8* proteins on a bicistronic transcript and is required for mesoderm and neurectoderm patterning. *Dev Cell* *1*, 103-114.

Leung, C.L., Sun, D., Zheng, M., Knowles, D.R., and Liem, R.K. (1999). Microtubule actin cross-linking factor (MACF): a hybrid of dystonin and dystrophin that can interact with the actin and microtubule cytoskeletons. *J Cell Biol* *147*, 1275-1286.

Lin, C.M., Chen, H.J., Leung, C.L., Parry, D.A., and Liem, R.K. (2005). Microtubule actin crosslinking factor 1b: a novel plakin that localizes to the Golgi complex. *J Cell Sci* *118*, 3727-3738.

Link, J., Leubner, M., Schmitt, J., Gob, E., Benavente, R., Jeang, K.T., Xu, R., and Alsheimer, M. (2014). Analysis of meiosis in SUN1 deficient mice reveals a distinct role of SUN2 in mammalian meiotic LINC complex formation and function. *Plos Genet* *10*, e1004099.

Lombardi, M.L., and Lammerding, J. (2011). Keeping the LINC: the importance of nucleocytoskeletal coupling in intracellular force transmission and cellular function. *Biochem Soc Trans* *39*, 1729-1734.

Lu, F.I., Thisse, C., and Thisse, B. (2011). Identification and mechanism of regulation of the zebrafish dorsal determinant. *Proc Natl Acad Sci U S A* *108*, 15876-15880.

Markussen, F.H., Michon, A.M., Breitwieser, W., and Ephrussi, A. (1995). Translational control of *oskar* generates short OSK, the isoform that induces pole plasma assembly. *Development* *121*, 3723-3732.

Marlow, F.L., and Mullins, M.C. (2008). Bucky ball functions in Balbiani body assembly and animal-vegetal polarity in the oocyte and follicle cell layer in zebrafish. *Dev Biol* *321*, 40-50.

Masui, Y. (1972). Hormonal and cytoplasmic control of the maturation of frog oocytes. *Sov J Dev Biol* *3*, 484-495.

Meinke, P., Nguyen, T.D., and Wehnert, M.S. (2011). The LINC complex and human disease. *Biochem Soc Trans* 39, 1693-1697.

Melton, D.A. (1987). Translocation of a localized maternal mRNA to the vegetal pole of *Xenopus* oocytes. *Nature* 328, 80-82.

Messitt, T.J., Gagnon, J.A., Kreiling, J.A., Pratt, C.A., Yoon, Y.J., and Mowry, K.L. (2008). Multiple kinesin motors coordinate cytoplasmic RNA transport on a subpopulation of microtubules in *Xenopus* oocytes. *Dev Cell* 15, 426-436.

Mosquera, L., Forristall, C., Zhou, Y., and King, M.L. (1993). A mRNA localized to the vegetal cortex of *Xenopus* oocytes encodes a protein with a nanos-like zinc finger domain. *Development* 117, 377-386.

Mowry, K.L., and Cote, C.A. (1999). RNA sorting in *Xenopus* oocytes and embryos. *Faseb J* 13, 435-445.

Mowry, K.L., and Melton, D.A. (1992). Vegetal messenger RNA localization directed by a 340-nt RNA sequence element in *Xenopus* oocytes. *Science* 255, 991-994.

Nagahama, Y., and Yamashita, M. (2008). Regulation of oocyte maturation in fish. *Dev Growth Differ* 50 Suppl 1, S195-219.

Nashchekin, D., Fernandes, A.R., and St Johnston, D. (2016). Patronin/Shot Cortical Foci Assemble the Noncentrosomal Microtubule Array that Specifies the *Drosophila* Anterior-Posterior Axis. *Dev Cell* 38, 61-72.

Nojima, H., Rothhamel, S., Shimizu, T., Kim, C.H., Yonemura, S., Marlow, F.L., and Hibi, M. (2010). Syntabulin, a motor protein linker, controls dorsal determination. *Development* 137, 923-933.

Nojima, H., Shimizu, T., Kim, C.H., Yabe, T., Bae, Y.K., Muraoka, O., Hirata, T., Chitnis, A., Hirano, T., and Hibi, M. (2004). Genetic evidence for involvement of maternally derived Wnt canonical signaling in dorsal determination in zebrafish. *Mech Dev* 121, 371-386.

Palmucci, L., Doriguzzi, C., Mongini, T., Restagno, G., Chiado-Piat, L., and Maniscalco, M. (1994). Unusual expression and very mild course of Xp21 muscular dystrophy (Becker type) in a 60-year-old man with 26 percent deletion of the dystrophin gene. *Neurology* 44, 541-543.

Pepling, M.E., Wilhelm, J.E., O'Hara, A.L., Gephardt, G.W., and Spradling, A.C. (2007). Mouse oocytes within germ cell cysts and primordial follicles contain a Balbiani body. *Proc Natl Acad Sci U S A* 104, 187-192.

Postel, R., Ketema, M., Kuikman, I., de Pereda, J.M., and Sonnenberg, A. (2011). Nesprin-3 augments peripheral nuclear localization of intermediate filaments in zebrafish. *J Cell Sci* 124, 755-764.

Rebagliati, M.R., Weeks, D.L., Harvey, R.P., and Melton, D.A. (1985). Identification and cloning of localized maternal RNAs from *Xenopus* eggs. *Cell* 42, 769-777.

Riemer, S., Bontems, F., Krishnakumar, P., Gomann, J., and Dosch, R. (2015). A functional Bucky ball-GFP transgene visualizes germ plasm in living zebrafish. *Gene Expr Patterns* 18, 44-52.

Rodler, D., and Sinowatz, F. (2013). Expression of intermediate filaments in the Balbiani body and ovarian follicular wall of the Japanese quail (*Coturnix japonica*). *Cells Tissues Organs* 197, 298-311.

Roper, K., and Brown, N.H. (2004). A spectraplakins is enriched on the fusome and organizes microtubules during oocyte specification in *Drosophila*. *Curr Biol* 14, 99-110.

Sanchez-Soriano, N., Travis, M., Dajas-Bailador, F., Goncalves-Pimentel, C., Whitmarsh, A.J., and Prokop, A. (2009). Mouse ACF7 and drosophila short stop modulate filopodia formation and microtubule organisation during neuronal growth. *J Cell Sci* 122, 2534-2542.

Sato, A., Isaac, B., Phillips, C.M., Rillo, R., Carlton, P.M., Wynne, D.J., Kasad, R.A., and Dernburg, A.F. (2009). Cytoskeletal forces span the nuclear envelope to coordinate meiotic chromosome pairing and synapsis. *Cell* *139*, 907-919.

Scherthan, H. (2001). A bouquet makes ends meet. *Nat Rev Mol Cell Biol* *2*, 621-627.

Schnapp, B.J., Arn, E.A., Deshler, J.O., and Highett, M.I. (1997). RNA localization in *Xenopus* oocytes. *Semin Cell Dev Biol* *8*, 529-540.

Schroeder, K.E., Condic, M.L., Eisenberg, L.M., and Yost, H.J. (1999). Spatially regulated translation in embryos: asymmetric expression of maternal Wnt-11 along the dorsal-ventral axis in *Xenopus*. *Dev Biol* *214*, 288-297.

Selman, K., Wallace, R.A., Sarka, A., and Qi, X.P. (1993). STAGES OF OOCYTE DEVELOPMENT IN THE ZEBRAFISH, BRACHYDANIO-RERIO. *Journal of Morphology* *218*, 203-224.

Shibuya, H., Ishiguro, K., and Watanabe, Y. (2014a). The TRF1-binding protein TERB1 promotes chromosome movement and telomere rigidity in meiosis. *Nat Cell Biol* *16*, 145-156.

Shibuya, H., Morimoto, A., and Watanabe, Y. (2014b). The dissection of meiotic chromosome movement in mice using an in vivo electroporation technique. *Plos Genet* *10*, e1004821.

Sive, H.L., Grainger, R.M., and Harland, R.M. (2007). Cortical Isolation from *Xenopus laevis* Oocytes and Eggs. *CSH Protoc* *2007*, pdb prot4753.

Smith, E.A., and Fuchs, E. (1998). Defining the interactions between intermediate filaments and desmosomes. *J Cell Biol* *141*, 1229-1241.

Smith, L.D. (1966). The role of a "germinal plasm" in the formation of primordial germ cells in *Rana pipiens*. *Dev Biol* *14*, 330-347.

Smith, S.M., and Maughan, P.J. (2015). SNP genotyping using KASPar assays. *Methods Mol Biol* *1245*, 243-256.

Song, H.W., Cauffman, K., Chan, A.P., Zhou, Y., King, M.L., Etkin, L.D., and Kloc, M. (2007). Hermes RNA-binding protein targets RNAs-encoding proteins involved in meiotic maturation, early cleavage, and germline development. *Differentiation* *75*, 519-528.

Sosa, B.A., Rothballer, A., Kutay, U., and Schwartz, T.U. (2012). LINC complexes form by binding of three KASH peptides to domain interfaces of trimeric SUN proteins. *Cell* *149*, 1035-1047.

Starr, D.A., and Fridolfsson, H.N. (2010). Interactions between nuclei and the cytoskeleton are mediated by SUN-KASH nuclear-envelope bridges. *Annual review of cell and developmental biology* *26*, 421-444.

Staudt, N., Molitor, A., Somogyi, K., Mata, J., Curado, S., Eulenberg, K., Meise, M., Siegmund, T., Hader, T., Hilfiker, A., *et al.* (2005). Gain-of-function screen for genes that affect *Drosophila* muscle pattern formation. *Plos Genet* *1*, e55.

Styers, M.L., Kowalczyk, A.P., and Faundez, V. (2006). Architecture of the vimentin cytoskeleton is modified by perturbation of the GTPase ARF1. *J Cell Sci* *119*, 3643-3654.

Subramanian, A., Prokop, A., Yamamoto, M., Sugimura, K., Uemura, T., Betschinger, J., Knoblich, J.A., and Volk, T. (2003). Shortstop recruits EB1/APC1 and promotes microtubule assembly at the muscle-tendon junction. *Curr Biol* *13*, 1086-1095.

Tao, Q., Yokota, C., Puck, H., Kofron, M., Birsoy, B., Yan, D., Asashima, M., Wylie, C.C., Lin, X., and Heasman, J. (2005). Maternal *wnt11* activates the canonical wnt signaling pathway required for axis formation in *Xenopus* embryos. *Cell* *120*, 857-871.

Tarbashevich, K., Koebernick, K., and Pieler, T. (2007). XGRIP2.1 is encoded by a vegetally localizing, maternal mRNA and functions in germ cell development and anteroposterior PGC positioning in *Xenopus laevis*. *Dev Biol* *311*, 554-565.

Tran, L.D., Hino, H., Quach, H., Lim, S., Shindo, A., Mimori-Kiyosue, Y., Mione, M., Ueno, N., Winkler, C., Hibi, M., *et al.* (2012). Dynamic microtubules at the vegetal cortex predict the embryonic axis in zebrafish. *Development* *139*, 3644-3652.

Trinh le, A., Hochgreb, T., Graham, M., Wu, D., Ruf-Zamojski, F., Jayasena, C.S., Saxena, A., Hawk, R., Gonzalez-Serricchio, A., Dixon, A., *et al.* (2011). A versatile gene trap to visualize and interrogate the function of the vertebrate proteome. *Genes Dev* *25*, 2306-2320.

Ukeshima, A., and Fujimoto, T. (1991). A fine morphological study of germ cells in asymmetrically developing right and left ovaries of the chick. *Anat Rec* *230*, 378-386.

Varga, M., Maegawa, S., Bellipanni, G., and Weinberg, E.S. (2007). Chordin expression, mediated by Nodal and FGF signaling, is restricted by redundant function of two beta-catenins in the zebrafish embryo. *Mech Dev* *124*, 775-791.

Wagner, D.S., Dosch, R., Mintzer, K.A., Wiemelt, A.P., and Mullins, M.C. (2004). Maternal control of development at the midblastula transition and beyond: mutants from the zebrafish II. *Dev Cell* *6*, 781-790.

Wang, J.T., Smith, J., Chen, B.C., Schmidt, H., Rasoloson, D., Paix, A., Lambrus, B.G., Calidas, D., Betzig, E., and Seydoux, G. (2014). Regulation of RNA granule dynamics by phosphorylation of serine-rich, intrinsically disordered proteins in *C. elegans*. *Elife* *3*, e04591.

Weakley, B.S. (1967). "Balbiani's body" in the oocyte of the golden hamster. *Z Zellforsch Mikrosk Anat* *83*, 583-588.

Weeks, D.L., and Melton, D.A. (1987). A maternal mRNA localized to the animal pole of *Xenopus* eggs encodes a subunit of mitochondrial ATPase. *Proc Natl Acad Sci U S A* *84*, 2798-2802.

WH, v.W. (1845). Dissertation: *Observationes quaedam de araneis ex ovo evolutione*. Halle, Germany: In Halis Saxonum.

- Whittington, P.M., and Dixon, K.E. (1975). Quantitative studies of germ plasm and germ cells during early embryogenesis of *Xenopus laevis*. *J Embryol Exp Morphol* *33*, 57-74.
- Wilhelmsen, K., Litjens, S.H., Kuikman, I., Tshimbalanga, N., Janssen, H., van den Bout, I., Raymond, K., and Sonnenberg, A. (2005). Nesprin-3, a novel outer nuclear membrane protein, associates with the cytoskeletal linker protein plectin. *J Cell Biol* *171*, 799-810.
- Wilk, K., Bilinski, S., Dougherty, M.T., and Kloc, M. (2005). Delivery of germinal granules and localized RNAs via the messenger transport organizer pathway to the vegetal cortex of *Xenopus* oocytes occurs through directional expansion of the mitochondrial cloud. *Int J Dev Biol* *49*, 17-21.
- Wu, X., Kodama, A., and Fuchs, E. (2008). ACF7 regulates cytoskeletal-focal adhesion dynamics and migration and has ATPase activity. *Cell* *135*, 137-148.
- Xanthos, J.B., Kofron, M., Wylie, C., and Heasman, J. (2001). Maternal VegT is the initiator of a molecular network specifying endoderm in *Xenopus laevis*. *Development* *128*, 167-180.
- Yan, W., Ma, L., Zilinski, C.A., and Matzuk, M.M. (2004). Identification and characterization of evolutionarily conserved pufferfish, zebrafish, and frog orthologs of GASZ. *Biol Reprod* *70*, 1619-1625.
- Yano, T., Lopez de Quinto, S., Matsui, Y., Shevchenko, A., Shevchenko, A., and Ephrussi, A. (2004). Hrp48, a *Drosophila* hnRNPA/B homolog, binds and regulates translation of oskar mRNA. *Dev Cell* *6*, 637-648.
- Yisraeli, J.K., and Melton, D.A. (1988). The maternal mRNA Vg1 is correctly localized following injection into *Xenopus* oocytes. *Nature* *336*, 592-595.
- Yisraeli, J.K., Sokol, S., and Melton, D.A. (1989). The process of localizing a maternal messenger RNA in *Xenopus* oocytes. *Development* *107 Suppl*, 31-36.

Yisraeli, J.K., Sokol, S., and Melton, D.A. (1990). A two-step model for the localization of maternal mRNA in *Xenopus* oocytes: involvement of microtubules and microfilaments in the translocation and anchoring of Vg1 mRNA. *Development* 108, 289-298.

Yoon, C., Kawakami, K., and Hopkins, N. (1997). Zebrafish vasa homologue RNA is localized to the cleavage planes of 2- and 4-cell-stage embryos and is expressed in the primordial germ cells. *Development* 124, 3157-3165.

Zhou, Y., and King, M.L. (1996a). Localization of Xcat-2 RNA, a putative germ plasm component, to the mitochondrial cloud in *Xenopus* stage I oocytes. *Development* 122, 2947-2953.

Zhou, Y., and King, M.L. (1996b). RNA transport to the vegetal cortex of *Xenopus* oocytes. *Dev Biol* 179, 173-183.

Zust, B., and Dixon, K.E. (1975). The effect of u.v. irradiation of the vegetal pole of *Xenopus laevis* eggs on the presumptive primordial germ cells. *J Embryol Exp Morphol* 34, 209-220.